Université de Montréal

A study of the Polycomb group complexes in the maintenance of heterochromatic genome stability and Alzheimer's disease

par
Jida El Hajjar

Programme de biologie moléculaire,
Faculté de Médecine, Université de Montréal

Thèse présentée à la Faculté de Médecine
en vue de l'obtention du grade de doctorat
en biologie moléculaire

Juillet, 2013

Résumé:

La démence d'Alzheimer est une maladie neurodégénérative caractérisée par une perte progressive et irreversible des fonctions cognitives et des compétences intellectuelles. La maladie d'Alzheimer se présente sous deux formes: la forme familiale ou précoce (EOAD) qui représente 5% des cas et elle est liée à des mutations génétiques affectant le métabolisme des peptides amyloïde; et la forme tardive ou sporadique (LOAD) qui représente 95% des cas mais son étiologie est encore mal définie. Cependant, le vieillissement reste le principal facteur de risque pour développer LOAD. Les changements épigénétiques impliquant des modifications des histones jouent un rôle crucial dans les maladies neurodégénératives et le vieillissement lié à l'âge. Des données récentes ont décrit LOAD comme un désordre de l'épigénome et ont associé ce trouble à l'instabilité génomique. Les protéines Polycomb sont des modificateurs épigénétiques qui induisent le remodelage de la chromatine et la répression des gènes à l'hétérochromatine facultative. Nous rapportons que les souris hétérozygotes pour une protéine Polycomb développent avec l'âge un trouble neurologique ressemblant à LOAD caractérisé par l'altération des fonctions cognitives, la phosphorylation de la protéine tau, l'accumulation des peptides amyloïde, et le dysfonctionnement synaptique. Ce phénotype pathologique est précédé par la décondensation de l'hétérochromatine neuronale et l'activation de la réponse aux dommages à l'ADN. Parallèlement, une réduction d'expression de polycomb, malformations de l'hétérochromatine neuronale, et l'accumulation de dommages à l'ADN étaient également présents dans les cerveaux de patients LOAD. Remarquablement, les dommages de l'ADN ne sont pas distribués de façon aléatoire sur le génome mais sont enrichis au niveau des séquences répétitives. Les conclusions présentées dans cette thèse ont identifié des modifications épigénétiques spécifiques qui conduisent à une instabilité génomique aberrante menant à la formation de LOAD. Ces résultats vont aider au développement de nouveaux traitements qui peuvent potentiellement ralentir la neurodégénérescence.

Mots clés: Polycomb, Maladie d'Alzheimer tardive, instabilité génomique, hétérochromatine.

Abstract:

Alzheimer's disease (AD) is the most common neurodegenerative disorder characterized by progressive and irreversible decline in cognitive functions and thinking skills. There are two types of AD: early-onset or familial AD (EOAD) that accounts for 5% of cases and is linked to mutations affecting the amyloid metabolism and late-onset or sporadic AD (LOAD), which accounts for 95% of cases, however the etiology of this type remains poorly delineated with ageing presenting the main risk factor. Epigenetic changes involving histone modifications play a critical role in ageing and age- related neurodegenerative diseases. Recent evidence describing LOAD as an epigenetic disorder has accrued, associating this disorder to global genomic instability. Polycomb group proteins are epigenetic modifiers initiating chromatin remodeling and gene repression at facultative heterochromatin. We report that mice heterozygous for a polycomb protein develop with advancing age a neurological disorder resembling LOAD characterized by impaired memory behaviour, tau phosphorylation, amyloid accumulation, and synaptic dysfunction. Interestingly, this phenotype was preceded by neuronal heterochromatin decondensation and activation of DNA damage response. Concomitantly, polycomb deficiency, de-compaction of neuronal heterochromatin, and accumulation of DNA damage machinery were also characteristic of LOAD brains. Remarkably, DNA damage was not randomly distributed on the genome but enriched at heterochromatin. The findings presented in this thesis identified specific epigenetic modifications that lead to aberrant genomic instability in LOAD and will aid in the development of novel therapeutics, which may potentially slow neurodegeneration.

Keywords: Polycomb, Late-Onset Alzheimer's disease, genomic instability, heterochromatin.

Table of contents:

List of tables and figures

List of Acronyms and Abbreviations

Abbreviation	Meaning
5-mC	5-methyl Cytosine
8-OHG	8-Oxoguanine
Aβ	Amyloid-beta peptides
AD	Alzheimer's disease
ADP	Adenosine diphosphate
AGO	Argonaute protein
ALS	Amyotrophic lateral sclerosis
ALU	Arthrobacter luteus element
AML	Acute myeloid leukemia
AOR	Antioxidant response gene
APP	Amyloid precursor protein
ASF1a	Anti-silencing function 1a
ATM	Ataxia telangiectasia mutated protein
ATP	Adenosine triphosphate
ATR	Ataxia telangiectasia and Rad3 related protein
ATRX	α-Thalassemia X-linked mental retardation
BACE1	Beta-site amyloid precursor protein–cleaving enzyme 1
BER	Base excision repair
BLM	Bloom
BMI1	B lymphoma Mo-MLV insertion region 1 homolog
BRCA1	Breast cancer type 1 susceptibility protein
CAF1	Chromatin assembly factor 1
CAT	Catalase
CBS	Cystathionine β-synthase
CBX	Chromobox protein
CDK	Cyclin dependent kinases
CDKN2A	Cyclin-dependent kinase inhibitor $p16^{INK4a}$

ChIP	Chromatin Immunoprecipitation
CHK1	Checkpoint protein 1
CHK2	Checkpoint protein 2
CNS	Central nervous system
CR	Caloric restriction
CS	Cockayne syndrome
DCR	Dicer protein
DDR	DNA damage response
DKC1	Dyskerin
DKC	Dyskeratosis congenital
DNA-PK	DNA-dependent protein kinase
DNMT	DNA methylase
DPP/TGF	Decapentaplegic/transforming growth factor-β
DSB	Double strand breaks
DsRNAs	Double strand RNAs
EMT	Epithelial–mesenchymal transition
EOAD	Early-onset Alzheimer's disease
ERCs	Extrachromosomal rDNA circles
ES cells	Embryonic stem cells
ETS	E-twenty six family
E(Z)	Enhancer of zeste
FA	Fanconi anemia
FOXO	Forkhead box
FXTAS	Fragile X-associated tremor/ataxia syndrome
(GG) NER	Global genome NER
GPx	Glutathione peroxidase
GSH	Glutathione
$H2A^{ub}$	Ubiquitylation of hisone 2A at lysine 117
H_2O_2	Hydrogen peroxide
$H3K9^{me3}$	Trimethylation of histone 3 at lysine 9
$H3K27^{me3}$	Trimethylation of histone 3 at lysine 27

HDAC	Histone deacetylase
HGPS	Hutchinson-Gilford progeria syndrome
HIRA	Histone repressor A
HMTases	Histone methyltransferases
HNE	4-Hydroxy-nonenal
HOX	Homeotic genes
HP1	Heterochromatin protein 1
HR	Homologous recombination
HSC	Hematopoietic stem cells
IAP	Interstitial A particles
ICF	Immunodeficiency, centromeric instability and facial anomalies
ICL	DNA inter-strand crosslink
IF	Immunofluorescence
IGF-1	Insulin-like growth factor 1
IHC	Immunohistochemistry
JARID-2	Jumonji AT-rich interaction domain 2
JMJD2A	Jumonji domain-containing protein 2A
JNK	c-Jun N-terminal Kinase
Kbp	Kilobase pair
Ku70	Lupus Ku autoantigen protein p70
LINE	Long interspersed nuclear element
LncRNA	Long non-coding RNA
LOAD	Late-onset Alzheimer's disease
LSC	Leukemic stem cells
LTP	Long term potentiation
LTR	Long terminal repeat
MATIIa	Methionine adenosyltransferase isozyme
MBD	Methyl–binding domain proteins
MBT	Malignant brain tumor domain
MCI	Mild cognitive impairment
MEC	Mammary epithelial cells

MeCP2	Methyl-CpG–binding protein 2
MEF	Mouse embryonic fibroblasts
MDM2	Mouse double minute 2
MRE11	Meiotic recombination 11 homolog
NAD	Nicotinamide adenine dinucleotide
NBS1	Nijmegen breakage syndrome associated protein 1
NER	Nucleotide excision repair
NF-κB	Nuclear factor kappa-light-chain-enhancer of activated B cells
NHEJ	Non-homologous end joining
NMDA	N-methyl-D-aspartate surface receptors
NoRC	Nucleolar remodeling complex
NSC	Neuronal stem cells
NuRD	Nucleosome remodeling and histone deacetylase complex
O_2	Oxygen singlet
O_2-	Superoxide anions
OH.	Hydroxyl radicals
PARP-1	Poly-ADP ribose polymerase 1
PAX3	Paired box protein 3
PC	Polycomb
PcG	Polycomb group
PCN1	Proliferating cell nuclear antigen
PDGF	Platelet derived growth factor
PEV	Position effect variegation
PGC-1α	Peroxisome proliferator receptor gamma coactivator 1-alpha
PH	Polyhomeotic
PHF	Paired helical filament structures
PHO	Pleihomeotic
PPARγ	Peroxisome proliferator activated receptor gamma
PRE	Polycomb response element
PSC	Posterior sex combs
PSEN	Presenilin

PUFAs	Polyunsaturated fatty acids
RAS	Rat sarcoma protein
RdRP	RNA-dependent RNA polymerase
RITS	RNA-induced transcriptional gene silencing complex
RNAi	RNA interference
RNA POL	RNA polymerase
RO.	Alkoxyl radicals
ROO.	Peroxyradicals
ROS	Reactive Oxygen Species
rRNA	Ribosomal RNA
RT-PCR	Real-time polymerase chain reaction
RYBP	Ring1 and YY1 binding protein
SAHFs	Senescence-associated heterochromatin foci
SAM	S-adenosyl-methyonine
SFMBT	Scm-related gene containing four MBT domains
SINE	Short interspersed nuclear element
Sir2	Silent information regulator 2
SiRNAs	Small interfering RNAs
SIRT	Silent mating type information regulator 2 homolog
SOD	Superoxide dismutase
Sp1	Specificity protein 1
SPOP	CULLIN3/Speckle-type POZ protein
SSB	Single strand break
SU(VAR)	Suppressor of variegation protein
SUZ12	Suppressor of zeste 12 homolog
(TC) NER	Transcription coupled NER
TERC	Telomerase RNA element
TERT	Telomerase reverse transcriptase
Tg	Transgenic
TIF	Telomere dysfunction induced foci
TOMM40	Translocase of outer mitochondrial membrane 40

TOR	Target of rapamycin
TORC	Target of rapamycin complex
TTD	CS-like brittle hair disorder trichothiodystrophy
Ubx	Ultrabithorax
UCP-1	Uncoupling protein 1
UV	Ultraviolet radiation
VNTR	Variable number of tandem repeats
WNT	Wingless
WRN	Werner gene
WS	Werner Syndrome
XFE	XPF-ERCC1 progeroid syndrome
YY1	Yin-Yang 1

To my daughter Naïad,

To my life companion Nathaniel,

To my family and my friends

Acknowledgments:

My deepest gratitude goes to my thesis director, Professor Gilbert Bernier, who has the attitude and the substance of a great mentor. He continually conveyed a spirit of mental and work support, competence, enthusiasm, and patience. Without his unlimited guidance and persistent help, this thesis would not have been possible.

I would like to express my sincere appreciation for Dr. Mohamed Abdouh and Dr. Nicolas Tetreault for their assistance in teaching me the technical tools and for their contribution in this study. I would like to thank as well my Ph.D committee members, Dr. Frédéric Charron and Dr. Stéphane Lefrancois, for their annual follow-up on my work and for their valuable advices.

Finally, I dedicate this work to my family and my friends for their unconditional affection and emotional support.

CHAPTER 1

Chapter 1 is a review of the literature and is divided into three main sections. In the first section, I describe the molecular mechanisms of the ageing process along with the numerous theories established so far to explain this phenomenon. Moreover, I emphasize on ageing related pathologies specifically Alzheimer's disease. The second section recapitulates the basic knowledge of chromatin formation and maintenance, highlighting the regulation of constitutive heterochromatin and its implication in genomic instability and neurodegeneration. In the third section, I introduce the Polycomb group complexes, which act as transcriptional repressors, and I will specifically describe the function of the Polycomb gene *Bmi1* in the brain.

CHAPTER 1

INTRODUCTION: SECTION 1

Ageing & Alzheimer's disease

1.1.1. Cellular and organismal ageing

Ageing is defined as the progressive degeneration of tissue function that ultimately leads to mortality. This functional decline can ensue from 1) impaired activity of post-mitotic cells or 2) from inability to replenish those dysfunctional cells due to failure of stem cells to sustain replication and cell divisions. Analyzing the ageing phenomenon first arose from evolutionary theories, dating back to Darwin and Wallace. Theorists aimed to understand why natural selection permits the global recession in health and fitness, the promoters of prolonged longevity [1]. Interestingly, Medawar in 1952 hypothesized that the driving force of natural selection decreases with age, due to exposure and submission of living organisms to extrinsic age-related causes of mortality. According to him, there is little or no advantage from guarding the germline from mutations that only confer damaging consequences at old stage [2]. Other elegant hypotheses have also been proposed, adjusting Medawar's original theory, including 1) the notion of antagonistic pleiotropy [3]. In this model, germline mutations that present beneficial effects in the early stage of life will be selected, even if they will confer detrimental effects later in life; as well as 2) the disposable soma theory, which describes ageing as an evolutionary exchange of resources between procreation and maintenance of somatic tissue [4,5]. Nonetheless, all these theories converge on the unique concept that, unlike many developmental processes, ageing is not a programmed phenomenon. The fact that ageing is a consequence of the decline with time in natural selection is significant when molecular notions of ageing are taken into consideration. It is important to determine if ageing pathways will be conserved among eukaryotes, if stochastic events will precipitate associated pathology and, whether the pathology related to ageing can be tracked back to the same original molecular causes in all cases [1].

Various studies have accrued to delineate ageing molecular pathways through analyses of invertebrate model organisms, mammals and mammalian cells in culture. Many different, yet intersecting mechanisms have been suggested such as reactive oxygen species (ROS) accumulation, caloric intake, growth signaling, telomere shortening, genomic instability, and heterochromatin loss.

1.1.1.1.ROS:

Considered as the most acclaimed theory of ageing, in 1950, Harman proposed that accumulation of reactive oxygen species highly contributes to organismal ageing [6]. Mitochondria are dynamic organelles that modulate nutrient usage to provide the cell with energy, even during dramatic changes in diet and development. These organelles are also, however, the main producers of toxic reactive oxygen species (ROS) within the cell [7]. ROS are intermediate oxygen metabolites with or without an unpaired electron, comprising superoxide anions (O_2-), hydroxyl radicals (OH.), alkoxyl radicals (RO.), peroxyradicals (ROO.), hydrogen peroxide (H_2O_2), and the oxygen singlet (O_2). Intrinsic oxygen radicals are the byproducts of incomplete oxygen reduction during normal mitochondrial respiration, generated by complexes I and III, glycerol 3-phosphate dehydrogenase, and alpha ketoglutarate dehydrogenase. Extrinsic ROS are caused by external sources such as ionizing radiation, pollutants, allergens, microbes, and drugs. Through a process called radiolysis ionizing radiation interacts with water, which comprises 60% of the human body, resulting in formation of damaging metabolites [8].
ROS, at low doses, function as second messengers in various physiological cascades involved in cell proliferation and differentiation, gene expression, and regulation of immune responses. For instance, Grune et al. demonstrated that 40 different genes are activated by H_2O_2 in mammalian cells. However, accumulation of free radicals promotes oxidative stress and is deleterious for cellular macromolecules, causing lipid peroxidation, cross-linked sulphur bridges in proteins, single and double DNA strand breaks, nucleic acid adducts such as 8-oxoguanine (8-OHG) and DNA cross-linking [9]. Cells possess several mechanisms to detoxify free radicals and prevent their oxidative damage. The antioxidant defense system includes endogenous enzymatic and non-enzymatic components such as superoxide dismutase (SOD), catalase (CAT), glutathione peroxidase (GPx), and glutathione (GSH), as well as exogenous antioxidants such as vitamin C, vitamin E, carotenoids, and polyphenols. Endogenous and exogenous antioxidants cooperate synergistically to preserve or re-establish redox homeostasis, for example during the regeneration of vitamin E by glutathione. Numerous studies have been carried out to either increase or decrease antioxidant activity and evaluate the effects on ageing. The conclusions, however, are highly equivocal with findings supporting

longevity associated either with increased activity or reduced activity, and other results supporting that neither increased nor reduced activity has effect on lifespan extension [10,11,12,13,14].

The central nervous system (CNS) is highly vulnerable to oxidative imbalance because it is enriched of polyunsaturated fatty acids (PUFAs) and has a high metabolic oxidative rate, but in contrast it possesses a relative paucity of antioxidant system compared with other organs. These observations corroborate further the key role of oxidative stress in the ageing phenomenon [15].

1.1.1.2 Calorie restriction/Sirtuins:

In 1935, McCay et al observed that caloric restriction (CR), a dietary regimen, in rats slows ageing and extends median and maximal lifespan [16]. Similar findings have been demonstrated in a variety of species including yeast, spiders, flies, fish, and mice [17,18]. Some observational studies also reported the impact of prolonged CR on health and longevity in humans. For example, Kagawa et al. documented the prevalence of centenarians on the island of Okinawa in Japan. School children in Okinawa consume 62% (i.e. 48% less) of the recommended intake of total energy in Japan. For adults, total protein and lipid intakes were similar, but energy consumption was 20% less than Japanese national average. Interestingly, the rates of mortality caused by cerebral vascular disease, malignancy, and heart disease were respectively 59%, 69%, and 59% in Okinawa, compared to those of the rest of Japan [19]. Lifespan extension by caloric restriction reflects an important deceleration of ageing emerged from evidence that restriction retards age-related changes in the properties of proliferative and non-proliferative cells in many tissues and various organ systems. Several theories have accrued to elaborate the mechanisms by which CR exerts its effect on longevity. An initial hypothesis suggested that delayed sexual maturation is a possible explanation, until it was proven that CR introduced in older animals also extends lifespan. Decreased metabolic rate is another potential mechanism, resulting in reduction of free radicals generation and altering insulin sensitivity [20]. It was also demonstrated that CR modifies

gene expression profiles; for instance in yeast, CR up-regulates *Sir2* activity, a member of the sirtuins gene family [21].

Abraham Lincoln once stated that God must have valued the common people because he created so many of them. Mother Nature must have felt the same way regarding the sirtuins, a large family of proteins that acquired enormous fame when *Sir2* (Silent information regulator 2) was shown to extend lifespan in multiple model organisms [22,23]. In yeast, *Sir2* promotes longevity by suppressing the generation of toxic extrachromosomal rDNA circles (ERCs) [24]. Moreover, an extra copy of the Sir2 gene increases replicative lifespan by 50%, whereas deleting *Sir2* shortens yeast lifespan [22]. The *Caenorhabditis elegans* homologue *Sir-2.1* also prolongs worm lifespan by binding to the worm forkhead protein DAF-16 [25]. Concomitantly in *Drosophila*, increased dosage of *Sir2* promotes longevity [23]. Even though, correlation between *Sir2* and longevity was well established, its enzymatic activity remained elusive for several years until 1999 when Tanny et al. solved the mystery and demonstrated that *Sir2* possess NAD-dependent ADP-ribosyltransferase activity [26]. Consequent studies revealed that *Sir2* mediates another catalytic reaction, NAD-dependent histone deacetylation. During deacetylation, sirtuins cleave NAD and produce the novel metabolites, 2' and 3'-*O*-acetyl-ADP-ribose, which are important regulators of physiology [27,28].

Mammals possess seven *Sir2* homologs (SIRT1–7) that bear a highly conserved NAD-dependent sirtuin core domain [29]. Mammalian sirtuins have various cellular locations, target numerous substrates, and affect a wide range of cellular functions. SIRT1, SIRT6, and SIRT7 are nuclear proteins with SIRT1 being the most extensively studied sirtuin to date [30]. SIRT1 mutant mice can survive into adulthood but demonstrate a severe phenotype including small size, delayed bone mineralization, defective skeletal closure, delayed eyelid opening, and sterility. SIRT1 protects the cell against oxidative stress and DNA damage [30]. Several physiological processes affected during ageing and altered by CR are regulated by SIRT1, which deacetylates a broad number of substrates such as p53, Ku70, NF-κB, and forkhead proteins [31,32,33]. SIRT1 deacetylates histones H1K26, H3K9, H3K14, and H4K16 as well as reduces the methylation of H3K79 [27,34]. SIRT1 also directs differentiation of muscle cells, adipogenesis, fat storage in white adipose

tissue, and metabolism in the liver, through regulation of nuclear receptor PPARγ and PGC-α hence linking SIRT1 with diets that promote longevity [30]. SIRT1 has also been described as a neuroprotective protein. Interestingly, CR guards against neurodegenerative pathology in mouse models for Alzheimer's and Parkinson's diseases [35,36]. SIRT1 induces survival in cultured neuronal cells and operates as an anti-apoptotic factor through downregulation of p53 and FOXO [37, 38]. β-amyloid-induced death of microglia is counteracted by overexpression of SIRT1 or by treatment with *Sir2*-activating polyphenol, resveratrol [39]. Overall, the above observations indicate that SIRT1 induction may be a novel strategy to treat neurodegenerative diseases.

SIRT6 is a nuclear protein widely expressed in mouse tissues. SIRT6 KO mice manifest premature ageing symptoms including loss of subcutaneous fat and decreased bone density. $SIRT6^{-/-}$ mice die within 4 weeks after birth and exhibit a deficiency in one specific form of DNA repair, the base excision repair (BER). $SIRT6^{-/-}$ MEFs show impaired proliferation, enhanced sensitivity to DNA damaging agents, genomic instability in the form of chromosomal translocations, and detached fragmented centromeres [40].

SIRT3 protein is localized at mitochondria, which is particularly enthralling because mitochondrial dysfunction is highly associated with mammalian ageing and with various diseases including neurodegenerative disorders and cancer. Lifespan analysis of animals with different SIRT3 dosage levels has not yet been achieved; however, there is growing indication associating mitochondrial sirtuins with energy usage and human lifespan. For instance, human population studies revealed that polymorphisms within the SIRT3 gene are linked to longevity. The G477T transversion, which do not change the amino acid sequence, promotes survivorship of elderly males and may imply a haplotype contributing to longevity [41]. The same authors also reported that different number of tandem repeats (VNTR) enhancer within SIRT3 gene correlates with increased lifespan (i.e. >90 yr) [42]. In brown adipose tissue of obese mice, overexpression of SIRT3 triggered upregulation of the uncoupling protein UCP1 in the mitochondrial inner membrane, which led to decreased energy expenditure and reduced oxidative stress. These observations suggest that SIRT3 may modulate longevity and raise the importance of performing lifespan experiments in mice that overexpress or lack SIRT3.

In conclusion, sirtuins have emerged as key anti-ageing genes in several model organisms (Figure 1). The NAD-dependence of these enzymes links them unavoidably to the metabolic activity of cells. In various models, sirtuins have been demonstrated to be regulated by and to mediate the effects of the dietary regimen CR. Moreover, mammalian sirtuins have been implicated in stress resistance and numerous metabolic pathways, including adipogenesis, gluconeogenesis, and insulin and glucose homeostasis. While it may be years before we know whether sirtuins regulate mammalian lifespan, current data suggests that these proteins are regulated by diet and in turn, regulate multiple facets of physiology, making them interesting therapeutic targets for metabolic and neurodegenerative diseases.

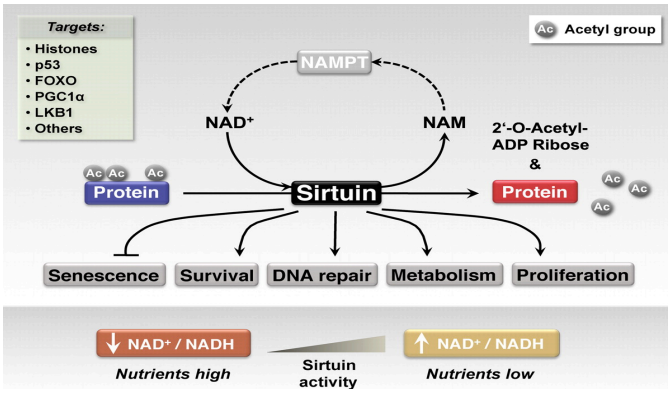

Figure 1: Sirtuins are NAD^+-dependent deacetylases that target histones and other non-histone substrates to regulate a wide range of cellular functions including cellular senescence, survival, DNA repair, metabolism, and cell cycle progression. The multi-facets of sirtuins function earn them the title of key anti-ageing genes. Adapted from Oellerich M.F. and Potente M. (2012) *Circulation Research* 110; 1238-1251.

1.1.1.3 Growth/Target of Rapamycin (TOR) signaling:

At first glance, ageing and growth are considered as mutually exclusive opposite events. Growth is described as synthesis of macromolecules from simple nutrients sustained by energy intake, and hence as increase of order and decrease of entropy. Ageing is synonymous to decay, meaning loss of order and greater entropy. However, interesting studies demonstrated that this rationale is erroneous and showed that reduced growth also decelerates the ageing process and prolongs lifespan. For instance caloric

restriction, as described in the paragraph above, inhibits growth and promotes longevity in various species from yeast to mice [43]. Rapamycin, an inhibitor of growth in yeast, decreases yeast aging. Repression of the growth-promoting insulin/IGF-1 signaling pathway extends lifespan, from worms to rodents. Therefore, growth and ageing are not antagonists but rather are complements of one another, determined by the same molecular pathway. In other words, excessive growth contributes to ageing and the molecular mechanism that drives both growth and ageing is the evolutionarily conserved TOR (target of rapamycin) pathway [43, 44].

TOR, as its name suggests, was originally identified in yeast as the target of the antifungal drug rapamycin, which is a natural secondary metabolite generated by soil bacteria to impede growth of fungal competitors. Interestingly, TOR is conserved structurally and functionally from yeast to human as crucial regulator of growth and metabolism [44]. In mammals, TOR (mTOR) modulates cell growth depending on nutrients (e.g., amino acids), growth factors (e.g., insulin, IGF-1), and cellular energy level (ATP) [45]. TOR activates anabolic processes such as transcription, translation, ribosome biogenesis, nutrient transport, as well as mitochondrial metabolism and in contrast inhibits catabolic activities such as mRNA degradation, ubiquitin-dependent proteolysis, and autophagy. TOR is an atypical serine/threonine kinase present in two functionally and structurally different multiprotein complexes: the rapamycin sensitive TORC1 and the rapamycin insensitive TORC2. mTORC1 regulates translation through phosphorylation of S6K and 4E-BP1; mTORC2 controls cell survival via phosphorylation of Akt/PKB [44, 45, 46, 47, 48].

Budding yeast *S. cerevisiae* is a particularly convenient system for ageing analysis since 1) it can be used to examine both replicative ageing (measured by the number of cell divisions) as well as chronological ageing (determined by the length of time a post-mitotic cell can survive); and 2) because of yeast's unicellularity where the cell is actually the organism and therefore it is a model for cell ageing and organismal longevity [49,50]. Inactivation of TORC1 signaling in yeast prolongs both replicative and chronological lifespan indicating that TOR engenders the ageing process regardless of physiological context (mitotic or post-mitotic cells). TOR also modulates longevity in multicellular organisms. Vellai et al. demonstrated that knocking down TOR in *C. elegans* doubles

maximal lifespan [51]. Subsequently Jia et al. observed that worms deficient in raptor, a TORC1-specific subunit, also presented extended lifespan [52]. In *Drosophila*, TOR is essential during larval development and genetic inhibition of TOR pathway prolongs lifespan. Remarkably, the lifespan extension is detected upon down regulation of TOR signaling in the fat body, underlining the role of fat in ageing. Furthermore, inhibition of TOR signaling in the fat body not only lengthens the life of the fly but also decreases the size of the entire organism associating again growth and ageing [53,54,55,56]. In mice, reduced insulin/IGF-1 signaling in adipose tissue deactivates downstream mTOR pathway and increases lifespan. Moreover, IGF-1 deficiency promotes lifespan extension in rodents. Similarly, downregulation of mTORC1 or mTORC1 effector S6K prevents age-and-diet induced obesity in mice [57, 58].

Numerous studies indicate that TORC1 regulates ageing through its downstream mechanisms such as autophagy, ribosome biogenesis, protein synthesis, transcription, and mitochondrial activity. TORC1 inhibits autophagy, which is defined by bulk degradation of proteins and organelles in lysosomes; autophagy is highly reduced in aging and age-related diseases. Additionally, autophagy is required for lifespan extension in worms. These observations indicate that TORC1 favors the ageing phenomenon in part via inhibition of autophagy [59,60,61,62].

TORC1 positively regulates ribosome and protein synthesis. Recent evidence showed that reduced ribosome biogenesis and repressed translation prolongs lifespan. Indeed, downregulation of ribosomal proteins and translation initiation factors promotes longevity in both yeast and worms. Therefore, TORC1 may drive the ageing process via activation of ribosome biogenesis and protein synthesis [63,64].

The nicotinamidase gene *PCN1* is associated with longevity and is transcriptionally activated upon TOR inhibition. Remarkably, nicotinamidase converts nicotinamide to NAD^+ that ultimately activates *Sir2* denoting that TOR and sirtuins are part of the same longevity pathway [65,66]. Accumulation of aggregation-prone proteins is a neurodegenerative feature. Studies revealed that TOR engenders neurodegeneration in a *Drosophila* tauopathy model and that it is implicated in Alzheimer's disease by initiating Tau protein synthesis [67,68]. In contrast, rapamycin increases clearance of pathologic proteins reducing their neurotoxicity [69].

Cell growth and division are the basic essential features of life. However, the growth-regulating TOR signaling pathway appears to also bear the seeds of death. Ageing and its pathological manifestations present excessive growth-driven signaling when growth is no longer attainable. Therefore, ageing may be considered as prolongation of the same process that modulates developmental growth.

1.1.1.4 Senescence:

In 1961, Hayflick and Moorfield were first to describe cellular senescence through their observation that cultured normal human fibroblasts had limited ability to replicate and proliferate, becoming eventually permanently arrested [70]. This finding spawned two interesting hypotheses: 1) since cultured cancer cells proliferate indefinitely, cellular senescence is a mechanism to prevent cancer formation and hence acts as tumor suppressive process; 2) tissue renewal and repair degenerate with age and therefore cellular senescence was anticipated to recapitulate the ageing of cells. Studies have ultimately demonstrated that these two hypotheses coalesced and brought new insights into the fields of cancer and ageing [71,72].

Hallmarks of cellular senescence consist of cell cycle arrest that occurs mostly in G1 phase, up-regulation of cell cycle inhibitors mainly p21 and p16, silencing of E2F target genes by chromatin reorganization into discrete foci called senescence associated heterochromatin foci (SAHFs), induced expression of secretory proteins that alter the tissue microenvironment, apoptotic resistance, active metabolism, and enlarged morphology [72,73,74]. Cells undergo senescence in response to 1) dysfunctional telomeres and other genotoxic stresses that ultimately induce a DNA damage response mediated by the tumor suppressor protein p53; or due to 2) up-regulation of $p16^{INK4A}$-pRb tumor suppressor pathway [75,76,77,78].

Telomere shortening:

Barbara McClintock and Herman Muller were the first investigators to demonstrate that chromosome ends consist of special structures required for chromosome stability [79,80]. Muller described these structures as *telomere* from the Greek for “end” *telos* and “part” *meros*. Telomeres are simple tandem non-coding DNA repeats (5’-TTAGGG-3’/5’-

CCCTAA-3') ending with single strand G-rich overhangs that fold into 3-dimensional structures termed "T-loops", ensuring perfect capping of the chromosome termini [81]. Standard DNA polymerases cannot replicate the entire DNA ends, a process called the "end-replication problem". Therefore, cells lose approximately 50 base pairs of telomeric DNA during each S phase, a phenomenon termed as telomere shortening [82]. Critically short telomeres are dysfunctional and only few such telomeres are sufficient to initiate a full senescence response in the affected cell [83,84].

Dysfunctional telomeres activate a DNA damage response (DDR) similar to that elicited by double strand breaks (DSB), leading to p53 up-regulation, p21 expression, and cellular senescence. DDR enables cells to sense the damage and to respond by arresting cell cycle progression and initiating repair if possible. DDR consists of nuclear foci containing the phosphorylated form of the histone variant H2AX, which co-localize with activated kinases such as ataxia telangiectasia mutated (ATM) and checkpoint-2 (CHK2) [85,86,87]. Such foci when physically present at telomeres are referred to as telomere dysfunction induced foci (TIF) [88,89]. Occurrence of TIF increases in dermal fibroblasts of aged primates [90].

Telomere attrition can also be accelerated by suppression of telomerase expression. Telomerase is an enzyme required to circumvent telomere shortening and promotes *de novo* synthesis of telomeres by extending the 3′ end of chromosomes through addition of TTAGGG repeats. The human core enzyme consists of 3 essential components: the telomerase RNA element (*hTERC*) serving as template for telomere sequence synthesis, the telomerase reverse transcriptase (*hTERT*) bearing the catalytic subunit activity, and the ribonucleoprotein dyskerin (*DKC1*) ensuring proper folding and stability of telomerase RNA [91,92,93,94,95]. In adult humans, telomerase remains only expressed in germ cells as well as certain stem cells and its expression is regulated at transcriptional level, alternative splicing, assembly, subcellular localization, and posttranslational modifications. Analyses of model organisms and studies on patients with telomerase mutations have revealed that short telomeres engender dire consequences. Though the phenotypes are quite different, all comprise some forms of age-associated pathology, premature ageing and early death [96]. Mice carrying homozygous deletion of the RNA

component *mTerc*-/- or of the catalytic subunit *mTert-/-* manifest progeroid phenotype, specifically affecting organ systems with high rate of cell turnover. Genetic mutations in *hTERC* were identified in patients with dyskeratosis congenita (DKC). Affected individuals present short stature, suffer from hypogonadism and infertility, have defects in the skin and in the hematopoietic system, and eventually die of bone marrow failure [97,98,99]. Mutations in *hTERT* have been correlated to several forms of anemia and idiopathic pulmonary fibrosis, which is an adult-onset lethal disease of progressive lung scarring, followed by respiratory failure [100,101]. Human segmental progeroid syndromes such as Werner's syndrome (WS) and Hutchinson-Gilford progeria syndrome (HGPS) gave important insights to cellular senescence, and cells from such patients present greatly reduced in vitro lifespans [102, 103]. Although the genetic defects in WS and HGPS are quite distinct, the observed accelerated cellular senescence was found to be associated with increased rates of telomere shortening [96,103,104]. A significant number of age-associated pathologies, such as cardiovascular disease, osteoarthritis, diabetes and Alzheimer's disease have also been correlated with telomere shortening [104,105,106,107]. Moreover, individuals with short telomeres had a 3.18 fold higher mortality rate from heart diseases, and 8.54 higher mortality rate from infectious diseases, compared to those with relatively long telomeres [96].

It is generally accepted that telomere attrition with age, which compromises the replicative lifespan of somatic cells in normal individuals, poses a barrier for the growth of aspiring malignant cells and hence operates as tumor suppressor mechanism; however, as a downside, it contributes to the collapse of cellular function and impaired organ maintenance. The intricate connection of telomere in both ageing and cancer ensures that pathways involving telomeres and telomerase will stay subject to intensive studies for many years to come. Understanding these pathways will help identify molecular targets for future therapies aiming to improve organ maintenance, tissue regeneration, and health in the growing population of the elderly.

Upregulation of the CDKN2A gene (cyclin-dependent kinase inhibitor $p16^{INK4a}$)

p16 inactivates cyclin dependent kinases CDK4 and CDK6 maintaining the

retinoblastoma protein (pRB) in its active hypophosphorylated form and consequently blocking cell cycle progression in G1 [108]. The expression of p16 is triggered by a wide variety of stresses such as oncogene activation as well as DDR signals and has been therefore stated as potent biomarker of senescence [109,110,111,112]. The p16 pathway is crucial for generating SAHFs to silence the genes required for replication and proliferation. SAHFs necessitate several days to form and implicate transient interactions among chromatin-modifying proteins such as HIRA (histone repressor A), ASF1a (anti-silencing function-1a) and HP1. Eventually, each SAHF includes portions of a single condensed chromosome, which is depleted for the linker histone H1 and enriched for HP1 and the histone variant macroH2A [71]. Although SAHFs are not found in all senescent cells, the p16–pRB pathway might establish chromatin conformations that are functionally equivalent to SAHFs in cells that do not develop these structures [71,74].

p16 expression is triggered by oncogenic RAS through activation of ETS transcription factors and is downregulated by the members of the polycomb family of repressors BMI1 and CBX7 [113,114,115,116,117]. The regulation of p16 is particularly important in the age-related decline of stem and progenitor cells. Several studies demonstrated that the induction of p16 correlated with the *in vivo* senescence of hematopoietic stem cells [118,119,120]. In parallel, Bmi1 deficient mice displayed a striking loss of hematopoietic cells and cerebellar neurons, which were correlated with p16 overexpression as well as replicative failure of stem cells [120,121,122]. In contrast, increased regenerative ability was found in bone marrow, pancreatic islets and forebrain of mice lacking p16 [123,124,125]. These observations underline the notion that age-associated upregulation of p16 restricts self-renewal and disturbs tissue homeostasis as well as associate p16-dependent senescence in three hallmarks of ageing: decrements in neurogenesis, haematopoiesis and pancreatic function. Another interesting association between cellular senescence and ageing was provided by studies of mice lacking the p53-related gene p63 [126]. Mutant animals displayed enhanced p16 expression, impaired stem cell renewal, widespread senescence, and accelerated ageing [127]. In humans, p16 overexpression was detected in ageing skin and kidneys [128,129]. Furthermore, upregulation of p16 has been observed in senescent human cardiomyocytes and hence has been proposed as

contributor to myocardial ageing [130,131,132].

In conclusion, cellular senescence is one of several factors that influence or may promote ageing and in order to establish a direct cause-effect relationship between cellular senescence and ageing, *in vivo* deceleration of cellular senescence rates is required along with concomitant demonstration of increased maximum lifespan.

1.1.1.5 DNA damage/repair:

Within the intricate cellular machinery, biomolecules (proteins, lipids and nucleic acids) are exposed to damaging reactions e.g. hydrolysis which may contribute ultimately for ageing. However impairment of certain macromolecules may be more detrimental for the cell than damage to other constituents [133]. Severe accelerated ageing phenotype was observed in a battery of human syndromes and in mice with genetic defects in DNA metabolism, denoting that genomic damage is a main culprit in the ageing process. In general, all biomolecules are renewable except for nuclear DNA, which is the irreplaceable blueprint for RNA and protein coding information. Normal cellular function depends on the integrity of the genome that must be conserved during the entire organism's lifetime and must be faithfully transmitted. Any acquired mutation in coding regions of DNA that was not properly repaired will trigger abnormal protein expression or function; moreover, chromosomal translocations or rearrangements induce apoptosis or senescence [134]. In order to preserve its genetic information, the cell developed complex maintenance network including numerous sophisticated systems to repair nuclear and mitochondrial DNA damage, checkpoint and effector machineries that allow cell survival or initiate senescence/cell death when DNA is severely impaired, as well as processes that guard the epigenetic code [135,136,137]. DNA damage is not only triggered by exogenous sources such as UV, ionizing radiation, and various chemicals but also by enemies from within the cell such as reactive oxygen species [138]. DNA lesions are greatly diverse and the immense size of the mammalian genome makes it more injury-prone, aggravating further the DNA problem. Some lesions are 1) mainly mutagenic promoting cancer formation; or 2) primarily cytotoxic initiating cell death or senescence and causing degenerative manifestations associated with ageing. Cytotoxic lesions are hard to repair and include double-strand breaks (DSBs) triggered by radiation

or ROS as well as inter-strand crosslinks induced by chemical agents such as cisplatin [139,140]. Apart from the sort of damage, the frequency of lesions and their position in the genome also affect the outcome. Despite the effort of the genome maintenance network in counteracting the wide range of potential threats, it cannot manage all the insults inflicted on the genome which will lead to gradual accumulation of DNA damage and eventually cellular malfunctioning, loss of organismal homeostasis, and ageing [141].

Consistent with the role of DNA damage in ageing, various DNA repair pathways have also been associated to the ageing process. Studies of mouse mutants deficient in DNA repair mechanisms have revealed premature appearance of various symptoms of ageing indistinguishable from the same phenotypes normally occurring much later in life. Also, rare progeroid human disorders were correlated with genetic defects in DNA repair response systems [142,143,144,145]. The cell ensures the removal of damaged bases and the repair of the resulting single stranded (ss) DNA lesions via the nucleotide excision repair (NER) mechanism. On the other hand, the repair of DSBs is mediated by non-homologous end joining (NHEJ) or by homologous recombination (HR). NER pathway represents a multi-step 'detect-excise-and-patch' repair system and is further divided into global genome (GG) NER and transcription coupled (TC) NER. Defects in TC-NER induce cell death, resulting from lesions that stall the RNA polymerase II, and underlie a variety of human progeroid disorders including Cockayne syndrome (CS) as well as CS-like brittle hair disorder trichothiodystrophy (TTD). Both conditions along with their associated mouse models show many symptoms of premature ageing, including progressive neurodevelopmental delay, cachexia, kyphosis, retinal degeneration and deafness. XFE is another progeroid syndrome caused by a defect in XPF-ERCC1, an endonuclease required for NER as well as for DNA inter-strand crosslink (ICL) repair. ICLs covalently link both strands of DNA, preventing transcription and replication, and hence are extremely cytotoxic. Failing defense against such spontaneous lesions triggers cell death and senescence, culminating in accelerated ageing, as observed in both Ercc1 and Xpf mouse mutants and the human XFE [146,147,148]. Ataxia telangiectasia is an autosomal recessive disorder characterized by the development of progressive cerebellar degeneration, skin abnormalities (telangiectasia, atrophy, pigmentary abnormalities and

hair greying), immunodeficiency and a wide range of malignant neoplasms. The disease is caused by various mutations in the *ATM* gene, which plays an essential role in DNA damage signaling, DNA repair and telomere maintenance. Fanconi anemia (FA) is an autosomal recessive disease resulting from mutations in Fanconi genes (encoding any of 12 Fanconi anemia complementation group proteins). These proteins are required for DNA damage and repair pathways. The disorder is coupled with accelerated telomere shortening, and abnormalities in telomere replication or repair are thought to play a role in the pathogenesis, specifically in the progression of the disease to immunodeficiency and bone marrow failure. Other "progeroid" genes that have been implicated in DNA replication and repair are the family of genes encoding the RecQ DNA helicases. One of the functions of these proteins is to aid in the resolution and repair of broken or stalled replication forks. Helicases that could be involved include RecQ protein-like 2 (RecQL2), RecQL3, and RecQL4 with known mutations that give rise to Werner (WRN), Bloom (BLM), and Rothmund Thompson syndromes, respectively [148].

Evidently, impairments in distinct DNA repair systems for cytotoxic lesions account for a bewildering but specific range of age-related pathologies, which may also explain the different segmental nature of progerias. It remains to know the sequence of events leading from DNA damage repair to the activation of longevity assurance pathways. It is likely that there are other protective mechanisms that can help postpone ageing. These include reduced production of metabolic byproducts through regulation of metabolism and oxidative phosphorylation, as well as improved anti-oxidant/detoxification defenses, which reduce the DNA damage load and its noxious effects. In addition, improved overall repair are predicted to extend lifespan next to other mechanisms, including epigenetic modifications and protein metabolism.

1.1.1.6 Heterochromatin loss:

In eukaryotes, the genomic DNA is organized in highly ordered chromatin structures. Chromatin is formed of nucleosomes, which are 146-7 base pairs of DNA wrapped around an octamer of four major core histone dimers H2A, H2B, H3, and H4 [149,150]. Designated as nuclear architecture, chromatin is organized into two

structurally distinct domains: 1) Euchromatin refers to open loose conformation where nucleosomes are distant, is rich in gene concentration, and is transcriptionally active. 2) Heterochromatin indicates closed condensed conformation where nucleosomes are tightly packed and is inaccessible for transcription factors. Trimethylation of histone H3 at lysine 9 ($H3K9^{me3}$) and recruitment of chromodomain proteins such as heterochromatin protein 1 (HP1) are hallmarks of heterochromatin assembly and maintenance. Heterochromatin is additionally subdivided into two compartments: 1) the constitutive heterochromatin, which includes large portions of noncoding repetitive DNA elements (centromeric, pericentromeric, telomeric, and intergenic regions), is localized to nuclear periphery and is transcriptionally impeded in all cell types; whereas 2) the facultative heterochromatin contains E2F target genes, regulates X chromosome inactivation, is present anywhere in the nucleus, and is formed in certain subset of cells [151,152,153,154]. The notion that long-term maintenance of nuclear architecture is required to enable permanent normal functioning of cells and tissues has reinvigorated interest in studying the association between chromatin malformations and the ageing process. Villeponteau was first to put forth the loss of heterochromatin model of ageing and proposed that heterochromatin domains formed in embryogenesis are disrupted with advancing age, leading to de-repression of silenced DNA and aberrant expression patterns [155]. The detrimental effect of abnormal heterochromatin formation is demonstrated in the Hutchinson-Gilford progeria syndrome (HGPS), which is an autosomal dominant disorder caused by gain-of-function mutation in the LMNA gene encoding for lamin A/C [101]. HGPS patients manifest premature ageing aspects including extreme short stature, aged facial features, alopecia, lipodystrophy, scleroderma, osteolysis as well as atherosclerosis and they pass away usually at the age of 12 years as a consequence of myocardial infarction or stroke [156]. Cells extracted from HGPS patients exhibit abnormal nuclear architecture characterized by reduced presence of $H3K9^{me3}$ and HP1 markers at the constitutive heterochromatin leading to de-repression of pericentric satellite III repeats [157]. Misteli et al. further delineated the mechanism of heterochromatin loss observed in HGPS patients and demonstrated that defects in the NURD chromatin remodeling complex associated with reduced HDAC1 activity are key modulators of premature ageing [158]. As mentioned earlier, Werner syndrome (WS) is a rare progeroid autosomal recessive

disorder caused by loss of function mutations in the WRN gene encoding a member of the RecQ helicase family implicated in DNA repair, DNA recombination, and telomere maintenance [159]. WS patients develop normally until puberty, at which time they stop growing and start displaying multiple progressive premature ageing pathologies including hair graying, pattern baldness, skin atrophy, senile bilateral cataracts, type 2 diabetes, hypogonadism, osteoporosis, and atherosclerosis. Patients present a significantly decreased life expectancy and death occurs at an average age of 47 usually as a result of cancer or myocardial infarction. WS cells express a dysfunctional RecQ helicase activity initiating hyper-recombination, chromosomal aberrations, and hence genomic instability especially at repetitive loci of constitutive heterochromatin [160]. This finding indicates that the accelerated ageing observed in WS patients stem from inefficient repression of deleterious recombination events and global genomic instability at constitutive heterochromatin. Several reports on different organisms further validated the association between loss of heterochromatin and ageing. In *C.elegans*, peripheral heterochromatin was disrupted in aged cells [161]. Progressive loss of heterochromatin correlated with advancing age in *Drosophila* and lamin proteins were shown to influence the impaired nuclear morphology and decreased lifespan [162,163]. Moreover, loss-of-function HP1 mutant flies manifest shortened lifespan however overexpression of HP1 in *Drosophila* extends lifespan and reduces the breakdown of muscle integrity that is characteristic of old animals [164]. Moreover, inhibiting the activity of Jumonji domain-containing protein 2A (JMJD2A), a histone demethylase that catalyzes demethylation of histone H3 at lysine 9, significantly extended the lifespan of *Drosophila* [165]. In humans, aged skin fibroblasts exhibited nuclear defects similar to those seen in HGPS cells involving histone modifications and increased DNA damage [166]. Age related loss of heterochromatic epigenetic silencing was actually described 20 years ago. Indeed, the major satellite repeats that constitute the pericentromeric heterochromatic domains were found to be overexpressed in old cardiac tissue, suggesting a gradual loss of silencing of these elements [167]. One mechanistic explanation to that phenomenon was proposed by Haider et al. who reported that aged individuals display impaired activity in their histone modifying enzymes engendering decondensation of perinuclear constitutive heterochromatin [168].

As stated earlier, ageing is also linked to increased formation of senescence associated heterochromatin foci, which occur however in facultative heterochromatin to silence specific genes. SAHFs are formed in sequential manner consisting of chromosomes decondensation, followed by H3K9 methylation, and binding of HP1 proteins. Therefore, ageing is associated with global decrease in constitutive heterochromatin levels but accompanied with increase of heterochromatin formation at specific gene loci i.e facultative heterochromatin. This phenomenon is defined as heterochromatin redistribution [169] (Figure 2). Another example underlining heterochromatin redistribution is the finding that DNA methylation, which is required for heterochromatin formation, gets depleted globally with advancing age specifically at constitutively heterochromatic repetitive DNA segments, but becomes enriched at gene specific loci involved in cancer and senescence. Redistribution of DNA methylation has been ascribed to the differential regulation of the DNA methyltransferases: Dnmt1, which maintains DNA methylation patterns and Dnmt3, which is a *de novo* DNA methyltransferase. Reports revealed that in ageing, expression and activity of Dnmt1 decreases concomitantly with upregulation of Dnmt3 [170,171,172,173,174,175].

In conclusion, these findings suggest that loss of global heterochromatin model for ageing is described as net reduction in constitutive heterochromatin and redistribution of heterochromatin markers ($H3K9^{me3}$ and HP1) for facultative heterochromatin, ultimately leading to altered transcriptional patterns associated with ageing. As stated before, understanding the complex molecular interactions related to ageing engendered multiple ageing models including ROS insult, genomic instability, programmed senescence, telomere shortening, calorie intake and growth signaling. All of these models can be unified with heterochromatin disruption as the overarching theme. Persistent activation of DNA damage response instigates alterations in chromatin organization and nuclear architecture, eventually promoting the inexorable changes associated with ageing.

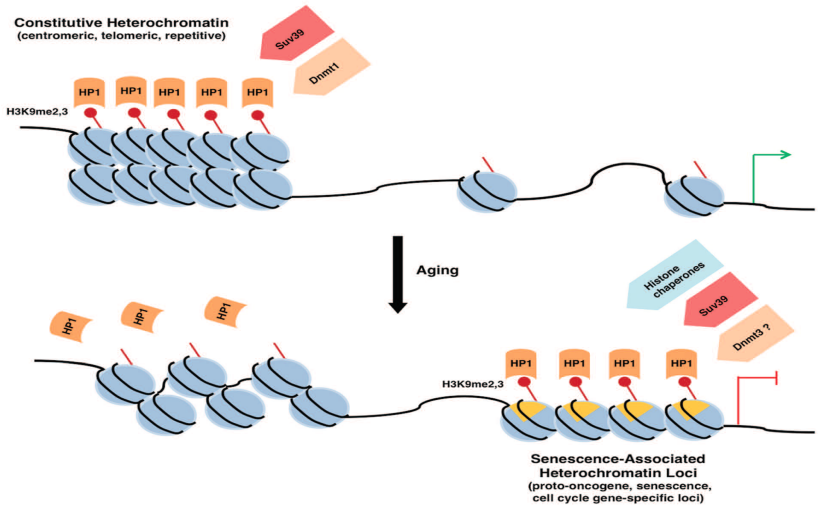

Figure 2: Heterochromatin redistribution during ageing, characterized by loss of constitutive heterochromatin demonstrated by decreased H3K9 methylation and delocalization of HP1. Conversely, facultative heterochromatin formation increases at specific loci, particularly at senescence-associated heterochromatin foci (SAHFs). Adapted from Tsurumi A and Li X.W. (2012) *Epigenetics* 7:7, 680-688.

1.1.2. Alzheimer's disease

Alzheimer's disease (AD), which was nearly anonymous to the public a generation ago, currently represents an enormous concern at individual level and is an imminent catastrophe for society. Greater than 35 million people worldwide are affected with Alzheimer's disease, a neurodegenerative protean disorder characterized by gradual progression from episodic memory problems to global decline of cognitive functions and learning skills, ultimately leading to death within 3 to 9 years after diagnosis. Sadly, patients affected with AD quickly learn that there is yet no efficient disease modifying treatment and that they are destined to experience the dire consequences. Nevertheless, scientific research is constantly attempting to vary this bleak situation [176].

1.1.2.1.Forms of AD:

There are two main forms of Alzheimer 's disease:

Familial early-onset AD (EOAD)

EOAD accounts for less than 5% of all AD patients and affects individuals under 65

years of age. This early-onset autosomal dominant form of AD is triggered by mutations in three genes (amyloid precursor protein (*APP*), presenilin 1 (*PSEN1*) and presenilin 2 (*PSEN2*)) as well as by duplication of the *APP* gene. From therapeutic perspective, targeting solely the pathological mechanisms inducing familial early-onset AD makes the implicit assumption that this form is fundamentally identical to the common sporadic late-onset form [177,178].

Sporadic late-onset AD (LOAD)

LOAD symptoms appear in people of 65 year-old and over, accounting for 95% of AD cases. The genetics of the more common form of AD are not yet elucidated and are presently subject to active investigation. The only genetic variant that has been identified as a risk factor for LOAD is the ε4 allele of the apolipoprotein E (*APOE*) gene, however even after a decade from the discovery of its role in AD progression, no consensus mechanism of pathogenesis has yet emerged [179]. The primary risk factor of LOAD is advancing age with incidence doubling every 5 years after 65 years of age. Additional potential risk genes identified by gene-expression profiling and whole-genome association studies include the Aβ chaperone clusterin, the mitochondrial transporter TOMM40, and the Sortillin-related receptor that functions to partition amyloid precursor protein away from β-secretase and γ-secretase. However, their underlying mechanisms are various, and whether any of these factors promote amyloid accumulation and tauopathy in humans is yet unknown [180,181,182,183].

1.1.2.2. AD hallmarks:

Several molecular lesions have been detected in AD patients but the overarching hallmarks are accumulation of misfolded proteins in the brain including amyloid plaques and neurofibrillary tangles, synaptic dysfunction, oxidative damage, and energy failure.

β-Amyloid

Cerebral plaques are loaded with β-amyloid peptides (Aβ), which are metabolites of 36 to 43 amino acids. Aβ40 peptides are much more predominant than the aggregation-prone and toxic Aβ42 monomers. β-amyloid peptides are produced from proteolysis of the amyloid precursor protein (*APP*) performed by the consecutive actions of the β-secretase beta-site amyloid precursor protein–cleaving enzyme 1 (*BACE-1*) and the γ-secretase presenilin 1(*PSEN1*) (Figure 3). The “amyloid hypothesis” of AD states that imbalance

between production, clearance, and aggregation of Aβ peptides promotes their aggregation and therefore initiates Alzheimer's disease. Aβ monomers possess natural self-aggregation potential and coexist in multiple physical forms. Primitive form comprises soluble oligomers of 2 to 6 peptides that coalesce into intermediate assemblies, and then arrange themselves into fibrils and eventually β-pleated sheets to establish the insoluble fibers of advanced amyloid plaques. Soluble oligomers and intermediate assemblies were demonstrated to be the most neurotoxic forms of Aβ, disrupting synaptic function. Moreover, the severity of cognitive impairment in AD patients correlated with high levels of oligomers in the brain and not with total Aβ burden [184,185,186,187,188,189,190].

In normal physiological levels, Aβ functions at the synaptic junction to dampen excitatory transmission and prevent neuronal hyperactivity. Maintaining steady-state levels of Aβ levels depends on the proteases neprilysin and insulin-degrading enzyme. Neprilysin is a zinc endopeptidase that degrades Aβ monomers and oligomers, however reduced expression of this protease triggers accumulation of cerebral Aβ. Insulin-degrading enzyme is a thiol metalloendopeptidase that cleaves small peptides including insulin and monomeric Aβ. Mice lacking insulin-degrading enzyme present 50% reduction in Aβ processing. Conversely, upregulation of neprilysin or insulin-degrading enzyme counteracts plaque accumulation [191,192].

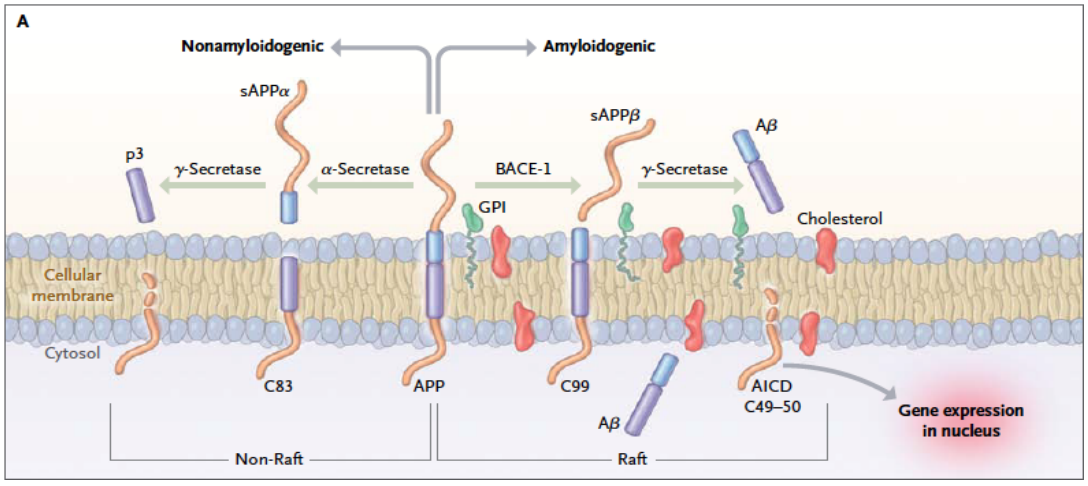

Figure 3: Processing of APP. Cleavage by α-secretase initiates nonamyloidogenic processing releasing a large amyloid precursor protein (sAPPα) ectodomain and an 83-

residue carboxy-terminal fragment. C83 is subsequently digested by γ-secretase, liberating extracellular p3 and the amyloid intracellular domain (AICD). Amyloidogenic processing is started by β-secretase beta-site amyloid precursor protein–cleaving enzyme 1 (BACE-1), releasing a shortened sAPPα. The remained C99 is also a γ-secretase substrate, generating Aβ and AICD. Soluble Aβ is prone to aggregation. Adapted from Querfurth H. and LaFerla F. *Alzheimer's disease*, NEJM 2010; 362:328-44.

Tau tangles

Neurofibrillary tangles are filamentous inclusions present in neurons of AD patients and comprise abnormally hyperphosphorylated and aggregated form of tau [193] (Figure 4). Tau is a soluble microtubule binding protein that is highly abundant in axons and is essential for stabilizing neuron's cytoskeleton as well as vesicle transport. Conversely hyperphosphorylated tau is insoluble, disintegrated from microtubules, and self-aggregated into paired helical filament structures (PHF) [194]. Activation of several kinases such as stress activated JNK kinase induces tau phosphorylation [195].

Similarly to Aβ oligomers, intermediate assemblies of hyperphosphorylated tau are the neurotoxic forms, impairing axonal transport and cognitive function. It was proposed that formation of insoluble helical filaments is a protective process through the sequestration of toxic intermediate tau species [196,197]. Several mutations in the *Tau* gene have been identified in patients with frontotemporal dementia, another neurodegenerative disorder. However, no *Tau* mutations have been detected in AD patients and the degree of neuron loss is out of proportion to the amount of neurofibrillary tangles [198]. Experimental evidence suggests that Aβ accumulation precedes and favors tau aggregation. Moreover, Aβ-induced degeneration of cultured neurons and cognitive deficits in mice with an Alzheimer's disease–like phenotype entail the presence of endogenous tau [199,200].

The ageing associated pathologies, such as increased oxidative stress, defective protein-folding function of the endoplasmic reticulum, as well as impaired proteasome-mediated and autophagic-mediated clearance of damaged proteins, accelerate the deposition of amyloid and tau proteins in Alzheimer's disease [201,202].

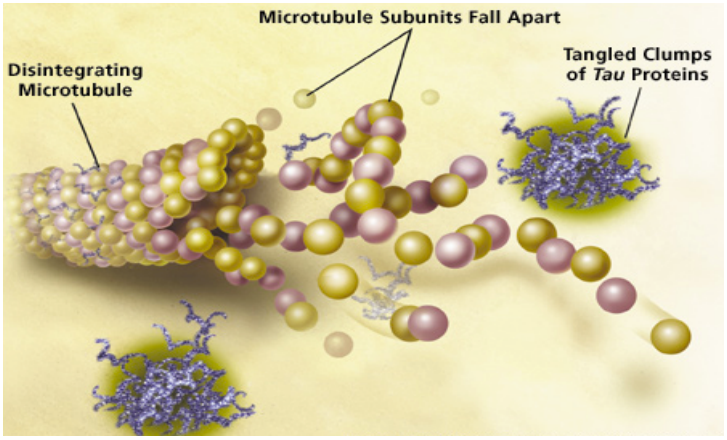

Figure 4: Formation of Tau tangles. Upon phosphorylation, tau protein detaches from microtubules and self-aggregates in form of tangled clumps. Adapted from Querfurth H. and LaFerla F. *Alzheimer's disease*, NEJM 2010; 362:328-44.

Synaptic dysfunction

Alzheimer's disease is described as a disorder of synaptic failure [203]. It is important to note though that ageing by itself promotes synaptic impairment, particularly affecting the dentate region of the hippocampus [204]. Synapses at the hippocampus start to degenerate in individuals with mild cognitive impairment (MCI), a transitional form between normal ageing and AD, and the remaining synaptic junctions will enlarge their sizes in order to compensate. In mild AD, there is 25% reduction in the expression of presynaptic vesicle protein synaptophysin, however with advancing pathology, synapses become excessively lost relative to neurons correlating with dementia progression [205,206]. Long-term potentiation assay, which is an experimental indicator of memory formation at synapses, is severely reduced in mice with Alzheimer's disease as well as after application of Aβ peptides on normal brain slices [207]. At the molecular level, impaired memory formation is caused by inhibition of crucial signaling molecules. Defective release of presynaptic neurotransmitters and postsynaptic glutamate-receptor ion currents ensues from endocytosis of *N*-methyl-D-aspartate (NMDA) surface receptors and endocytosis of α-amino-3-hydroxy-5-methyl-4-isoxazole propionic acid surface receptors [208,209]. These events further decline the synaptic activity through permanent depression of the currents after a high-frequency stimulus. Intraneuronal Aβ was shown to trigger early these synaptic deficits [210].

Oxidative Stress

Another hallmark of Alzheimer's disease is increased oxidative stress. Dysfunctional mitochondria generate oxidizing free radicals, triggering considerable oxidative damage in AD brains. Aβ peptides perturb mitochondrial function by directly impairing extracellular transport chain complex activities, blocking mitochondrial import channels, disrupting calcium storage, and highly increasing ROS levels. Moreover, the receptor for advanced glycation end products is required for mediating Aβ's pro-oxidant effects on neurons and microglial cells [213,214]. Similarly, Tau oligomers engender mitochondrial dysfunction and oxidative stress by decreasing the levels of NADH-ubiquinone oxidoreductase, which forms the mitochondrial electron transport chain complex I [215].

Although animal models and most cross-sectional studies in ageing populations present an association between antioxidant intake and cognitive performance, randomized trials of antioxidants have generally failed in improving cognitive function in AD [216].

DNA damage/Repair/ Cell-Cycle Reentry

Accumulation of DNA damage is particularly deleterious in post-mitotic cells such as neurons, which cannot be renewed through cell proliferation. Mounting evidence suggests that AD neurons have elevated levels of oxidative DNA damage leading to slow build-up of DNA adducts such as 8-OHG, DNA single strand breaks, DNA-DNA and DNA-protein cross linking [217,218]. Suram et al. demonstrated that soluble Aβ oligomers have DNA nicking activities similar to nucleases, causing a direct DNA damage [219]. Markers of aberrant cell-cycle reentry were detected in AD neurons but are mostly prominent at the G1–S phase boundary with some evidence showing cell cycle progression till the G2 phase. These abortive cell cycle events may proceed to complete DNA replication, forming tetraploid neurons and activation of mitotic cyclins as well as cyclin dependent kinases [220,221]. However, mitoses are absent hence these inductions are not indicative of neuronal cell division but are either the prelude of programmed cell death or the mechanism required for repairing DNA damage. PARP-1 is a DNA binding protein that is activated by SSBs as well as DSBs and is required for DNA repair processes. PARP-1 activity is induced by Aβ and it is increased in AD brains [222]. The Mre11 DNA repair complex consisting of Rad50, Mre11, and Nbs1 proteins is reduced in the neurons of AD cortex [223]. The non-homologous end joining (NHEJ) mechanism is

the predominant DNA repair process in neurons and requires the kinase DNA-PK complex. Shakelford et al. demonstrated that the level of DNA-PK catalytic subunit was significantly decreased in AD extracts, indicating that NHEJ pathway is less efficient in AD patients [224].

1.1.2.3.Models of disease and limitations:

Animal models are the best systems to analyze which disease-modifying strategy to pursue. Unfortunately, there is no animal model designed to recapitulate all the main hallmarks of AD. For instance, transgenic mice based on the amyloid hypothesis of AD, such as Tg2576 that overexpresses a mutant form of *APP* and deposits Aβ in a temporal and spatial pattern similar to human AD do not develop neuronal tangles or major neuronal loss. Similarly, tau transgenic models such as Tg4510, which overexpresses a mutant form of tau, develop neurofibrillary tangles, brain atrophy and functional deficits, but do not show amyloid deposition. Moreover, the transgenic mouse models used in AD studies mainly represent EOAD pathology and not LOAD pathology since they are based on overexpressing genes related to amyloid or tau metabolism without taking into account the ageing risk factor. The success of treatments in animals designed to model a pathological pathway predicts only that the treatment may successfully interfere with the pathway in patients, not that interference with the pathway will have efficacy in AD [176].

1.1.2.4.Biomarkers:

AD is currently diagnosed only via clinical assessments and confirmed by postmortem brain pathology. However, neurodegeneration in AD is estimated to start 20 to 30 years before the first clinical symptoms become apparent. Hence, the development of validated biomarkers for Alzheimer's disease is essential to improve early diagnosis, to differentiate AD from other dementias, and to accelerate the development of new therapies that will be most effective before pathological changes spread throughout the brain. Clinical diagnosis of AD is based on medical records, physical and neurological examination, laboratory tests, neuroimaging, and neuropsychological evaluation. Neuroimaging markers predict AD progression from a pre-AD state of mild cognitive impairment (MCI), and can be used to monitor efficacies of disease-modifying therapies.

Measurements of cerebrospinal fluid (CSF) markers including levels of Aβ40, Aβ42, total tau, and phosphorylated tau are also useful in predicting the risk of progression from MCI to AD [225].

There is no single linear chain of events that could summarize the heterogeneity of pathways initiating Alzheimer's disease. Thus, developing a multi-targeted approach to prevent or symptomatically treat AD is indispensable. Some studies put forth the notion that other pathological conditions, but not amyloid or tangle deposition, account for dementia in the elderly (80 years of age or older). It remains probable that many of these mechanisms and models, including the amyloid hypothesis, are minimal or incorrect and that some critical ageing-related process is the disease trigger.

CHAPTER 1

INTRODUCTION: SECTION 2

Constitutive heterochromatin and neurodegeneration

1.2.1. Chromatin

The human cells contain enough DNA to extend from earth to sun more than 300 times back and forth. How is that humongous DNA packaged so densely into chromosomes and squeezed into a microscopic nucleus?

The nucleus is the most prominent organelle within the eukaryotic cell, ranging from five to seven microns in diameter. It is a double membrane bound structure, which isolates the genetic material from the cytoplasm of the cell. The nuclear lamina consists of intermediate fibers named lamins, which are cytoskeletal proteins localized in the inner side of the nuclear membrane and are required to attach and position the chromatin within the nucleus [226]. Chromatin defines the state in which DNA is packaged within the nucleus. The repeating fundamental unit of chromatin is the nucleosome, which is composed of 147 base pairs of DNA wrapped in 1.7 superhelical turns around an octamer of four core histones (H3, H4, H2A, H2B). The nucleosomal array, described as beads-on-a-string fiber with a diameter of 11-nm, forms the first level of chromatin organization. Binding of linker histones (H1 or H5) wraps another 20 base pairs and further folds the nucleosomal arrays into a more compact 30-nm chromatin structure, which represents the second structural level of DNA organization. DNA coiling requires energy that is provided by histones mainly in the form of electrostatic interactions. Since DNA is negatively charged due to the phosphate groups in its phosphate-sugar backbone and the histones are positively charged proteins due to their lysine residues at the N-terminal tails, hence they bind with each other very tightly leading to chromatin condensation. As a result, chromatin will compress into a much smaller spatial volume within the nucleus compared to unwound DNA [149,150]. Chromatin conformation is highly dynamic affecting nuclear architecture, DNA repair, genomic stability as well as gene expression patterns and is regulated by post-translational covalent modifications of histones or by displacement of histones via chromatin remodeling complexes. These two processes are reversible, so modified or remodeled chromatin can be restored to its compact state after transcription, replication, or DNA repair are complete [226]. Post-translational modifications of histones include:

1) Methylation, acetylation, ubiquitylation, and sumoylation of lysine residues.
2) Methylation of arginine residues.
3) Phosphorylation of threonine and serine residues.
4) ADP-ribosylation of glutamate.

In the early twentieth century, Emil Heitz identified cytologically detectable differences in the staining of chromatin. He noted that certain regions remain visible throughout interphase whereas other parts become invisible after exit of mitosis. He suggested the terms heterochromatin and euchromatin, respectively [227]. I already discussed the differences between these two conformations earlier in this chapter, however in this section, I will expand more about the formation of constitutive heterochromatin describing its imperative role in genomic stability.

1.2.2. Constitutive heterochromatin

Eukaryotic and human genes contain some repetitive DNA sequences, however, the majority of highly repetitive DNA sequences are localized outside the coding information and are described as constitutive heterochromatin [228]. There are two main types of repetitive heterochromatic DNA (Figure 5):

1) Highly repetitive sequences are short sequences of 5-10 bp, which are not interspersed with different non-repetitive sequences. The main family of highly tandem repeats includes satellite DNA. They are represented by monomer sequences, usually less than 2000-bp long, tandemly reiterated up to 10^5 copies per haploid animals and are present in certain sub-chromosomal compartments including centromeres, telomeres, as well as pericentromeric domains [229]. Satellite DNA forms 1 to 65% of the total DNA of numerous organisms including animals, plants, and prokaryotes. Satellites are large arrays of AT rich DNA sequence motifs, which evolved within and across the species through nucleotide changes and copy number variations. The precise function of satellite DNA remains unclear, although they are being increasingly utilized as a versatile tool for genome analysis, genetic mapping and for understanding chromosomal organization [230]. Some human satellite DNAs are implicated in the function of centromeres, whose DNA consists very largely of various families of satellite DNA. The centromere is an

epigenetically defined domain. Its function is independent of the underlying DNA sequence; instead, its function depends on its particular chromatin organization, which, once established, has to be stably maintained through multiple cell divisions [231].

2) Moderately or dispersed repetitive sequences include short (150 to 300-bp) sequences or long ones (5-kbp) amounting about 40% and 1-2% of the total genome, respectively. These repeats are dispersed throughout the euchromatin having 10^3 to 10^5 copies per haploid genome, hence forming the intergenic heterochromatin. These sequences operate as regulators of gene expression. On the basis of their mode of amplification, repetitive DNA sequences may be tandemly arranged or interspersed in the genome [232].

a. Interspersed repeats also named transposable elements are mobile DNA sequences that can migrate to different regions of the genome and account for more than 40% of the total human DNA sequence [233]. There are primarily two types of transposable elements comprising DNA transposons and retrotransposons. DNA transposons are described as fossils since they are inactive in the human genome due to their high mutational rate. Retrotransposons are the most important and most abundant active transposable segments. In order to displace, reverse transcriptase converts the RNA transcript of the retrotransposon into cDNA, which will eventually integrate into the genome at a new location. The predominant families of retrotransposons are long interspersed nuclear elements (LINEs) and short interspersed nuclear elements (SINEs). LINEs are very successful autonomous transposons since they can make all the products needed for retrotransposition, including the essential reverse transcriptase. Human LINEs consist of three distantly related families: LINE-1, LINE-2, and LINE-3, however, LINE-1 (or L1) is the only family that continues to have actively transposing members. To integrate into genomic DNA, the LINE-1 endonuclease cuts a DNA duplex at the cleavage site TTTTA; hence the preference for incorporating into gene-poor AT-rich regions imposes a lower mutational burden and makes it easier for the host to accommodate them. However, LINE-1 occasionally promotes disease progression by disrupting gene function after insertion into an important conserved sequence [233,234,237]. The LINE-1 machinery is also responsible for

most of the reverse transcription in the genome, allowing retrotransposition of the nonautonomous SINEs and also of copies of mRNA, giving rise to processed pseudogenes and retrogenes. SINEs are retrotransposons that have been very successful in colonizing mammalian genomes, resulting in various interspersed DNA families, some with extremely high copy numbers. Unlike LINEs, SINEs cannot transpose independently and they are mobilized by neighboring LINEs. The human Alu family is the most prominent SINE family in terms of copy number originating from the short RNA component of the signal recognition particle 7SL RNA and occurring on average more than once every 3 kb. Interestingly, newly transposing Alu repeats show a preference for AT-rich DNA, but progressively older Alu repeats show a progressively stronger bias toward GC-rich DNA. The bias in the overall distribution of Alu repeats toward GC-rich and, accordingly, gene-rich regions must result from strong selection pressure. It suggests that Alu repeats are not just genome parasites but are making a useful contribution to cells containing them. Some Alu sequences are known to be actively transcribed and may have been recruited to a useful function. The BCYRN1 gene, which encodes the BC200 neural cytoplasmic RNA, arose from an Alu monomer and is one of the few Alu sequences that are transcriptionally active under normal circumstances. In addition, Alu repeats has recently been shown to act as a trans-acting transcriptional repressors during the cellular heat shock response [235,237].

b. Tandem repeats includes minisatellites and microstellites. Minisatellites comprises tandem copies of repeats that are 6-100 nucleotides in length. Alec Jeffrey first identified minisatellites in 1985, from the non-coding (intron) regions of the human myoglobin gene. Also named as variable number of tandem repeats (VNTR), majority of the minisatellites have a rich GC content and strong strand asymmetry. The degree of repetition varies from two to several hundreds. Repeat unit within a minisatellite usually presents small variations in sequence and mutations consist of gains or losses of one or more repeat units. Such mutations at hypervariable minisatellite loci are up to 1000 times more common than mutations in protein coding genes [236,237].

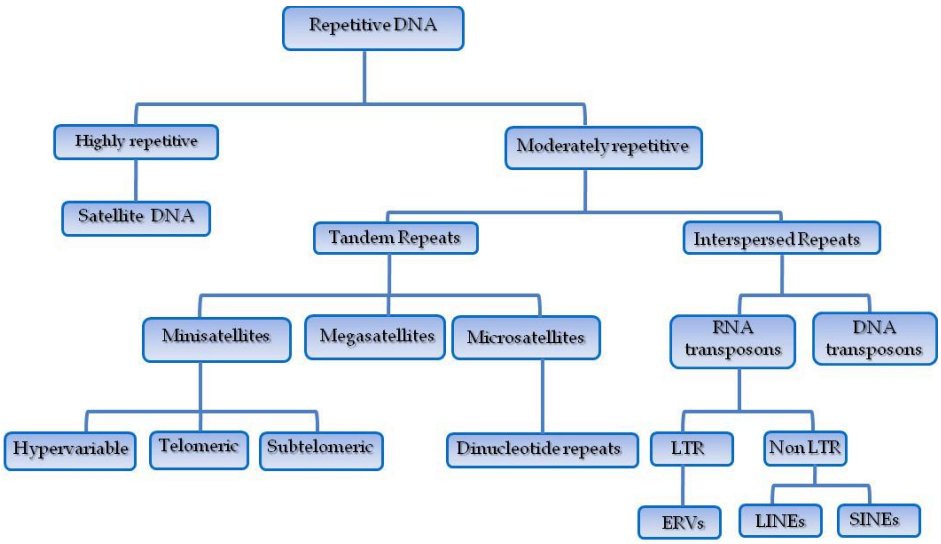

Figure 5: Schematic diagram representing the biological categories of the different DNA repetitive sequences. Adapted from Pathak D. and Ali S. (2012), *Functional Genomics*, ISBN: 978-953-51-0727-9.

Constitutive heterochromatin has a characteristic histone-modification profile, which is distinguished by hypoacetylation and H3K9 trimethylation. Constitutive heterochromatin nucleation is directly associated with the presence of repetitive DNA elements and several lines of evidence denote the importance of non-coding RNAs and RNAi in this process. RNAi defines a post-transcriptional silencing mechanism that involves the Dicer protein (Dcr), Argonaute (Ago), and RNA-dependent RNA polymerase (RdRP). Briefly, RdRP generates double strand RNAs (dsRNAs) that will eventually be processed by Dicer into small interfering RNAs (siRNAs) [238,239,240]. A mechanistic insight into RNAi based heterochromatic silencing was demonstrated by purification of the RITS (RNA-induced transcriptional gene silencing) complex from *Schizosaccharomyces pombe*. RITS machinery includes Ago protein, siRNAs processed primarily from heterochromatic repeats, and the fission yeast HP1 homolog Chp1. Ago deficient yeast presented defects in chromosome segregation, implying heterochromatin malformation [241]. Yeast lacking Dicer present loss of siRNAs as well as delocalization of RITS from centromeric regions. Furthermore, RITS was shown to be required for initiating H3K9 methylation at centromeric repeats [242,243]. Overall, these findings suggest that siRNAs wihin RITS complex provide specificity for RITS localization on the genome

and are needed for the subsequent recruitment of histone methyltransferases (HMTases) (Figure 6). DNA-binding proteins can also nucleate constitutive heterochromatin, working in parallel with RNAi-directed nucleation. For instance in *S. pombe*, transcription factors Atf1 and Pcr1 cooperate with the HDAC protein Clr3 to initiate heterochromatin [244]. Once nucleated, H3K9me3 mark serves as a molecular anchor tethering more HP1 proteins to chromatin, which in turn trigger further recruitment of HDACs and HMTases allowing heterochromatin to propagate to neighboring sequences, a process described as heterochromatinization. Moreover, studies have shown that Hp1 also recruits Dnmt1 to methylate DNA at cytosine bases of CpG dinucleotides, a process highly associated to heterochromatin organization [245].

Constitutive heterochromatin contributes to several biological processes. It was first described to prevent illegitimate recombination between scattered repetitive DNA elements to protect genome integrity. Interestingly, control of transposable segments has been suggested as the original evolutionary benefit of heterochromatic silencing. Heterochromatin is important for the organization of nuclear domains. The peripheral localization of heterochromatin against the nuclear membrane favors the concentration of euchromatic active domains towards the center of the nucleus, allowing euchromatin to replicate and be transcribed with maximum efficiency. Heterochromatin is also required for normal function of centromeres and has been suggested that centromeric heterochromatin is necessary for the cohesion of sister chromatids, permitting normal segregation of mitotic chromosomes [228]. Mounting evidence indicates that heterochromatin operates as a dynamic platform controlling gene repression. Genes that are usually located in euchromatin can be silenced *in cis* and *in trans* when placed next to heterochromatic domains.

Inactivation in cis

Following chromosomal rearrangements, a euchromatic domain may be juxtaposed with a heterochromatic region. Rearrangement promotes the removal of normal barriers that protect the euchromatin, allowing for the heterochromatic structure to propagate *in cis* to the adjacent euchromatin and thus inactivating the genes enclosed therein. This mechanism has been identified in position effect variegation (PEV) in *Drosophila* and also in the inactivation of certain transgenes in mouse.

Inactivation in trans

During cell differentiation, certain active genes are transposed into heterochromatic nuclear domains resulting in their silencing. Such a mechanism has been suggested to explain the co-localization in lymphocyte nuclei of the protein IKAROS and its downstream genes with centromeric heterochromatin [246].

Overall, although constitutive heterochromatin is apparently nebulous, isolated in the periphery of the nucleus, and previously considered as "Junk" DNA, growing evidence indicates that it is crucial in the organization and function of the genome.

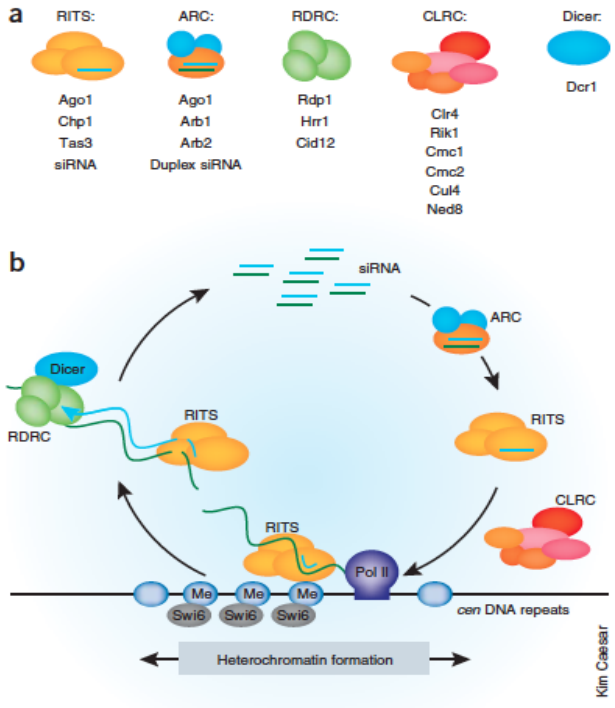

Figure 6: RNAi-mediated heterochromatin formation in fission yeast. RITS complex mediates heterochromatin assembly by associating with nascent transcripts via siRNA base-pairing, and with methylated H3K9 via the chromodomain of its Chp1 subunit. The chromosome-associated siRNA synthesis loop is essential for the spreading of H3K9 methylation and silencing. The coupling of the siRNA synthesis loop to H3K9 methylation forms a stable feedback loop that epigenetically maintains heterochromatin. Adapted from Buhler M. and Moazed D., *Transcription and RNAi in heterochromatic gene silencing*. Nature struct.mol. bio. 2007.

1.2.3. Constitutive heterochromatin, genomic instability, and neurodegeneration

Correct formation of constitutive heterochromatin is critical to genome stability. Heterochromatin is usually refractory to DNA damage because of its condensed conformation and the protection given by its associated proteins. Per se, knockdown of heterochromatic proteins or induced decondensation of heterochromatin can sensitize cells to DNA damage [247]. Indeed, loss of HP1 renders nematodes highly sensitive to DNA damage [248]. In *Drosophila*, reduction of H3K9^{me2} levels through inactivation of the histone methyltransferase Su(var)3-9 favors genomic instability and constitutive DDR at the heterochromatin in both somatic and germ-line cells [249]. Moreover, flies lacking Su(var)3-9 exhibit reduced lifespan, muscle degeneration and loss of rRNA transcription silencing, whereas increasing heterochromatin formation through HP1 over-expression promotes longevity [163]. In mice, deletion of the SUV39h1/h2 methyltransferases leads to reduced viability, loss of H3K9^{me3} and genomic instability [250]. Interestingly, the neuroprotective SIRT1 protein was shown to regulate SUV39H1 through deacetylation during heterochromatin formation. Loss of SIRT1 affects H3K9^{me3} deposition and impairs HP1 localization [251]. Mice lacking the methyltransferase PRSET-7PA that is necessary for constitutive heterochromatin formation, display early embryonic lethality, defects in chromosomal condensation, and accumulation of DNA damage [252]. Neuronal cells from HP1β-deficient mice exhibit heterochromatin decondensation and genomic instability [253]. Inactivation of chromatin remodeling proteins, such as those of the NURD complex, result in DDR and cellular senescence that is preceded by heterochromatin alteration [158]. In human cells, downregulation of SU(V)39H1 via its methylation by SET7/9 leads to significant reduction in H3K9^{me3} levels, increased expression of satellite repeats, genomic instability, and inhibition of cell proliferation [254]. The HGPS syndrome associated with heterochromatin defects and introduced earlier in this chapter is also characterized by genomic instability. Cells from patients with ICF (Immunodeficiency, Centromeric instability and Facial anomalies) syndrome, a rare recessive disease that is linked to mutations of the gene DNMT3B, are characterized by mitotic catastrophe and genomic instability. DNA methylation mediated by DNMT3B is required for setting the histone code in pericentric and centromeric heterochromatin and loss of DNMT3B promotes the demethylation of GC rich satellite repeats causing

abnormal segregation of the sister chromatids, formation of multiradial figures, deletions, and micronuclei [255].

Perturbations in constitutive heterochromatin and active restrotranspositions are reported to trigger neurodegenerative diseases through engendering genomic plasticity in neurons by initiating variation in genomic DNA sequences and by altering the transcriptome of individual cells. Fragile X-associated tremor/ataxia syndrome (FXTAS) is a neurodegenerative disease linked to fragile X premutation carriers. In an FXTAS *Drosophila* model, activation of a specific LTR retrotransposon, gypsy, modulates neurodegeneration [256]. Aberrant overexpression of Alu repeats is also found to directly cause age-related macular degeneration [257]. Mutations in DNMT1, which is crucial for the maintenance of methylation in constitutive heterochromatin, cause central and peripheral neurodegeneration in hereditary sensory and autonomic neuropathy (HSAN1) with dementia and hearing loss [258]. Mutations in ATRX (α-thalassemia X-linked mental retardation) cause several X-linked mental retardation syndromes featuring facial dismorphism, urogenital defects, and α-thalassemia [259]. ATRX protein resides predominantly in repetitive DNA sequences and impaired ATRX activity causes aberrant methylation pattern, genomic instability, and DDR [260]. Mutations in CREBBP (c-AMP-responsive element binding protein (CREB) binding protein) gene cause Rubinstein Taybi syndrome, an autosomal dominant disorder of growth retardation, facial abnormalities, and mental retardation. CREBBP functions as a histone acetylase (HAT) promoting the decondensation of chromatin [261].

In conclusion, all these findings and observations point to a surprisingly active role for constitutive heterochromatin malformation in genomic instability and neurodegeneration. The phenotypic variations associated with mutations in chromatin modifying complexes, even though all converging into heterochromatin decondensation and genomic instability, reflect the functional diversity, redundancy, and environmental modulation of the affected processes.

CHAPTER 1

INTRODUCTION: SECTION 3

Polycomb proteins: epigenetic modifiers

1.3.1. Polycomb complexes

Polycomb group (PcG) proteins were originally identified in *Drosophila melanogaster* functioning as transcriptional repressors of homeotic (Hox) genes. PcG protein activity begins at gastrulation preventing homeotic gene reactivation at the time when the early repressors start to disappear [262]. Therefore PcG proteins operate as a maintenance system guarding the repressed state of target genes, which was already established early in development. This process results in variegated expression i.e. silencing of the gene in some cells but not in others, producing mosaic tissues. Several genome wide studies revealed widespread PcG roles in repressing hundreds of developmental decision makers and signaling factors [263,264,265,266]. Polycomb silencing function appears to be sensitive to dosage and involves cooperation of multiprotein complexes that selectively occupy chromatin sites [267]. These complexes include the PRC1, PRC2 and PhoRC groups and are described below.

The PRC1 complex

PRC1 complex biochemically purified from *Drosophila melanogaster* comprises a central core consisting of Polycomb (PC), Polyhomeotic (PH), Posterior sex combs (PSC), and RING1. The mammalian PRC1 complexes were identified using HeLa cells that express tagged protein components [268]. In mice and humans, some PcG proteins have several homologues that presumably operate as alternatives at different targets or in different tissues. The mammalian purified complexes consist of HPC (chromobox proteins CBX), HPH (1, 2 and 3), PCGF (BMI1 and its homologue MEL18), as well as RING1 (A and B), which are analogous respectively to the fly PC, PH, PSC and RING [269]. A common view has been that PRC1 targets chromatin via its PC chromodomain subunit CBX, which binds specifically to the PRC2 complex histone mark H3K27^{me3} [270,271,272]. Recently, it has been shown that PRC1 complexes are further distinguished by comprising CBX subunits or not, dividing PRC1 family into CBX-containing and CBX-lacking subgroups. Interestingly, PRC1 complexes lacking CBX proteins do not include the chromodomain subunit of PC, raising recent questions about the mode of PRC1 recruitment to chromatin. Indeed, genome wide ChIP analysis

revealed that CBX-comprising PRC1 co-localizes with H3K27^{me3} at chromatin whereas PRC1 missing CBX subunits are independent of this mark; and that loss of H3K27^{me3} dislodges CBX-containing, but not CBX-lacking PRC1 complexes from chromatin domains [273,274]. Therefore, different PRC1 groups may target to chromatin by other mechanisms, with only CBX-containing complexes recruited via H3K27^{me3}. Interestingly, emerging studies are implicating long non-coding RNAs (lncRNAs) in targeting PcG complexes to chromatin. A key example is the interaction of PRC1 with the lncRNA ANRIL to regulate the INK4A/ARF locus [275]. Other studies demonstrated conventional interactions of PRC1 with DNA binding factors such as Runx1 and REST, promoting PRC1 recruitment to genomic sites [276].

The PRC2 complex

A key function of PRC2 is trimethylation of histone H3 on K27, widely viewed as the operative chromatin mark initiating PcG silencing. The key catalytic subunit of PRC2 is the SET domain of the H3 methyltransferase Enhancer of *zeste* (E(Z)). However, when on its own, E(Z) has no histone methyltransferase activity and must be assembled with SUZ12 and EED to methylate H3K27 [277,278,279,280]. Moreover, knockout of *SUZ12* decreases the level of EZH2 protein, the mammalian E(Z), suggesting that formation of the complex stabilizes EZH2 [281]. Another PRC2 component includes P55 (RBAP46/RBAP48), a histone-binding protein that is also associated with the chromatin assembly factor CAF1 [282]. Evidence identified JARID-2 as another prominent PRC2-associated protein in embryonic stem cells. JARID-2 is member of the Jumonji (Jmj) family of histone demethylases, influencing PRC2 chromatin recruitment and modulating PRC2 histone methyltransferase activity [283]. *In vivo*, trimethylation of H3K27 characterizes PcG target genes, which as mentioned earlier is specifically recognized by the PC chromodomain of PRC1 complex. *In vitro*, the PRC2 complex also methylates H3K9 and H3K9 trimethylation has been reported *in vivo* at PcG target genes [284]. Other studies showed that PRC2 could also methylate itself and other proteins such as GATA4 and histone H1 on K26, which has an amino acid context similar to that of H3K27 [285,286]. Therefore, while H3K27 methylation is a hallmark of PRC2 activity, this complex like the PRC1 group does not have monolithic composition and is unlikely

to have monolithic function.

Other E(Z) complexes have been identified including PRC3 and PRC4 complexes, which differ biochemically by the presence of different isoforms of EED. PRC4 complex is assembled when EZH2 is overexpressed in cultured cells. It comprises an EED isoform that is only expressed in undifferentiated ES cells as well as the histone deacetylase SIRT1 [287].

The PhoRC complex

PHO and its closely related homologue, PHOL, are the only PcG proteins that are recognized to bind directly to DNA. These two *D. melanogaster* proteins are analogous to the mammalian factor Yin-Yang 1 (YY1), so called because it has both activating and repressive activities. Although it has been reported that PHO interacts molecularly with both PRC1 and PRC2 complexes in flies and mammals, it is not an important component of either of these two purified complexes [288]. The *Drosophila* PHO-containing complex, PhoRC, is implicated in homeotic gene silencing and contains an MBT-domain protein SFMBT (*Scm*-related gene containing four MBT domains). Although not previously recognized, SFMBT protein operates as a bona fide PcG protein and is required for PcG silencing. Its MBT repeats bind specifically to mono- and dimethylated H3K9 and H4K20. Widespread H3K9 and H4K20 methylation has been reported at the PcG target gene *Ubx* in *Drososphila*, providing other interactions to stabilize the binding of PcG proteins. These interactions provide a mechanistic insight for the spread of PcG silencing, by allowing polycomb complexes bound to a specific loci to interact with methylated nucleosomes and methylate any neighbouring nucleosomes that lack methyl marks [289].

PcG mechanisms of transcriptional repression

PRC1 group promotes gene silencing through two distinct mechanisms including ubiquitylation of histone H2AK119 and polynucleosome compaction. RING1 in flies and RING1A and B in mammals have been shown to function as E3 ubiquitin ligases that orchestrate the mono-ubiquitylation of lysine 119 of histone H2A. The presence of BMI1,

which also encompasses a RING-domain, enhances the catalytic activity of RING1A and RING1B [290]. H2A ubiquitylation plays an important role in PRC1-mediated gene silencing, but the exact mechanism by which this specific ubiquitylation initiates repression is still unknown [290,291]. Moreover, recent studies conducted on RING1B-mutant mouse cells along with presence or absence of RING1A defined two separate classes of PcG target genes: those that critically necessitate H2A ubiquitylation for silencing and those that display significant silencing without ubiquitylation. For instance, de Napoles et al. demonstrated that ubiquitylation-impaired RING1B renders *PAX3* almost totally derepressed, whereas numerous *HOX* genes are partially silenced [292]. Overall, these findings suggest that H2A ubiquitylation is a major contributor in PRC1 repression, however there are other mechanisms that are also required such as polynucleosome compaction. Switch of the beads-on-a-string arrangement of nucleosome arrays into condensed knot-like structures is a non-enzymatic function of many PRC1 family complexes. Compaction does not necessitate H2A ubiquitylation, as it is unaffected when mouse RING1B is made catalytically inactive [293]. In vertebrates, positively charged CBX subunits are the sole PRC1 components demonstrated to produce compaction. Since they also bind H3K27^{me3} thereby recruiting PRC1 complexes to regions containing this mark, they probably connect compaction with targeting by H3K27^{me3}. Interestingly, densely packed nucleosomal arrays can trigger K27 methylation by PRC2 providing an attractive positive feedback loop between the compacted conformation and the covalent histone mark that is targeted by PRC1 complexes responsible for further compaction [294]. Unfortunately, the extent to which these findings reflect the situation *in vivo* is yet difficult to evaluate.

Other proposed mechanisms of PcG silencing involve the primary chromatin fibre rather than higher order structures. For instance, when the well-defined polycomb response element (PRE) from the *Ubx* gene was placed in front of *lacZ* reporter driven by the heat shock-inducible *hsp26* promoter, silencing did not mainly interfere with the binding of RNA polymerase II (RNA POL II) or of transcription factors, instead it blocked initiation of RNA synthesis by POL II. Another insight comes from the finding that chromatin insulators can block PcG silencing. One insulator placed between PRE and the promoter

inhibits silencing, however two insulators in tandem favor bypass of the block and lead to promoter silencing. This observation indicates that continuous DNA linkage is not required for silencing, and that the bound PcG complexes potentially loop out to contact the target promoter. The insulator also prevents the spreading of H3K27 trimethylation from the PRE concomitantly with the block imposed on silencing, suggesting that this chromatin mark might be directly involved in repression, or result from the same process that induces repression [295].

Biological functions

In addition to the Hox clusters, PcG proteins regulate numerous genes especially key developmental regulators, and are centrally integrated in processes ranging from chromosome X inactivation to spermatogenesis, self-renewal of neural and haematopoietic stem cells, senescence and cell cycle progression [296,297,298]. PcG target genes encode transcriptional regulators, as well as morphogens, receptors and signalling proteins that are involved in all of the main developmental pathways. PcG complexes also modulate the majority of cell differentiation pathways, elucidating the concept that epigenetically stable silencing being established in the early embryo and preserved for the rest of development is not the common rule. This indicates that there are ways to bypass or overcome PcG silencing and switch target genes to the active state. In *D. melanogaster*, this can be accomplished by active transcriptional activity preceding the establishment of PcG silencing in the early embryo. Various studies revealed that transcription through the PRE interferes with PcG silencing, suggesting another potential mechanism for switching or resetting the epigenetic state [296]. According to this model, activation of neighboring transcription region that crosses the PRE promotes the derepression of silenced gene. Another suggested mechanism to bypass PcG silencing is massive production of an activator that is targeted to the repressed gene. For instance, PcG repression of Gal4–UAS reporter construct in the *D. melanogaster* embryo was counteracted by significant overexpression of Gal4. Larval imaginal discs, whose developmental identity has been established in the embryo and maintained by PcG silencing, can be influenced to change identity by cutting them and allowing them to regenerate. Studies have demonstrated that cells switching identity are subject to intense

signaling by strong morphogens such as Wingless/WNT, Decapentaplegic/transforming growth factor-β (DPP/TGF) and Hedgehog [296]. During wound healing in *Drosophila,* Lee et al. noted that JNK pathway is activated leading to downregulation of PcG genes. Similar mechanisms are suggested to operate in mammals and various signaling pathways in mammalian cells engender surprising effects on the PRC2 complex. Induction of integrins, T-cell receptor, platelet derived growth factor (PDGF) and related pathways favors re-localization of the PRC2 complex into the cytoplasm, where it appears to interact with the signal response pathway. PRC2 is required for the restructuring of the actin cytoskeleton in response to signaling. Covalent modifications of PcG proteins might be another way to dislodge them from target genes. Phosphorylation of PcG proteins promotes their dissociation from chromatin [295]. Activation of MAPKAP kinase 3, which is associated to PcG complexes, phosphorylates their components and causes their detachment from chromatin. Another mechanism involves PI3K–AKT, which enters the nucleus and phosphorylates EZH2. It is not established yet if these kinases are targeted to specific genes, thereby inducing local derepression rather than a global loss of silencing [295].

In conclusion, PcG role in orchestrating patterns of gene transcription appears to be pervasive, mainly targeting genes critical in differentiation pathways. Many questions about PcG-mediated silencing remain to be determined, including the most essential one such as the mechanism of repression. It will be interesting to delineate if repression is due to blockage of transcription initiation or transcription elongation. The effects of PcG complexes are fully accounted for by the chromatin modifictions, but it is entirely plausible that histone methylation and ubiquitylation patterns as well as the PcG-complex distribution are only devices to deliver the crucial function to the right places.

1.3.2. *Bmi1*

Bmi1 (B lymphoma Mo-MLV insertion region 1 homolog), first identified as an oncogene that cooperated with c-Myc in the generation of murine lymphomas, plays essential roles in cell cycle regulation, cell immortalization, and cell senescence [299]. *Bmi1* is a member of the PRC1 complex, which promotes chromatin compaction and

gene repression through its E3-mono-ubiquitin ligase activity mediated by Ring1a/b on histone H2A at lysine 119 ($H2A^{ub}$) [300,301]. The human *BMI1* gene is localized on short arm of chromosome 10 (10p11.23) and contains 10 exons and 9 introns. The human gene encodes a 37kDa protein consisting of 326 amino acids, whereas mouse *Bmi1* gene encodes a protein of 45–47kDa [302].

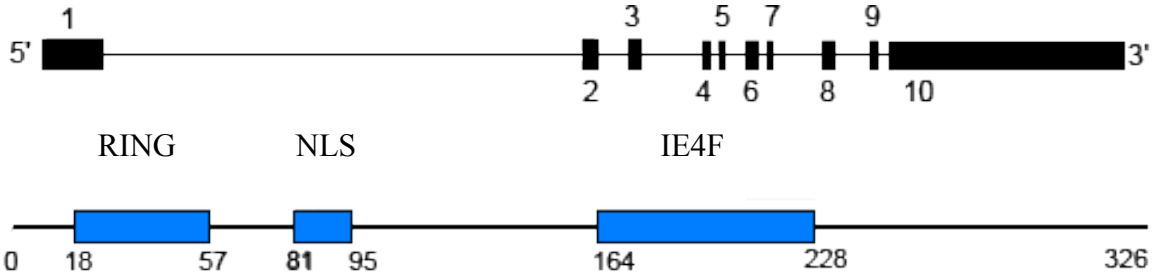

Figure 7: Schematic representation of human BMI1 gene (upper scheme) and BMI1 protein (lower scheme). RING represents the ring finger domain; NLS represents the nuclear localization domain; and IE4F1 represents the interaction site with E4F1. Adapted from Cao L., Bombard J., et al., *Bmi1 as a novel target for drug discovery in cancer*. J. Cell Biochem. 2011. 112:2729-41.

With respect to amino acid sequence, a high degree of homology is present between human BMI1 and murine *Bmi1*. BMI1 protein comprises a central helix-turn-helix domain, which is essential for inducing telomerase activity, and a conserved RING-finger domain near the NH_2 terminus, which was shown to be important for the generation of lymphomas in Eμ-*Bmi1* transgenic mice. BMI1 is predominantly localized at the nucleus, mediated by two nuclear localization signals (KRRR and KRMK) located in the C-terminal region of this protein [302,303]. BMI1 has a ubiquitous pattern of expression in almost all tissues and its expression levels are observed to be high in the brain, esophagus, salivary gland, thymus, kidney, lungs, gonads, placenta, blood, and bone marrow [303]. $Bmi1^{-/-}$ mice exhibit reduced post-natal growth and lifespan as well as defects in hematopoiesis, skeletal patterning, neurological functions, and cerebellar development [304,305,306]. Our group previously reported that *Bmi1*-null mice also display a premature ocular- and brain-aging phenotype associated with p53-mediated apoptosis and repression of anti-oxidant response genes in neurons [307].

Bmi1 and stem cells:

Hematopoietic stem cells (HSCs) and neuronal stem cells (NSCs) express high levels of *Bmi1*, which is required for efficient self-renewing cell divisions of adult HSCs as well as adult peripheral and central nervous system NSCs [308,309,310]. Indeed, transplantation of *Bmi1*$^{-/-}$ fetal liver cells led to only transient hematopoietic cell reconstitution, indicating that the transplanted mutant fetal liver HSCs failed to generate more HSCs. Similarly, the reduced self-renewal of *Bmi1*-deficient NSCs resulted in their postnatal depletion *in vivo* [311]. Moreover, BMI1 is reported to play a crucial role during the self-renewal and maintenance of prostate, intestinal, lung epithelial and bronchioalveolar stem cells [303].

Bmi1 and cancer:

Bmi1 is associated with the initiation and progression of various types of tumor promoting cells and is overexpressed in numerous types of human cancers including mantle cell lymphoma, non-small cell lung cancer, B-cell non-Hodgkin's lymphoma, pancreatic adenocarcinoma, breast cancer, colorectal cancer, prostate cancer, and nasopharyngeal carcinoma. For example, in approximately 11% of cases of mantle cell lymphoma, the malignant cells have a three to seven-fold amplification of *Bmi1* DNA and express high levels of the protein [312,313]. Consistent with its implication in the progression of carcinomas, various studies have demonstrated that *Bmi1* is required for the self-renewal of cancer stem cells through multiple pathways. For example, in a mouse model of AML, *Bmi1* was essential for the proliferation and maintenance of leukemic stem cells (LSCs). *Bmi1*-expressing LSCs were able to induce leukemia progression when transplanted into irradiated mice, whereas *Bmi1*-deficient LSCs had limited proliferative capacity and were unable to trigger malignant formation [314]. One mechanism by which *Bmi1* overexpression drives transformation is through preventing senescence and activation of telomerase. There is evidence that *Bmi1* regulates telomerase expression in human mammary epithelial cells (MECs) and may play a role in the development of human breast cancer. Overexpression of *Bmi1* immortalizes MECs and is associated with human telomerase reverse transcriptase (*hTERT*) expression, which leads to induction of telomerase activity. Deletion analysis of the *Bmi1* protein suggested that the *RING* finger, as well as the conserved helix-turn-helix domain, was required for

its ability to induce telomerase and immortalization [315]. Another mechanism is via promoting stem-like properties associated with induction of epithelial–mesenchymal transition (EMT) favoring invasion and metastasis [316]. A recent report demonstrated that in head and neck cancer, BMI1 upregulates the mitotic kinase Aurora A leading to chromosome instability and EMT through stabilization of *Snail* [317]. Our group also demonstrated that BMI1 confers radioresistance to cancerous stem cells in glioblastoma through recruitment of DNA damage machinery [318]. Operating as an important modulator in tumorigenesis, *Bmi1* can be used as a valuable marker for the assessment and prognosis of different cancers as well as a potent target candidate in cancer stem cells for cancer therapy. Indeed, Wang et al. successfully examined 1,2-dioleoyl-sn-glycero-3-phosphatidylcholine nanoparticles carrying small inhibitory RNA to target BMI1 and demonstrated an inhibition in the growth of chemoresistant ovarian tumors implanted in a xenograft mouse model [319]. Moreover, Siddique et al recently showed that targeted inhibition of BMI1 by adopting gene therapy approach led to reduced invasive potential and tumorigenic potential of prostate cancer cells [319].

Bmi1 and senescence:

Several lines of evidence point to a clear role for *Bmi1* in preventing senescence. In human fetal lung fibroblasts, *Bmi1* is downregulated when the cells undergo replicative senescence, but not quiescence. *Bmi1* overexpression extends replicative lifespan in mouse and human fibroblasts [320]. WT mouse embryo fibroblasts (MEF) enter senescence after 8 passages in culture, whereas $Bmi1^{-/-}$ fibroblasts undergo senescence after 3 passages. Moreover, re-expression of *Bmi1* rescued the premature senescent phenotype and increased MEF lifespan. Furthermore, unlike human fibroblasts, *Bmi1* could immortalize MEFs. One key target of *Bmi1* is the *Ink4a/Arf* locus that encodes two structurally and functionally distinct proteins: the $p16^{Ink4a}$ and the $p19^{Arf}$ ($p14^{ARF}$ in humans) proteins [320]. $p16^{Ink4a}$ is an inhibitor of the cell cycle while $p19^{Arf}$ regulates p53 stability. As stated earlier, $p16^{Ink4a}$ regulates the retinoblastoma activity. During the cell cycle, pRB is hyperphosphorylated by the cyclin D/cyclin-dependent kinases 4 and 6 complex, disabling its inhibition of E2F transcription factor and allowing transcription of E2F target genes that are important for the G1/S transition. In the absence of *Bmi1*, $p16^{Ink4a}$ is upregulated resulting in hypophosphorylated pRB,

which binds to E2F and inhibits E2F-mediated transcription leading to cell cycle arrest and senescence. $p19^{Arf}$ also plays an important role in senescence though sequestering mouse double minute 2 (MDM2). MDM2 is an E3 ubiquitin ligase that targets p53 for proteasomal degradation. Thus, by repressing MDM2, ARF stabilizes p53 favoring cell cycle arrest in G1 and G2/M phases or apoptosis. Lifespan extension by *Bmi1* is mediated partially by suppression of the $p16^{Ink4a}$-dependent senescence pathway and requires the RING finger and helix-turn-helix domains of *Bmi1*. Indeed, deletion of RING finger region induced $p16^{Ink4a}$ expression and premature senescence [321,322]. Mice lacking *Bmi1* showed induction of both $p16^{Ink4a}$ and $p19^{Arf}$ in various hematopoietic and neuronal tissues. Point mutations and deletion of $p16^{Ink4a}$ and $p19^{Arf}$ are frequently found in many types of human cancers, involving them as key regulators of immortalization and/or senescence checkpoints. Interestingly, *Ink4a/Arf* locus is upregulated not only in senescing cultured cell lines but also in several tissues of ageing animals. Concomitantly, Itahana et al. showed that *Bmi1* levels are reduced in senescent diploid fibroblasts [303,322,323].

Bmi1 and CNS:

Several studies associated the important function of *Bmi1* in the central nervous system (CNS). Bmi1 null mice exhibit smaller brains with profound defects in cerebellar growth after 2 weeks of age [306]. They also develop generalized astriogliosis, ataxia, and epilepsy in the first month after birth [304]. Our group reported that *Bmi1* is highly expressed in neurons and that *Bmi1* mutant mice manifest a progeroid phenotype at 4 week-old. This progeroid phenotype is characterized by lens cataracts formation, apoptosis of cortical neurons, and increase of reactive oxygen species (ROS) concentrations, due to p53-mediated repression of antioxidant response (AOR) genes. We also found that *Bmi1* expression progressively declines in the neurons of ageing mouse and human brains and that *Bmi1*-deficient neurons were hypersensitive to β-amyloid-induced apoptosis [307,324]. Conversely, *Bmi1* overexpression in cortical neurons conferred robust protection against DNA damage-induced cell death or mitochondrial poisoning, and resulted in suppression of ROS through activation of AOR genes [324]. Since *Bmi1* regulates key genes implicated in senescence and ageing and *Bmi1* genetic deficiency recapitulates aspects of physiological brain aging, it is of interest to determine

if *Bmi1* is implicated in ageing related diseases and test if *Bmi1* overexpression is a potential therapeutic modality against neurodegeneration.

Bmi1 regulation (Figure 7):

Evidence revealed that *Bmi1* is regulated at the transcriptional and post-translational levels. BMI1 is positively regulated by c-MYC, E2F1, sp1, and FoxM1 at the transcriptional level [319]. BMI1 can be ubiquitylated by the E3 ubiquitin ligase CULLIN3/Speckle-type POZ protein (SPOP) *in vitro*, however this ubiquitylation does not affect BMI1 protein levels and most likely has no bearing on protein stability [325]. Bmi1 can also be phosphorylated leading to its dissociation from chromatin [326, 327]. Moreover, the nature of phosphorylation sites is important for *Bmi1* function. Indeed, Kim et al. reported that in the progeroid Ataxia-telangectasia mutated disorder, the defective proliferation of $Atm^{-/-}$ NSCs was due to *Bmi1* downregulation, mediated by its phosphorylation via p38 MAP-kinase. Conversely, *Bmi1* downregulation could be rescued by Akt phosphorylation, which renders *Bmi1* resistant to the proteasomal degradation, leading to its stabilization and accumulation in the nucleus [328]. Treatment of breast cancer cells with histone deacetylase inhibitors (HDACi) downregulates the expression of BMI1, associated by a decrease in histone 2A lysine 119 ubiquitination (H2AK119Ub) [329]. Few observations hint on the role of miRNAs in *Bmi1* regulation. For instance, miRNA 200c was shown to downregulate BMI1 in breast cancer [330]. miRNA-218 initiates apoptosis by downregulating BMI1 in colon cancer [331]. miR-128a inhibits the growth of medulloblastoma cells by reducing BMI1 expression, which resulted in changes of the intracellular redox state of the tumor cells, thus promoting cellular senescence [319].

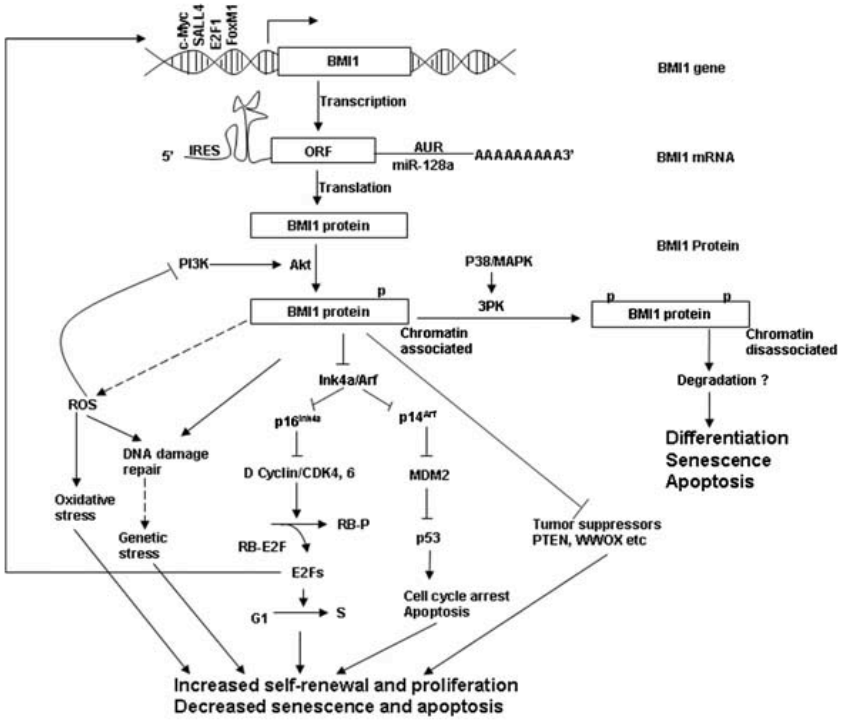

Figure 8: Schematic representation of different mechanisms regulating Bmi1 expression and its downstream signaling pathways. Adapted from Cao L., Bombard J., et al., *Bmi1 as a novel target for drug discovery in cancer*. J. Cell Biochem. 2011. 112:2729-41.

Since we demonstrated that *Bmi1* deficiency promotes progeria and ageing, we hypothesized that it is also implicated in ageing-related neurodegenerative disorders such as late onset Alzheimer's disease. Furthermore, since *Bmi1* acts as a chromatin remodeler via its mediated H2A ubiquitylation, we speculate that this pathological phenomenon is due to altered chromatin formation. We used aged *Bmi1* heterozygous mice to analyze for LOAD hallmarks and defective chromatin structure.

References:

1. Burtner CR, Kennedy BK., *Progeria syndromes and ageing: what is the connection?* Nat Rev Mol Cell Biol. 2010. 11(8):567-78.

2. MedawarP., *An unsolved problem in biology* (H.K. lewis, London, 1952).

3. Williams, G. C., *Pleiotropy, natural selection and the evolution of senescence*. Evolution, 1957. 11, 398–411.

4. Kirkwood. T.B., *Evolution of ageing*. Nature, 1977. 270, 301-304.

5. Kirkwood T. B. & Holliday R., *The evolution of ageing and longevity*. Proc. R. Soc. Lond. B Biol. Sci. 1979. 205,531–546.

6. Harman D., *Aging: a theory based on free radical and radiation chemistry*. J.Gerontol. 1956. 11, 298-300.

7. Loeb LA., Wallace DC., et al., *The mitochondrial theory of aging and its relationship to reactive oxygen species damage and somatic mtDNA mutations*. Proc Natl Acad Sci U S A. 2005. 102(52):18769-70.

8. Bouayed J, Bohn T., *Exogenous antioxidants - Double-edged swords in cellular redox state: Health beneficial effects at physiologic doses versus deleterious effects at high doses*. Oxid Med Cell Longev. 2010. 3(4):228-237.

9. Sanz A., Stefanatos RK., *The mitochondrial free radical theory of aging: a critical view.* Curr Aging Sci. 2008. 1(1):10-21.

10. Schriner, S. E. et al., *Extension of murine life span by overexpression of catalase targeted to mitochondria.* Science 2005. 308, 1909–1911.

11. Landis G. N. & Tower J., *Superoxide dismutase evolution and life span regulation*. Mech. Ageing Dev. 2005. 126, 365–379.

12. Van Raamsdonk, J. M. & Hekimi, S. , *Deletion of the mitochondrial superoxide dismutase sod-2 extends lifespan in Caenorhabditis elegans*. PLoS Genet. 2009. 5, e1000361.

13. Perez, V. I., et al., *Is the oxidative stress theory of aging dead?* Biochim. Biophys. Acta 2009. 1790, 1005–1014.

14. Gems, D. & Doonan, R., *Antioxidant defense and aging in C. elegans: is the oxidative damage theory of aging wrong?* Cell Cycle 2009. 8, 1681–1687.

15. Clark TA, Lee HP, et al., *Oxidative Stress and its Implications for Future Treatments and Management of Alzheimer Disease*. Int J Biomed Sci. 2010. 6(3):225-227.

16. McCay CM, Crowell MF, Maynard LA., *The effect of retarded growth upon the length of life span and upon the ultimate body size 1935*. Nutrition 1989. 5(3):155-71

17. Barrows CH, Kokkonen GC., *Dietary restriction and life extension, biological mechanisms*. Nutritional approaches to aging research. Boca Raton, FL: CRC Press Inc, 1982:219–43.

18. Weindruch R., Walford RL., *The retardation of aging and disease by dietary restriction*. Springfield, IL: Charles C Thomas Publisher, 1988.

19. Kagawa Y., *Impact of westernization on the nutrition of Japanese: changes in physique, cancer, longevity and centenarians.* Prev Med 1978. 7:205–17.

20. Heilbronn LK, Ravussin E., *Calorie restriction and aging: review of the literature and implications for studies in humans.* Am J Clin Nutr. 2003.78(3):361-9.

21. Lin SJ., Kaeberlain M., et al., *Calorie restriction extends Saccharomyces cerevisiae lifespan by increasing respiration.* Nature. 2002. 418(6895):344-8.

22. Kaeberlein M, McVey M, Guarente L., *The SIR2/3/4 complex and SIR2 alone promote longevity in Saccharomyces cerevisiae by two different mechanisms.* Genes.Dev. 1999. (19):2570-80.

23. Rogina B, Helfand SL., *Sir2 mediates longevity in the fly through a pathway related to calorie restriction.* Proc Natl Acad Sci U S A. 2004. 101(45):15998-6003.

24. Sinclair DA, Guarente L., *Extrachromosomal rDNA circles--a cause of aging in yeast.* Cell. 1997. 91(7):1033-42.

25. Tissenbaum HA, Guarente L., *Increased dosage of a sir-2 gene extends lifespan in Caenorhabditis elegans.* Nature. 2001. 410(6825):227-30.

26. Tanny JC, Dowd GJ, et al., *An enzymatic activity in the yeast Sir2 protein that is essential for gene silencing.* Cell. 1999. 99(7):735-45.

27. Imai S, Johnson FB, et al., *Sir2: an NAD-dependent histone deacetylase that connects chromatin silencing, metabolism, and aging.* Cold Spring Harb Symp Quant Biol. 2000. 65:297-302.

28. Landry J, Slama JT, Sternglanz R., *Role of NAD(+) in the deacetylase activity of the SIR2-like proteins.* Biochem Biophys Res Commun. 2000. 278(3):685-90.

29. Frye RA., *Phylogenetic classification of prokaryotic and eukaryotic Sir2-like proteins.* Biochem Biophys Res Commun. 2000. 273(2):793-8.

30. Guarente L., *Sirtuins in aging and disease*. Cold Spring Harb Symp Quant Biol. 2007.72:483-8.

31. Luo J, Nikolaev AY,et al., *Negative control of p53 by Sir2alpha promotes cell survival under stress.* Cell. 2001. 107(2):137-48.

32. Cohen HY, Miller C, et al., *Calorie restriction promotes mammalian cell survival by inducing the SIRT1 deacetylase.* Science. 2004.305(5682):390-2.

33. Bitterman KJ, Wall NR, et al., *Modulation of NF-kappaB-dependent transcription and cell survival by the SIRT1 deacetylase.* EMBO J. 2004. 23(12):2369-80.

34. Yeung F, Hoberg JE, *Human SirT1 interacts with histone H1 and promotes formation of facultative heterochromatin.* Mol Cell. 2004. 16(1):93-105.

35. Jiang M, Wang J, et al., *Neuroprotective role of Sirt1 in mammalian models of Huntington's disease through activation of multiple Sirt1 targets*. Nat Med. 2011. 18(1):153-8.

36. Cheng HL, Mostoslavsky R, et al., *Developmental defects and p53 hyperacetylation in Sir2 homolog (SIRT1)-deficient mice*. Proc Natl Acad Sci U S A. 2003. 100(19):10794-9.

37. Brunet A, Sweeney LB, et al., *Stress-dependent regulation of FOXO transcription factors by the SIRT1 deacetylase.* Science. 2004. 303(5666):2011-5.

38. Motta MC, Divecha N, et al., *Mammalian SIRT1 represses forkhead transcription factors.* Cell. 2004. 116(4):551-63.

39. Chen J, Zhou Y, et al., *SIRT1 protects against microglia-dependent amyloid-beta toxicity through inhibiting NF-kappaB signaling*. J Biol Chem. 2005. 280(48):40364-74.

40. Kanfi Y, Naiman S, et al., *The sirtuin SIRT6 regulates lifespan in male mice.* Nature. 2012. 483(7388):218-21.

41. Rose G, Dato S, et al., *Variability of the SIRT3 gene, human silent information regulator Sir2 homologue, and survivorship in the elderly*. Exp Gerontol. 2003. 38(10):1065-70.

42. Bellizzi D, Rose G, et al., *A novel VNTR enhancer within the SIRT3 gene, a human homologue of SIR2, is associated with survival at oldest ages.* Genomics. 2005. 85(2): 258-63.

43. Blagosklonny MV., Hall M., *Growth and ageing: a common molecular mechanism.* Aging 2009. 1 (4): 357-362.

44. Wullschleger S, Loewith R, Hall MN., *TOR signaling in growth and metabolism*. Cell. 2006. 124:471-484.

45. Avruch J, Hara K, et al., *Insulin and amino-acid regulation of mTOR signaling and kinase activity through the Rheb GTPase*. Oncogene. 2006. 25:6361-6372.

46. Manning BD, Cantley LC., *AKT/PKB signaling: navigating downstream*. Cell. 2007.129:1261-1274.

47. Powers T. *TOR signaling and S6 kinase 1: Yeast catches up*. Cell Metab. 2007;6:1-2.

48. Kaeberlein M, Powers RWr, et al., *Regulation of yeast replicative life span by TOR and Sch9 in response to nutrients*. Science 2005. 310:1193-1196.

49. Powers RWr, Kaeberlein M, et al., *Extension of chronological life span in yeast by decreased TOR pathway signaling*. Genes Dev. 2006. 20:174-184.

50. Kennedy BK, Austriaco NRJ, Guarente L., *Daughter cells of Saccharomyces cerevisiae from old mothers display a reduced life span*. J Cell Biol. 1994. 127:1985-1993.

51. Vellai T, Takacs-Vellai K, et al., *Genetics: influence of TOR kinase on lifespan in C. elegans*. Nature 2003. 426:620.

52. Jia K, Chen D, Riddle DL. *The TOR pathway interacts with the insulin signaling pathway to regulate C. elegans larval development, metabolism and life span.* Development 2004. 131:3897-3906.

53. Luong N, Davies CR, et al., *Activated FOXO-mediated insulin resistance is blocked by reduction of TOR activity.* Cell Metab. 2006. 4:133-142.

54. Pinkston JM, Garigan D, Hansen M, Kenyon C. *Mutations that increase the life span of C. elegans inhibit tumor growth.* Science. 2006;313:971-975.

55. Blüher M, Kahn BB, Kahn CR. *Extended longevity in mice lacking the insulin receptor in adipose tissue.* Science. 2003;299:572-574.

56. Guarente L, Kenyon C. *Genetic pathways that regulate ageing in model organisms.* Nature. 2000;408:255-262.

57. Bartke A. *Long-lived Klotho mice: new insights into the roles of IGF-1 and insulin in aging*. Trends Endocrinol Metab. 2006;17:33-35.

58. Sonntag WE, Carter CS, et al., *Adult-onset growth hormone and insulin-like growth factor I deficiency reduces neoplastic disease, modifies age-related pathology, and increases life span.* Endocrinology. 2005;146:2920-2932.

59. Klionsky DJ. *Autophagy: from phenomenology to molecular understanding in less than a decade.* Nat Rev Mol Cell Biol. 2007.

60. Rubinsztein DC. *The roles of intracellular protein degradation pathways in neurodegeneration.* Nature. 2006;443:780-786.

61. Gu Y, Wang C, Cohen A. *Effect of IGF-1 on the balance between autophagy of dysfunctional mitochondria and apoptosis*. FEBS Lett. 2004;577:357-360.

62. Melendez A, Talloczy Z, Seaman M, Eskelinen EL, Hall DH, Levine B. *Autophagy genes are essential for dauer development and lifespan extension in C. elegans.* Science. 2003;301:1387-1391.

63. Syntichaki P, Troulinaki K, Tavernarakis N. *eIF4E function in somatic cells modulates ageing in Caenorhabditis elegans*. Nature. 2007;445:922-926.

64. Pan KZ, Palter JE, Rogers AN, Olsen A, Chen D, Lithgow GJ, Kapahi P. *Inhibition of mRNA translation extends lifespan in Caenorhabditis elegans*. Aging Cell. 2007;6:111-119.

65. Hansen M, Taubert S, Crawford D, Libina N, Lee SJ, Kenyon C. *Lifespan extension by conditions that inhibit translation in Caenorhabditis elegans.* Aging Cell. 2007;6:95-110.

66. Medvedik O, Lamming DW, Kim KD, Sinclair DA. *MSN2 and MSN4 Link Calorie Restriction and TOR to Sirtuin-Mediated Lifespan Extension in Saccharomyces cerevisiae*. PLoS Biol. 2007;5:e261.

67. Khurana V, Lu Y, Steinhilb ML, Oldham S, Shulman JM, Feany MB. *TOR-mediated cell-cycle activation causes neurodegeneration in a Drosophila tauopathy model.* Curr Biol. 2006;16:230-241.

68. An WL, Cowburn RF, Li L, et al., *Up-regulation of phosphorylated/activated p70 S6 kinase and its relationship to neurofibrillary pathology in Alzheimer's disease.* Am J Pathol. 2003;163:591-607.

69. Berger Z, Ravikumar B, et al., *Rapamycin alleviates toxicity of different aggregate-prone proteins.* Hum Mol Genet. 2006;15:433-442.

70. Hayflick, L., Moorhead, P.S., *The serial cultivation of human diploid cell strains*. Exp. Cell Res.1961. 25, 585–621.

71. Campisi, J., d'Adda di Fagagna, F. *Cellular senescence: when bad things happen to good cells.* Nat. Rev. Mol. Cell Biol. 2007. 8, 729–740.

72. Sedivy, J.M., Munoz-Najar, U.M., Jeyapalan, J.C., Campisi, J. *Cellular senescence: a link between tumor suppression and organismal aging?* In: Guarente, L., Partridge, L. (Eds.), The Molecular Biology of Aging. 2007. Cold Spring Harbor Laboratory Press, Cold Spring Harbor, NY.

73. DiLeonardo, A., Linke, S. P., Clarkin, K. & Wahl, G. M. *DNA damage triggers a prolonged p53-dependent G1 arrest and long-term induction of Cip1 in normal human fibroblasts.* Genes Dev. 1994. 8, 2540–2551.

74. Narita, M. et al., *Rb–mediated heterochromatin formation and silencing of E2F target genes during cellular senescence*. Cell 2003. 113, 703–716.

75. Herbig, U., Jobling, W. A., Chen, B. P., Chen, D. J. & Sedivy, J. *Telomere shortening triggers senescence of human cells through a pathway involving ATM, p53, and p21(CIP1), but not p16(INK4a)*. Mol. Cell 2004. 14, 501–513.

76. Ogryzko, V. V., Hirai, T. H., Russanova, V. R., Barbie, D. A. & Howard, B. H. *Human fibroblast commitment to a senescence-like state in response to histone deacetylase inhibitors is cell cycle dependent*. Mol. Cell. Biol. 1996. 16, 5210–5218.

77. Serrano, M., Lin, A. W., McCurrach, M. E., Beach, D. & Lowe, S. W. *Oncogenic ras provokes premature cell senescence associated with accumulation of p53 and p16INK4a.* Cell 1997. 88, 593–602.

78. Hampel, B., Malisan, F., Niederegger, H., Testi, R. & Jansen-Durr, P. *Differential regulation of apoptotic cell death in senescent human cells*. Exp. Gerontol. 2004.

39,1713–1721.

79. McClintock B. *The behavior in successive nuclear divisions of a chromosome broken at meiosis*. Proc Natl Acad Sci USA 1939. 25: 405–416.

80. Muller HJ. *The re-making of chromosomes.* Collecting Net, Woods Hole 1938. 13: 181–198.

81. Moyzis RK, Buckingham JM, Cram LS, Dani M, Deaven LL, Jones MD, Meyne J, Ratliff RL, Wu JR. *A highly conserved repetitive DNA sequence, (TTAGGG)n, present at the telomeres of human chromosomes*. Proc Natl Acad Sci USA 1988. 85: 6622–6626.

82. Olovnikov AM. *A theory of marginotomy. The incomplete copying of template margin in enzymic synthesis of polynucleotides and biological significance of the phenomenon*. J Theor Biol 1973. 41: 181–190.

83. Bodnar AG, Ouellette M, Frolkis M, Holt SE, Chiu CP, Morin GB, Harley CB, Shay JW, Lichtsteiner S, Wright WE. *Extension of life-span by introduction of telomerase into normal human cells*. Science 1998. 279: 349–352.

84. Hathcock KS, Hemann MT, Opperman KK, Strong MA, Greider CW, Hodes RJ. *Haploinsufficiency of mTR results in defects in telomere elongation*. Proc Natl Acad Sci USA 2002. 99: 3591–3596.

85. d'Adda di Fagagna F, Hande MP, Tong WM, Roth D, Lansdorp PM, Wang ZQ, Jackson SP. *Effects of DNA nonhomologous end-joining factors on telomere length and chromosomal stability in mammalian cells*. Curr Biol 2001. 11: 1192–1196.

86. Von Zglinicki T. *Role of oxidative stress in telomere length regulation and replicative senescence.* Ann NY Acad Sci 2000. 908: 99–110.

87. Jeyapalan JC, Ferreira M, Sedivy JM, Herbig U. *Accumulation of senescent cells in mitotic tissue of aging primates*. Mech Ageing Dev 2007. 128: 36–44.

88. d'Adda di Fagagna F, Reaper PM, Clay-Farrace L, Fiegler H, Carr P, Von Zglinicki T, Saretzki G, Carter NP, Jackson SP. *A DNA damage checkpoint response in telomere-initiated senescence*. Nature 2003. 426: 194–198.

89. Takai H, Smogorzewska A, de Lange T. *DNA damage foci at dysfunctional telomeres.* Curr Biol 2003. 13: 1549–1556.

90. Jeyapalan JC, Ferreira M, Sedivy JM, Herbig U. *Accumulation of senescent cells in mitotic tissue of aging primates*. Mech Ageing Dev 2007. 128: 36–44.

91. Autexier C, Lue NF. *The structure and function of telomerase reverse transcriptase*. Annu Rev Biochem 2006. 75: 493–517.

92. Collins K. *The biogenesis and regulation of telomerase holoenzymes*. Nat Rev Mol Cell Biol 2006. 7: 484–494.

93. Harrington L, McPhail T, Mar V, Zhou W, Oulton R, Bass MB, Arruda I, Robinson MO. *A mammalian telomerase-associated protein.* Science 1997. 275: 973–977.

94. Meyerson M, Counter CM, Eaton EN, Ellisen LW, Steiner P, Caddle SD, Ziaugra L, Beijersbergen RL, Davidoff MJ, Liu Q, Bacchetti S, Haber DA, Weinberg RA. *hEST2, the putative human telomerase catalytic subunit gene, is up-regulated in tumor cells and during immortalization*. Cell 1997. 90: 785–795.

95. Feng J, Funk WD, Wang SS, Weinrich SL, Avilion AA, Chiu CP, Adams RR, Chang E, Allsopp RC, Yu J. *The RNA component of human telomerase*. Science 1995. 269: 1236–1241.

96. Aubert G., Landsdorp P., *Telomeres and aging*. Physiological reviews 2008. 88(2): 557-579.

97. Vulliamy T, Marrone A, Goldman F, Dearlove A, Bessler M, Mason PJ, Dokal I. *The RNA component of telomerase is mutated in autosomal dominant dyskeratosis congenita*. Nature 2001. 413: 432–435.

98. Vulliamy T, Marrone A, Szydlo R, Walne A, Mason PJ, Dokal I. *Disease anticipation is associated with progressive telomere shortening in families with dyskeratosis congenita due to mutations in TERC*. Nat Genet 2004. 36: 447–449.

99. Vulliamy TJ, Walne A, Baskaradas A, Mason PJ, Marrone A, Dokal I. *Mutations in the reverse transcriptase component of telomerase (TERT) in patients with bone marrow failure*. Blood Cells Mol Dis 2005. 34: 257–263.

100. Yamaguchi H, Calado RT, Ly H, Kajigaya S, Baerlocher GM, Chanock SJ, Lansdorp PM, Young NS. *Mutations in TERT, the gene for telomerase reverse transcriptase, in aplastic anemia*. N Engl J Med 2005. 352: 1413–1424.

101. Armanios MY, Chen JJ, Cogan JD, Alder JK, Ingersoll RG, Markin C, Lawson WE, Xie M, Vulto I, Phillips JA 3rd, Lansdorp PM, Greider CW, Loyd JE. *Telomerase mutations in families with idiopathic pulmonary fibrosis*. N Engl J Med 2007. 356: 1317–1326.

101. Eriksson M, Brown WT, Gordon LB, Glynn MW, Singer J, Scott L, Erdos MR, Robbins CM, Moses TY, Berglund P, Dutra A, Pak E, Durkin S, Csoka AB,

Boehnke M, Glover TW, Collins FS. *Recurrent de novo point mutations in lamin A cause Hutchinson-Gilford progeria syndrome*. Nature 2003. 423: 293–298.

102. Crabbe L, Verdun RE, Haggblom CI, Karlseder J. *Defective telomere lagging strand synthesis in cells lacking WRN helicase activity*. Science 2004. 306: 1951–1953.

103. Chang S, Multani AS, Cabrera NG, Naylor ML, Laud P, Lombard D, Pathak S, Guarente L, DePinho RA. *Essential role of limiting telomeres in the pathogenesis of Werner syndrome*. Nat Genet 2004. 36: 887–882.

104. Epel ES, Blackburn EH, Lin J, Dhabhar FS, Adler NE, Morrow JD, Cawthon RM. *Accelerated telomere shortening in response to life stress*. Proc Natl Acad Sci USA 2004. 101: 17312–17315.

105. Minamino T, Komuro I. *Vascular cell senescence: contribution to atherosclerosis*. Circ Res 2007. 100: 15–26.

106. Epel ES, Lin J, Wilhelm FH, Wolkowitz OM, Cawthon R, Adler NE, Dolbier C, Mendes WB, Blackburn EH. *Cell aging in relation to stress arousal and cardiovascular disease risk factors*. Psychoneuroendocrinology 2006. 31: 277–287.

107. Panossian LA, Porter VR, Valenzuela HF, Zhu X, Reback E, Masterman D, Cummings JL, Effros RB. *Telomere shortening in T cells correlates with Alzheimer's disease status.* Neurobiol Aging. 2003. 24(1):77-84.

108. Sherr, C.J., Roberts, J.M., *CDK inhibitors: positive and negative regulators of G1-phase progression*. Genes Dev. 1999. 13, 1501–1512.

109. Gil, J., Peters, G. *Regulation of the INK4b-ARF-INK4a tumour suppressor locus:*

all for one or one for all. Nat. Rev. Mol. 2006. Cell Biol. 7, 667–677

110. Kim,W.Y., Sharpless, N.E. *The regulation of INK4/ARF in cancer and aging*. Cell 2006. 127, 265–275.

111. Michaloglou, C., Vredeveld, L.C., Soengas, M.S., Denoyelle, C., Kuilman, T., van der Horst, C.M., Majoor, D.M., Shay, J.W., Mooi, W.J., Peeper, D.S. *BRAFE600- associated senescence-like cell cycle arrest of human naevi*. Nature 2005. 436, 720–724.

112. Ressler, S., Bartkova, J., Niederegger, H., Bartek, J., Scharffetter-Kochanek, K., Jansen-Durr, P., Wlaschek, M. *p16INK4A is a robust in vivo biomarker of cellular aging in human skin*. Aging Cell 2006. 5, 379–389.

113. Passegue´ , E., Wagner, E.F. *JunB suppresses cell proliferation by transcriptional activation of p16(INK4a) expression*. EMBO 2000. J. 19, 2969–2979.

114. Ohtani, N., Zebedee, Z., Huot, T.J., Stinson, J.A., Sugimoto, M., Ohashi, Y., Sharrocks, A.D., Peters, G., Hara, E. *Opposing effects of Ets and Id proteins on p16INK4a expression during cellular senescence*. Nature 2001. 409, 1067–1070.

115. Krishnamurthy, J., Torrice, C., Ramsey, M.R., Kovalev, G.I., Al-Regaiey, K., Su, L., Sharpless, N.E. *Ink4a/Arf expression is a biomarker of aging*. J. Clin. Invest. 2004. 114, 1299–1307.

116. Yogev, O., Anzi, S., Inoue, K., E S. *Induction of transcriptionally active Jun proteins regulates drug-induced senescence*. J. Biol. Chem. 2006. 281, 34475–34483.

117. Bracken, A.P., Kleine-Kohlbrecher, D., Dietrich, N., Pasini, D., Gargiulo, G.,

Beekman, C., Theilgaard-Monch, K., Minucci, S., Porse, B.T., Marine, J.C., Hansen, K.H., Helin, K. *The Polycomb group proteins bind throughout the INK4A-ARF locus and are disassociated in senescent cells*. Genes Dev.2007. 21, 525–530.

118. Lewis, J.L., Chinswangwatanakul, W., Zheng, B., Marley, S.B., Nguyen, D.X., Cross, N.C., Banerji, L., Glassford, J., Thomas, N.S., Goldman, J.M., Lam, E.W., Gordon, M.Y.*The influence of INK4 proteins on growth and self-renewal kinetics of hematopoietic progenitor cells*. Blood 2001. 97, 2604–2610.

119. Meng, A., Wang, Y., Van Zant, G., Zhou, D. *Ionizing radiation and busulfan induce premature senescence in murine bone marrow hematopoietic cells*. Cancer Res. 2003. 63, 5414–5419.

120. Park, I.K., Qian, D., Kiel, M., Becker, M.W., Pihalja, M., Weissman, I.L., Morrison, S.J., Clarke, M.F. *Bmi-1 is required for maintenance of adult self-renewing haematopoietic stem cells*. Nature 2003. 423, 302–305.

121. Lessard, J., Sauvageau, G. *Bmi-1 determines the proliferative capacity of normal and leukaemic stem cells*. Nature 2003. 423, 255–260.

122. Molofsky, A.V., Pardal, R., Iwashita, T., Park, I.K., Clarke, M.F., Morrison, S.J. *Bmi-1 dependence distinguishes neural stem cell self-renewal from progenitor proliferation.* Nature 2003. 425, 962–967.

123. Janzen, V., Forkert, R., Fleming, H.E., Saito, Y., Waring, M.T., Dombkowski, D.M.,Cheng, T., DePinho, R.A., Sharpless, N.E., Scadden, D.T. *Stem-cell ageing modified by the cyclin-dependent kinase inhibitor p16INK4a.* Nature 2006. 443, 421–426.

124. Krishnamurthy, J., Ramsey, M.R., Ligon, K.L., Torrice, C., Koh, A., Bonner-

Weir, S., Sharpless, N.E. *p16INK4a induces an age-dependent decline in islet regenerative potential*. Nature 2006. 443, 453–457.

125. Molofsky, A.V., Slutsky, S.G., Joseph, N.M., He, S., Pardal, R., Krishnamurthy, J., Sharpless, N.E., Morrison, S.J. *Increasing p16INK4a expression decreases forebrain progenitors and neurogenesis during ageing*. Nature 2006. 443, 448–452.

126. Keyes, W.M., Wu, Y., Vogel, H., Guo, X., Lowe, S.W., Mills, A.A. *p63 deficiency activates a program of cellular senescence and leads to accelerated aging*. GenesDev. 2005. 19, 1986–1999.

127. Keyes, W.M., Mills, A.A. *p63: a new link between senescence and aging*. Cell Cycle 2006. 5, 260–265.

128. Melk, A., Ramassar, V., Helms, L.M., Moore, R., Rayner, D., Solez, K., Halloran, P.F. *Telomere shortening in kidneys with age*. J. Am. Soc. Nephrol. 2000. 11, 444–453.

129. Chkhotua, A.B., Gabusi, E., Altimari, A., D'Errico, A., Yakubovich, M., Vienken, J., Stefoni, S., Chieco, P., Yussim, A., Grigioni, W.F. *Increased expression of p16(INK4a) and p27(Kip1) cyclin-dependent kinase inhibitor genes in aging human kidney and chronic allograft nephropathy*. Am. J. Kidney Dis. 2003. 41, 1303–1313.

130. Kajstura, J., Pertoldi, B., Leri, A., Beltrami, C.A., Deptala, A., Darzynkiewicz, Z., Anversa, P. *Telomere shortening is an in vivo marker of myocyte replication and aging*. Am. J. Pathol.2000. 156, 813–819.

131. Chimenti, C., Kajstura, J., Torella, D., Urbanek, K., Heleniak, H., Colussi, C., Di Meglio, F., Nadal-Ginard, B., Frustaci, A., Leri, A., Maseri, A., Anversa, P.

Senescence and death of primitive cells and myocytes lead to premature cardiac aging and heart failure. Circ. Res. 2003. 93, 604–613.

132. Torella, D., Rota, M., Nurzynska, D., Musso, E., Monsen, A., Shiraishi, I., Zias, E., Walsh, K., Rosenzweig, A., Sussman, M.A., Urbanek, K., Nadal-Ginard, B., Kajstura, J., Anversa, P., Leri, A.*Cardiac stem cell and myocyte aging, heart failure, and insulin-like growth factor-1 overexpression*. Circ. Res. 2004. 94, 514-524.

133. Kirkwood, T. B. *Understanding the odd science of aging*. Cell 2005. 120, 437–447.

134. Garinis G., Van der Horst G., et al., *DNA damage and ageing: new-age ideas for an age-old problem*. Nature cell biology 2008. 10 (11) 1241-1247.

135. d'Adda di Fagagna, F., Teo, S. H. & Jackson, S. P. *Functional links between telomeres and proteins of the DNA-damage response*. Genes Dev. 2004. 18, 1781–1799.

136. Harper, J. W. & Elledge, S. J. *The DNA damage response: ten years after*. Mol. Cell 2007. 28, 739–745.

137. Hoeijmakers, J. H. *Genome maintenance mechanisms for preventing cancer*. Nature 2001. 411, 366–374.

138. De Bont, R. & van Larebeke, N. *Endogenous DNA damage in humans: a review of quantitative data*. Mutagenesis 2004. 19, 169–185.

139. Grillari, J., Katinger, H. & Voglauer, R. *Contributions of DNA interstrand cross-links to aging of cells and organisms*. Nucleic Acids Res. 2007. 35, 7566–7576.

140. Beeharry, N. & Broccoli, D. *Telomere dynamics in response to chemotherapy*. Curr. Mol. Med. 2005. 5, 187–196.

141. Vijg, J. *Somatic mutations and aging: a re-evaluation*. Mutat. Res. 2000. 447, 117–135.

142. Plosky, B. S. & Woodgate, R. *Switching from high-fidelity replicases to low-fidelity lesion-bypass polymerases*. Curr. Opin. Genet. 2004. Dev. 14, 113–119.

143. Martin, G. M. *Genetic modulation of senescent phenotypes in Homo sapiens*. Cell 2005. 120, 523–532.

145. Vilhem Bohr, D. W., de Souza Pinto, N. C., van der Pluijm, I. & Hoeijmakers, J. H. *DNA Repair and Aging*, (Cold Spring Harbor Laboratory Press, New York, 2008).

146. Hasty, P. & Vijg, J. Rebuttal to Miller: *'Accelerated aging': a primrose path to insight?*' Aging Cell 2004. 3, 67–69.

147. Miller, R. A. *'Accelerated aging': a primrose path to insight?* Aging Cell 2004. 3, 47–51.

148. Sinclair D., Oberdoerffer P., *The ageing epigenome: Damaged beyond repair?* Ageing Res. Reviews. 2009. 8:189-198.

149. Hansen JC. *Conformational dynamics of the chromatin fiber in solution: determinants, mechanisms and functions*. Annu Rev Biophys Biomol Struct 2002. 31:361-92.

150. Luger K, Mäder AW, Richmond RK, Sargent DF, Richmond TJ. *Crystal structure of the nucleosome core particle at 2.8 A resolution*. Nature 1997. 389:251-60.

151. Wallrath LL. *Unfolding the mysteries of heterochromatin*. Curr Opin Genet Dev 1998. 8:147-53;

152. Grewal SI, Moazed D. *Heterochromatin and epigenetic control of gene expression*. Science 2003; 301:798-802.

153. Martin C, Zhang Y. *The diverse functions of histone lysine methylation*. Nat Rev Mol Cell Biol 2005. 6:838-49.

154. Eissenberg JC, Elgin SC. *The HP1 protein family: getting a grip on chromatin*. Curr Opin Genet Dev 2000. 10:204-210.

155. Villeponteau B. *The heterochromatin loss model of aging*. Exp Gerontol 1997. 32:383-94.

156. Hennekam RC. *Hutchinson-Gilford progeria syndrome: review of the phenotype.* Am J Med Genet A. 2006. 140(23):2603-24.

157. Shumaker DK, Dechat T. *Mutant nuclear lamin A leads to progressive alterations of epigenetic control in premature aging*. Proc Natl Acad Sci U S A. 2006. 103(23): 8703-8.

158. Pegoraro G, Misteli T. *Ageing-related chromatin defects through loss of the NURD complex.* Nat Cell Biol. 2009 Oct;11(10):1261-7.

159. Yu CE, Oshima J, Fu YH, Wijsman EM, Hisama F, Alisch R, Matthews S, Nakura J, Miki T, Ouais S, Martin GM, Mulligan J, Schellenberg GD. *Positional cloning of the Werner's syndrome gene*. Science. 1996. 272(5259):258-62.

160. Salk D. *Werner's syndrome: a review of recent research with an analysis of*

connective tissue metabolism, growth control of cultured cells, and chromosomal aberrations. Hum Genet. 1982. 62(1):1-5.

161. Haithcock E, Dayani Y, Neufeld E, Zahand AJ, Feinstein N, Mattout A, et al. *Age-related changes of nuclear architecture in Caenorhabditis elegans*. Proc Natl Acad Sci USA 2005. 102:16690-5.

162. Brandt A, Krohne G, Grosshans J. *The farnesylated nuclear proteins KUGELKERN and LAMIN B promote aging-like phenotypes in Drosophila flies*. Aging Cell 2008. 7:541-51.

163. Larson K, Yan SJ, Tsurumi A, Liu J, Zhou J, Gaur K, et al. *Heterochromatin formation promotes longevity and represses ribosomal RNA synthesis.* PLoS Genet 2012. 8:1002473.

164. Demontis F, Perrimon N. *Integration of Insulin receptor/Foxo signaling and dMyc activity during muscle growth regulates body size in Drosophila*. Development 2009. 136:983-93.

165. Nakagawa-yagi Y., Sato Y., et al., *Pharmacological modulation of histone demethylase activity by a small molecule isolated from subcritical water extracts of Sasa senanensis leaves prolongs the lifespan of Drosophila melanogaster.* BMC Complementary and Alternative medicine 2012. 12:101.

166. Scaffidi P, Misteli T. *Lamin A-dependent nuclear defects in human aging*. Science 2006. 312:1059-63.

167. Gaubatz JW, Cutler RG. *Mouse satellite DNA is transcribed in senescent cardiac muscle*. J Biol Chem 1990. 265:17753-17758.

168. Haider S., Cordeddu L., et al., *The landscape of DNA repeat elements in human*

heart failure. Genome biology 2012. 13:R90.

169. Sedivy JM, Banumathy G, Adams PD. *Aging by epigenetics—a consequence of chromatin damage?* Exp Cell Res 2008. 314:1909-17.

170. Richardson B. *Impact of aging on DNA methylation*. Ageing Res Rev 2003. 2:245-61.

171. Bollati V, Schwartz J, Wright R, Litonjua A, Tarantini L, Suh H, et al. *Decline in genomic DNA methylation through aging in a cohort of elderly subjects.* Mech Ageing Dev 2009. 130:234-9.

172. Bellizzi D, D'Aquila P, Montesanto A, Corsonello A, Mari V, Mazzei B, et al. *Global DNA methylation in old subjects is correlated with frailty*. Age (Dordr) 2012. 34:169-79.

173. Wilson VL, Jones PA. *DNA methylation decreases in aging but not in immortal cells*. Science 1983. 220:1055-7.

174. Lopatina N, Haskell JF, Andrews LG, Poole JC, Saldanha S, Tollefsbol T. *Differential maintenance and de novo methylating activity by three DNA methyltransferases in aging and immortalized fibroblasts*. J Cell Biochem 2002. 84:324-34.

175. Casillas MA Jr, Lopatina N, Andrews LG, Tollefsbol TO. *Transcriptional control of the DNA methyltransferases is altered in aging and neoplastically transformed human fibroblasts*. Mol Cell Biochem 2003. 252:33-43.

176. Selkoe D., Mandelkow E., et al., *Deciphering Alzheimer's disease*. Cold Spring Harbor Perspect Med 2012. 2:a011460.

177. Campion D, Dumanchin C. *Early-onset autosomal dominant Alzheimer disease: prevalence, genetic heterogeneity, and mutation spectrum*. Am J Hum Genet. 1999. 65(3):664-70.

178. Harvey RJ, Skelton-Robinson M, Rossor MN. *The prevalence and causes of dementia in people under the age of 65 years.* J Neurol Neurosurg Psychiatry. 2003. 74(9):1206-9.

179. Corder, E.H., Saunders, A.M., Strittmatter, W.J., Schmechel, D.E., Gaskell, P.C., Small, G.W., Roses, A.D., Haines, J.L., and Pericak-Vance, M.A. *Gene dose of apolipoprotein E type 4 allele and the risk of Alzheimer's disease in late onset families*. Science 1993. 261, 921–923.

180. Rogaeva E, Meng Y, Lee JH, et al. *The neuronal sortilin-related receptor SORL1 is genetically associated with Alzheimer disease*. Nat Genet 2007. 39:168-77.

181. Lambert JC, Heath S, Even G, et al. *Genome-wide association study identifies variants at CLU and CR1 associated with Alzheimer's disease*. Nat Genet 2009. 41:1094-9.

182. Sager KL, Wuu J, Leurgans SE, et al. *Neuronal LR11/sorLA expression is reduced in mild cognitive impairment*. Ann Neurol 2007. 62:640-7.

183. Rogaeva E, Meng Y, Lee JH, et al. *The neuronal sortilin-related receptor SORL1is genetically associated with Alzheimer disease*. Nat Genet 2007. 39:168-77.

184. Haass C, Selkoe DJ. *Soluble protein oligomers in neurodegeneration: lessons from the Alzheimer's amyloid beta-peptide*. Nat Rev Mol Cell Biol 2007. 8:101-12.

185. Busciglio J, Pelsman A, Wong C, et al. *Altered metabolism of the amyloid beta precursor protein is associated with mitochondrial dysfunction in Down's syndrome*. Neuron 2002. 33:677-88.

186. Selkoe DJ. *Alzheimer's disease: genes, proteins, and therapy*. Physiol Rev 2001. 81:741-66.

187. Tanzi RE, Bertram L. *Twenty years of the Alzheimer's disease amyloid hypothesis: a genetic perspective.* Cell 2005. 120: 545-55.

188. Kayed R, Head E, Thompson JL, et al. *Common structure of soluble amyloid oligomers implies common mechanism of pathogenesis.* Science 2003. 300:486-9.

189. Klein WL, Krafft GA, Finch CE. *Targeting small Abeta oligomers: the solution to an Alzheimer's disease conundrum?* Trends Neurosci 2001. 24:219-24.

190. Walsh DM, Selkoe DJ. *A beta oligomers: a decade of discovery*. J Neurochem 2007;101:1172-84.

191. Kanemitsu H, Tomiyama T, Mori H. *Human neprilysin is capable of degrading amyloid beta peptide not only in the monomeric form but also the pathological oligomeric form.* Neurosci Lett 2003;350:113-6.

192. Qiu WQ, Walsh DM, Ye Z, et al. *Insulin-degrading enzyme regulates extracellular levels of amyloid beta-protein by degradation*. J Biol Chem 1998;273:32730-8.

193. Lee VM, Goedert M, Trojanowski JQ. *Neurodegenerative tauopathies*. Annu Rev Neurosci 2001;24:1121-59.

194. Iqbal K, Alonso Adel C, Chen S, et al. *Tau pathology in Alzheimer disease and*

other tauopathies. Biochim Biophys Acta 2005;1739:198 210.

195. Yoshida H, Hastie CJ, McLauchlan H, Cohen P, Goedert M. *Phosphorylation of microtubule-associated protein tau by isoforms of c-Jun N-terminal kinase (JNK).* J Neurochem. 2004. 90(2):352-8.

196. Khlistunova I, Biernat J, Wang Y, et al. *Inducible expression of Tau repeat domain in cell models of tauopathy: aggregation is toxic to cells but can be reversed by inhibitor drugs.* J Biol Chem 2006;281:1205-14.

197. Santacruz K, Lewis J, Spires T, et al. *Tau suppression in a neurodegenerative mouse model improves memory function.* Science 2005;309:476-81.

198. Goedert M, Jakes R. *Mutations causing neurodegenerative tauopathies.* Biochim Biophys Acta 2005;1739:240-50.

199. Gotz J, Chen F, van Dorpe J, Nitsch RM. *Formation of neurofibrillary tangles in P301l tau transgenic mice induced by Abeta 42 fibrils.* Science 2001;293:1491-5.

200. Lewis J, Dickson DW, Lin WL, et al. *Enhanced neurofibrillary degeneration in transgenic mice expressing mutant tau and APP.* Science 2001;293:1487-91.

201. Lopez Salon M, Morelli L, Casta.o EM, Soto EF, Pasquini JM. *Defective ubiquitination of cerebral proteins in Alzheimer's disease.* J Neurosci Res 2000;62: 302 10.

202. Hoozemans JJ, Veerhuis R, Van Haastert ES, et al. *The unfolded protein response is activated in Alzheimer's disease.* Acta Neuropathol 2005;110:165-72.

203. Selkoe DJ. *Alzheimer's disease is a synaptic failure*. Science 2002;298:789-91.

204. Scheff SW, Price DA, Schmitt FA, DeKosky ST, Mufson EJ. S*ynaptic alterations in CA1 in mild Alzheimer disease and mild cognitive impairment*. Neurology 2007;68:1501-8.

205. Masliah E, Mallory M, Alford M, et al. *Altered expression of synaptic proteins occurs early during progression of Alzheimer's disease*. Neurology 2001;56:127-9.

206. DeKosky ST, Scheff SW. Synapse loss in frontal cortex biopsies in Alzheimer's disease: correlation with cognitive severity. Ann Neurol 1990;27:457-64.

207. Larson J, Lynch G, Games D, Seubert P. Alterations in synaptic transmission and long-term potentiation in hippocampal slices from young and aged PDAPP mice. Brain Res 1999;840:23-35.

208. Shankar GM, Bloodgood BL, Townsend M, Walsh DM, Selkoe DJ, Sabatini BL. Natural oligomers of the Alzheimer amyloid- beta protein induce reversible synapse loss by modulating an NMDA-type glutamate receptor-dependent signaling pathway. J Neurosci 2007;27:2866-75.

209. Snyder EM, Nong Y, Almeida CG, et al.Regulation of NMDA receptor trafficking by amyloid-beta. Nat Neurosci 2005;8:1051-8.

210. Mucke L, Masliah E, Yu GQ, et al. High-level neuronal expression of abeta 1-42 in wild-type human amyloid proteinprecursor transgenic mice: synaptotoxicity without plaque formation. J Neurosci 2000;20:4050-8.

211. Nunomura A, Perry G, Aliev G, et al. Oxidative damage is the earliest event in Alzheimer disease. J Neuropathol Exp Neurol 2001;60:759-67.

212. Hensley K, Carney JM, Mattson MP, et al. A model for beta-amyloid aggregation

and neurotoxicity based on free radical generation by the peptide: relevance to Alzheimer disease. Proc Natl Acad Sci U S A 1994;91:3270-4.

213. Yan SD, Chen X, Fu J, et al. RAGE and amyloid-beta peptide neurotoxicity in Alzheimer's disease. Nature 1996;382:685-91.

214. Keller JN, Mark RJ, Bruce AJ, et al. 4-Hydroxynonenal, an aldehydic product of membrane lipid peroxidation, impairs glutamate transport and mitochondrial function in synaptosomes. Neuroscience 1997;80:685-96.

215. Lasagna-Reeves CA, Castillo-Carranza DL, Sengupta U, Clos AL, Jackson GR, Kayed R. *Tau oligomers impair memory and induce synaptic and mitochondrial dysfunction in wild-type mice.* Mol Neurodegener. 6:39.

216. Pratico D. *Oxidative stress hypothesis in Alzheimer's disease: a reappraisal.* Trends Pharmacol Sci 2008;29:609-15.

217. Lovell MA, Markesbery WR. *Oxidative DNA damage in mild cognitive impairment and late-stage Alzheimer's disease.* Nucleic Acids Res. 2007;35(22):7497-504.

218. Markesbery WR, Lovell MA. *DNA oxidation in Alzheimer's disease.* Antioxid Redox Signal. 2006. 8(11-12):2039-45.

219. Suram A, Hegde ML, Rao KS *A new evidence for DNA nicking property of amyloid beta-peptide (1-42): relevance to Alzheimer's disease.* Arch Biochem Biophys. 2007. 463(2):245-52.

220. Yang Y, Mufson EJ, Herrup K. *Neuronal cell death is preceded by cell cycle events at all stages of Alzheimer's disease.* J Neurosci 2003;23:2557-63.

221. Liu DX, Greene LA. *Neuronal apoptosis at the G1/S cell cycle checkpoint.* Cell Tissue Res 2001;305:217-28.

222. Love S, Barber R, Wilcock GK. *Increased poly(ADP-ribosyl)ation of nuclear proteins in Alzheimer's disease.* Brain 1999. 122 (Pt 2):247-53.

223. Jacobsen E, Beach T, et al., *Deficiency of the Mre11 DNA repair complex in Alzheimer's disease brains.* Brain Res Mol Brain Res. 2004. 128(1):1-7.

224. Shackelford DA. *DNA end joining activity is reduced in Alzheimer's disease.* Neurobiol Aging. 2006. 27(4):596-605.

225. Chintamaneni M., Bhaskar M., *Biomarkers in Alzheimer's disease: a review*. ISRN pharmacology 2012. 984786.

226. Michelle G. *Cell nucleus and chromatin structure.* Fundamentals of biochemistry, cell biology and biophysics. Vol II. Book Chapter.

227. Heitz, E., 1928. *Das heterochromatin der moose*. I. Jahrb.Wiss. Botanik 69, 762–818.

228. Dillon N. *Heterochromatin structure and function.* Biology of the cell 2004. 96:631-637.

229. Charlesworth B., Sniegowski P., Stephan W. *The Evolutionary Dynamics Of Repetitive DNA In Eukaryotes.* Nature 1994. 371215220.

230. Kit S. *Equilibrium Sedimentation In Density Gradients Of DNA Preparations From Animal Tissues*. J. Mol. Biol. 1961. 3711716.

231. Ugarkovic D., Plohl M. *Variation In Satellite DNA Profiles-Causes And Effects*.

EMBO 2002. 2159555959.

232. Patience C., Takeuchi Y., Weiss R.A. *Infection Of Human Cells By An Endogenous Retrovirus Of Pigs*. Nat. Med. 1997. 3276282

233. Richard C., Mark B. *The impact of retrotransposons on human genome evolution*. Nature Reviews Genetics 2009. 1010691703

234. Capy P. *Evolutionary biology. A plastic genome*. Nature 1998. 39667115223

235. Brown T. A. *The Repetitive DNA Content Of Genomes*. Genomes 2002. 5964

236. Debrauwere H., G. C. Gendrel, S. Lechat, M. Dutreix. *Differences and similarities between various tandem repeat sequences: Minisatellites and microsatellites*. Biochimie 1997. 79577586

237. Deepali P. and Sher A. Repetitive DNA: A Tool to Explore Animal Genomes/Transcriptomes, Functional Genomics 2012. ISBN: 978-953-51-0727-9.

238. Buhler M., Verdel A. & Moazed D. *Tethering RITS to a nascent transcript initiates RNAi- and heterochromatin-dependent gene silencing*. Cell 2006.125, 873–886.

239. Djupedal I. et al. *RNA Pol II subunit Rpb7 promotes centromeric transcription and RNAi-directed chromatin silencing*. Genes Dev.2005. 19, 2301–2306.

240. Kato H. et al. *RNA polymerase II is required for RNAi-dependent heterochromatin assembly*. Science 2005. 309, 467–469.

241. Verdel A. et al. *RNAi-mediated targeting of heterochromatin by the RITS complex*. Science 2004. 303, 672–676.

242. Motamedi M.R. et al. *Two RNAi complexes, RITS and RDRC, physically interact and localize to noncoding centromeric RNAs*. Cell 2004.119, 789–802.

243. Moazed D. et al. *Studies on the mechanism of RNAi-dependent heterochromatin assembly*. Cold Spring Harb. Symp. Quant. Biol.2006. 71, 461–471.

244. Shimada A., Dohke K., et al., *Phosphorylation of Swi6/HP1 regulates transcriptional gene silencing at heterochromatin.* Gen. Dev. 2009. 23(1):18-23.

245. Smallwood A., Estève P.O*., Functional cooperation between HP1 and DNMT1 mediates gene silencing.* Gen. Dev. 2007. 21(10):1169-78.

246. Mattei M.G., Luiani J. *Heterochromatin from chromosome to protein*. Atlas of genetics and cytogenetics in oncology and haematology 2006. 1-8.

247. Greenberg R. *Histone tails: directing the chromatin response to DNA damage*. FEBS letters 2011. 585:2883-90.

248. Luijsterburg MS., Dinant C., et al*. Heterochromatin protein 1 is recruited to various types of DNA damage.* J. Cell. Bio. 2009. 185(4):577-86.

249. Peng JC, Karpen GH, et al. *Heterochromatic genome stability requires regulators of histone H3 K9 methylation.* PLoS Genet. 2009. 5(3):e1000435.

250. Peters AH, O'Carroll D. et al*. Loss of the Suv39h histone methyltransferases impairs mammalian heterochromatin and genome stability*. Cell. 2001.107(3):323-37.

251. Vaquero A, Scher M, Erdjument-Bromage H, Tempst P, Serrano L, Reinberg D. *SIRT1 regulates the histone methyl-transferase SUV39H1 during heterochromatin*

formation. Nature. 2007. 450(7168):440-4.

252. Oda, H., Okamoto, I., Murphy, N., Chu, J., Price, S.M., Shen, M.M., et al. *Monomethylation of histone H4-lysine 20 is involved in chromosome structure and stability and is essential for mouse development.* Mol. Cell. Biol 2009. 29(8): 2278–2295.

253. Dinant, C., and Luijsterburg, M.S. *The emerging role of HP1 in the DNA damage response.* Mol. Cell. Biol 2009. 29(24): 6335–6340.

254. Wang D., Zhou J., et al. *Methylation of SUV39H1 by SET7/9 results in heterochromatin relaxation and genomic instability.* PNAS 2013. 110(14):5516-5521.

255. Hansen S., Wijmenga C., et al., *The DNMT3B DNA methyltransferase gene is mutated in the ICF immunodeficiency syndrome*. PNAS 1999. 96(25):14417.

256. Tan H, Qurashi A. *Retrotransposon activation contributes to fragile X premutation rCGG-mediated neurodegeneration*. Hum Mol Genet. 2012. 21(1):57-65.

257. Kaneko H, Dridi S, et al. *DICER1 deficit induces Alu RNA toxicity in age-related macular degeneration*. Nature. 2011. 471(7338):325-30

258. Christopher J. Klein1, Maria-Victoria Botuyan. *Mutations in DNMT1 cause hereditary sensory neuropathy with dementia and hearing loss.* Nat Genet . 2011. 43(6): 595–600

259. Gibbons RJ, Higgs DR. *Molecular-clinical spectrum of the ATR-X syndrome.* Am J Med Genet 2000, 97:204-212.

260. Lovejoy CA, Li W. et al. *Loss of ATRX, genome instability, and an altered DNA*

damage response are hallmarks of the alternative lengthening of telomeres pathway. PLoS Genet. 2012;8(7):e1002772.

261. Guan Z, Giustetto M, Lomvardas S, Kim JH, Miniaci MC, Schwartz JH, Thanos D, Kandel ER. *Integration of long-term-memory-related synaptic plasticity involves bidirectional regulation of gene expression and chromatin structure*. Cell 2002, 111:483-493.

262. Sparmann, A. and M. van Lohuizen, *Polycomb silencers control cell fate, development and cancer.* Nat Rev Cancer, 2006. 6(11): p. 846-56.

263. Schuettengruber, B., et al., *Genome regulation by polycomb and trithorax proteins*. Cell, 2007. 128(4): p. 735-45.

264. Schwartz, Y.B. and V. Pirrotta, *Polycomb silencing mechanisms and the management of genomic programmes*. Nat Rev Genet, 2007. 8(1): p. 9-22.

265. Breen, T.R., V. Chinwalla, and P.J. Harte, *Trithorax is required to maintain engrailed expression in a subset of engrailed-expressing cells*. Mech Dev, 1995. 52(1): p. 89-98.

266. Hanson, R.D., et al., *Mammalian Trithorax and polycomb-group homologues are antagonistic regulators of homeotic development*. Proc Natl Acad Sci U S A, 1999. 96(25): p. 14372-7.

267. Franke, A., et al., *Polycomb and polyhomeotic are constituents of a multimeric protein complex in chromatin of Drosophila melanogaster*. EMBO J, 1992. 11(8): p. 2941-50.

268. Levine, S.S., et al., *The core of the polycomb repressive complex is compositionally and functionally conserved in flies and humans*. Mol Cell Biol,

2002. 22(17): p. 6070-8.

269. Alkema, M.J., et al., *Identification of Bmi1-interacting proteins as constituents of a multimeric mammalian polycomb complex*. Genes Dev, 1997. 11(2): p. 226-40.

270. Shao, Z., et al., *Stabilization of chromatin structure by PRC1, a Polycomb complex*. Cell, 1999. 98(1): p. 37-46.

271. Hernandez-Munoz, I., et al., *Association of BMI1 with polycomb bodies is dynamic and requires PRC2/EZH2 and the maintenance DNA methyltransferase DNMT1*. Mol Cell Biol, 2005. 25(24): p. 11047-58.

272. Otte, A.P. and T.H. Kwaks, *Gene repression by Polycomb group protein complexes: a distinct complex for every occasion?* Curr Opin Genet Dev, 2003. 13(5): p. 448-54.

273. Gao, Z., Zhang, J., Bonasio, R., Strino, F., Sawai, A., Parisi, F., Kluger, Y., and Reinberg, D. (2012). *PCGF homologs, CBX proteins, and RYBP define functionally distinct PRC1 family complexes*. Mol. Cell 45, 344–356.

274. Tavares, L., Dimitrova, E., Oxley, D., Webster, J., Poot, R., Demmers, J., Bezstarosti, K., Taylor, S., Ura, H., Koide, H., et al. (2012). *RYBP-PRC1 complexes mediate H2A ubiquitylation at polycomb target sites independently of PRC2 and H3K27me3*. Cell 148, 664–678.

275. Yap, K.L., Li, S., Mun˜ oz-Cabello, A.M., Raguz, S., Zeng, L., Mujtaba, S., Gil, J.,Walsh, M.J., and Zhou, M.M. (2010). *Molecular interplay of the noncoding RNA ANRIL and methylated histone H3 lysine 27 by polycomb CBX7 in transcriptional silencing of INK4a*. Mol. Cell 38, 662–674.

276. Yu, M., Mazor, T., Huang, H., Huang, H.T., Kathrein, K.L., Woo, A.J.,

Chouinard, C.R., Labadorf, A., Akie, T.E., Moran, T.B., et al. (2012). *Direct recruitment of polycomb repressive complex 1 to chromatin by core binding transcription factors*. Mol. Cell 45, 330–343.

277. Nekrasov, M., B. Wild, and J. Muller, *Nucleosome binding and histone methyltransferase activity of Drosophila PRC2*. EMBO Rep, 2005. **6**(4): p. 348-53.

278. Ketel, C.S., et al., *Subunit contributions to histone methyltransferase activities of fly and worm polycomb group complexes*. Mol Cell Biol, 2005. **25**(16): p. 6857-68.

279. Cao, R., et al., *Role of histone H3 lysine 27 methylation in Polycomb-group silencing*. Science, 2002. 298(5595): p. 1039-43.

280. Czermin, B., et al., *Drosophila enhancer of Zeste/ESC complexes have a histone H3 methyltransferase activity that marks chromosomal Polycomb sites*. Cell, 2002. 111(2): p. 185-96.

281. Muller, J., et al., *Histone methyltransferase activity of a Drosophila Polycomb group repressor complex*. Cell, 2002. 111(2): p. 197-208.

282. Taylor-Harding, B., et al., *p55, the Drosophila ortholog of RbAp46/RbAp48, is required for the repression of dE2F2/RBF-regulated genes*. Mol Cell Biol, 2004. 24(20): p. 9124-36.

283. Pasini D, Cloos PA,Walfridsson J, Olsson L, Bukowski JP, et al. 2010. *JARID2 regulates binding of the Polycomb repressive complex 2 to target genes in ES cells*. Nature 464:306–10

284. Xu C., Bian C., et al. *Binding of different histone marks differentially regulates*

the activity and specificity of polycomb repressors complex 2 (PRC2). PNAS 2010. 107(45):19266-71.

285. He, A., Shen, X., Ma, Q., Cao, J., von Gise, A., Zhou, P., Wang, G., Marquez, V.E., Orkin, S.H., and Pu, W.T. (2012). *PRC2 directly methylates GATA4 and represses its transcriptional activity*. Genes Dev. 26, 37–42.

286. Kuzmichev, A., Jenuwein, T., Tempst, P., and Reinberg, D. (2004). *Different EZH2-containing complexes target methylation of histone H1 or nucleosomal histone H3*. Mol. Cell 14, 183–193.

287. Furuyama, T., et al., *SIR2 is required for polycomb silencing and is associated with an E(Z) histone methyltransferase complex*. Curr Biol, 2004. 14(20): p. 1812-21.

288. Mohd-Sarip, A., et al., *Synergistic recognition of an epigenetic DNA element by Pleiohomeotic and a Polycomb core complex*. Genes Dev, 2005. 19(15): p. 1755-60.

289. Klymenko, T., et al., *A Polycomb group protein complex with sequence-specific DNA-binding and selective methyl-lysine-binding activities*. Genes Dev, 2006. 20(9): p. 1110-22.

290. Cao, R., Y. Tsukada, and Y. Zhang, *Role of Bmi-1 and Ring1A in H2A ubiquitylation and Hox gene silencing*. Mol Cell, 2005. **20**(6): p. 845-54.

291. Wang, H., et al., *Role of histone H2A ubiquitination in Polycomb silencing*. Nature, 2004. 431(7010): p. 873-8.

292. de Napoles M, Mermoud JE, Wakao R, Tang YA, Endoh M, et al. 2004. *Polycomb group proteins Ring1A/B link ubiquitylation of histone H2A to*

heritable gene silencing and X inactivation. Dev. Cell 7:663–76

293. Grau D.J., Chapman B., et al. *Compaction of chromatin by diverse polycomb groups requires localized regions of high charges*. Gen. Dev.2011. 25:2210-21.

294. Simon J., Kingston R. *Occupying Chromatin: polycomb mechanisms for getting to genomic targets, stopping transcriptional traffic, and staying put*. Molecular Cell 2013. 49:808-824.

295. Shwartz Y., Pirotta V. *Polycomb silencing mechanisms and the management of genomic programmes*. Nat. Gen. Reviews 2007.8:9-22.

296. Schwartz, Y.B. and V. Pirrotta, Polycomb complexes and epigenetic states. Curr Opin Cell Biol, 2008. 20(3): p. 266-73.

297. Lessard, J. and G. Sauvageau, *Polycomb group genes as epigenetic regulators of normal and leukemic hemopoiesis.* Exp Hematol, 2003. 31(7): p. 567-85.

298. Lessard, J., S. Baban, and G. Sauvageau, *Stage-specific expression of polycomb group genes in human bone marrow cells*. Blood, 1998. 91(4): p. 1216-24.

299. Haupt, Y., et al*., bmi-1 transgene induces lymphomas and collaborates with myc in tumorigenesis*. Oncogene, 1993. **8**(11): p. 3161-4.

300. Buchwald, G., et al., *Structure and E3-ligase activity of the Ring-Ring complex of polycomb proteins Bmi1 and Ring1b*. EMBO J, 2006. **25**(11): p. 2465-74.

301. Li, Z., et al., *Structure of a Bmi-1-Ring1B polycomb group ubiquitin ligase complex*. J Biol Chem, 2006. **281**(29): p. 20643-9.

302. Van Lohuizen, M., et al*., Identification of cooperating oncogenes in E mu-myc*

transgenic mice by provirus tagging. Cell, 1991. 65(5): p. 737-52.

303. Park IK, Morrison S., et al., *Bmi1, stem cells, and senescence regulation*. Journal of clinical investigation 2004. 113:175-9.

304. Van der Lugt, N.M., et al., *Posterior transformation, neurological abnormalities, and severe hematopoietic defects in mice with a targeted deletion of the bmi-1 proto-oncogene.* Genes Dev, 1994. **8**(7): p. 757-69.

305. Lessard, J. and G. Sauvageau, *Bmi-1 determines the proliferative capacity of normal and leukaemic stem cells.* Nature, 2003. 423(6937): p. 255-60.

306. Leung, C., et al., *Bmi1 is essential for cerebellar development and is overexpressed in human medulloblastomas*. Nature, 2004. 428(6980): p. 337-41.

307. Chatoo W., Abdouh M., et al. *The polycomb gene Bmi1 regulates antioxidant defenses in neurons by repressing p53 prooxidant activity*. J.of.Neuroscience 2009. 29(2):529-542.

308. Park, I.K., et al., *Bmi-1 is required for maintenance of adult self-renewing haematopoietic stem cells*. Nature, 2003. 423(6937): p. 302-5.

309. Iwama, A., et al., *Enhanced self-renewal of hematopoietic stem cells mediated by the polycomb gene product Bmi-1*. Immunity, 2004. 21(6): p. 843-51.

310. Molofsky, A.V., et al., *Bmi-1 dependence distinguishes neural stem cell self-renewal from progenitor proliferation*. Nature, 2003. 425(6961): p. 962-7.

311. He, S., et al., *Bmi-1 over-expression in neural stem/progenitor cells increases proliferation and neurogenesis in culture but has little effect on these functions in*

vivo. Dev Biol, 2009. 328(2): p. 257-72.

312. Bea S, Tort F, Pinyol M, Puig X, Hernandez L, Hernandez S, Fernandez PL, van Lohuizen LM, Colomer D, Campo E. 2001. *BMI-1 gene amplification and overexpression in hematological malignancies occur mainly in mantle cell lymphomas*. Cancer Res 61: 2409–2412.

313. Chiba T, Seki A, Aoki R, Ichikawa H, Negishi M, Miyagi S, Oguro H, Saraya A, Kamiya A, Nakauchi H, Yokosuka O, Iwama A. 2010.*Bmi1 promotes hepatic stem cell expansion and tumorigenicity in both Ink4a/Arf-dependent and -independent manners in mice.* Hepatology 52: 1111–1123.

314. van Gosilga D, Schepers H, Rizo A, van der Kolk D, Vellenga E, Schuringa JJ. 2007. *Establishing long-term cultures with self-renewing acute myeloid leukemia stem/progenitor cells*. Exp Hematol 35: 1538–1549.

315. Dimri GP, Martinez JL, et al., *The Bmi-1 oncogene induces telomerase activity and immortalizes human mammary epithelial cells*. Cancer Res. 2002. 62(16):4736-45.

316. Singh A, Settleman J. 2010. EMT, *cancer stem cells and drug resistance: An emerging axis of evil in the war on cancer*. Oncogene 29:4741–4751.

317. Chou CH., Yang NK., et al., *Chromosome instability modulated by BMI1-AURKA signaling drives progression in head and neck cancer*. Cancer. Res. 2013. 73(2):953-66.

318. Abdouh M, Facchino S, Chatoo W, Balasingam V, Ferreira J, Bernier G. 2009. *BMI1 sustains human glioblastoma multiforme stem cell renewal*. J Neurosci 29: 8884–8896.

319. Cao L., Bombard J., et al., *Bmi1 as a novel target for drug discovery in cancer*. J. Call Biochem. 2011. 112:2729-41.

320. Jacobs, J.J., et al., *The oncogene and Polycomb-group gene bmi-1 regulates cell proliferation and senescence through the ink4a locus*. Nature, 1999. 397(6715): p. 164-8.

321. Gil, J. and G. Peters, *Regulation of the INK4b-ARF-INK4a tumour suppressor locus: all for one or one for all*. Nat Rev Mol Cell Biol, 2006. **7**(9): p. 667-77.

322. Bracken, A.P., et al., *The Polycomb group proteins bind throughout the INK4AARF locus and are disassociated in senescent cells*. Genes Dev, 2007. **21**(5): p.525-30.

323. Agherbi, H., et al., *Polycomb mediated epigenetic silencing and replication timing at the INK4a/ARF locus during senescence*. PLoS One, 2009. **4**(5): p.e5622.

324. Abdouh M., Chatoo W., et al., *Bmi1 is downregulated in the aging brain and displays antioxidant and protective activities in neurons*. PLos one 2012. 7(2):e31870.

325. Niessen H., Demmers J., *Talking to chromatin: post-translational modulation of polycomb group function.* Epigenetics and chromatin 2009. 2:10.

326. Voncken, J.W., et al., *Chromatin-association of the Polycomb group protein BMI1 is cell cycle-regulated and correlates with its phosphorylation status*. J Cell Sci, 1999. 112 (Pt 24): p. 4627-39.

327. Voncken, J.W., et al., *MAPKAP kinase 3pK phosphorylates and regulates chromatin association of the polycomb group protein Bmi1*. J Biol Chem, 2005.

280(7): p. 5178-87.

328. Kim J., Hwangbo J., Wong P. *p38 MAPK-Mediated Bmi-1 Down-Regulation and Defective Proliferation in ATM-Deficient Neural Stem Cells Can Be Restored by Akt Activation.* PLos One 2011. 6(1): e16615

329. Bomni PV., Dimri M., et al., *The polycomb group protein BMI1 is a transcriptional target of HDAC inhibitors.* Cell cycle 2010. 9(13):2663-73.

330. Liu S., Tetziaff MT., et al., *miR-200c inhibits melanoma progression and drug resistance through downregulation of BMI-1*. Am.J.Patho.2012. 181(5):1823-35.

331. He X., Dong Y., et al. *MicroRNA-218 inhibits cell cycle progression and promotes apoptosis in colon cancer by downregulating BMI1 polycomb ring finger oncogene.* Mol.Med 2013. 18:491-8.

CHAPTER 2:

Chapter 2 is the first article included in the thesis. In this study, we analyzed the novel function of *Bmi1* in formation and maintenance of constitutive heterochromatin. This function is PRC2-independent and requires ubiquitylation of histone H2A.

I am second author on this article where I contributed to the experiments in figure 4 as well as in the writing of the manuscript.

CHAPTER 2

ARTICLE

BMI1 is required for heterochromatin formation and repeat-DNA silencing

Mohamed Abdouh[1], Jida El Hajjar[1], Vicky Plamondon[1], and Gilbert Bernier[1, 2]

(Manuscript in revision at *Cell reports*)

[1] Stem Cell and Developmental Biology Laboratory, Hôpital Maisonneuve-Rosemont, 5415 Boul. l'Assomption, Montreal, Canada, H1T 2M4

[2] Faculty of Medicine, University of Montreal, Montreal, Canada

SUMMARY

Mono-ubiquitination of histone H2A at lysine 119 (H2Aub) is associated with the inactive chromatin at pericentromeric satellite repeat-DNA, X chromosome and silenced developmental genes. The Polycomb Repressive Complex 1 protein BMI1 was shown to promote H2Aub and transcriptional repression at developmental and tumor suppressor genes. We report here that BMI1 deficiency results in defective heterochromatin formation and activation of repeat-DNA sequences in mouse and human cells. BMI1 localized at intergenic and pericentromeric satellite repeat-DNA and was required for H2Aub deposition and H3K9me3 loading in an EZH2- and H3K27me3-independent manner. BMI1 co-purified with architectural heterochromatin proteins and with H3K9me3. Notably, H2Aub and heterochromatin defects associated with BRCA1 deficiency could be rescued by BMI1 over-expression. These findings uncover a critical function for BMI1 in heterochromatin formation and maintenance in mammalian cells.

INTRODUCTION

Chromosomes are structurally organized in distinct sub-compartment as determined by the local DNA sequence and chromatin organization. Euchromatin defines "open" chromatin regions containing actively transcribed genes. In contrast, heterochromatin defines "close" chromatin regions containing protein-encoding genes (the facultative heterochromatin) or not (the constitutive heterochromatin) [1]. The constitutive heterochromatin is found at the center and ends of chromosomes and is mostly constituted of repetitive DNA sequences [1]. Numerous (about 10,000) repetitive A/T rich DNA elements of 231 bp are also found in the pericentric heterochromatin of mouse and human chromosomes. Furthermore, about 40% of the mammalian genome is constituted of retro-elements located in intergenic regions of chromosomes [2, 3]. Active repression of repetitive elements of retroviral origins is important to maintain genomic stability as these can self-replicate and randomly integrate the genome. During mitosis, repetitive elements can also recombine by non-homologous recombination, resulting in chromosomes deletion, translocation and fusion [4].

Polycomb group proteins form large multimeric complexes that are involved in gene silencing through modifications of chromatin organization [5]. They are classically subdivided into two groups, namely Polycomb Repressive Complex 1 (PRC1) and PRC2 [6]. The sequential histone modifications induced by the PRC2 complex (which includes EZH2, EED and SUV12) and the PRC1 complex (which includes BMI1, RING1a and RING1b) allows stable silencing of gene expression in euchromatin and facultative heterochromatin [7-9]. The PRC2 contains histone H3 tri-methylase activity at lysine 27 ($H3K27^{me3}$) while the PRC1 contains histone $H2AK119^{ub}$ ($H2A^{ub}$) ligase activity [7-9]. Cells deficient for *Bmi1* proliferate poorly owing to de-repression of the *Ink4a/Arf* locus. Mice lacking *Bmi1* also display neurological abnormalities, depletion of neural stem cells, increased reactive oxygen species and premature aging [10-12].

Although Polycomb group proteins have not been directly implicated in constitutive heterochromatin formation or maintenance in mammalian somatic cells, several line of evidences support this possibility: **1)** Immuno-gold localization of BMI1 by electron microscopy in U-2 OS cells revealed high enrichment in electron-dense

heterochromatin, consistent with BMI1 immuno-localization at pericentric heterochromatin in some human cell lines [13-16]; **2)** co-inactivation of Eed and Ring1b in mouse embryonic stem cells resulted in activation of intergenic retro-elements [17]; **3)** inhibition of Eed and Ring1b in mouse embryonic stem cells resulted in re-activation of major satellite repeat-DNA in the parental allele of mouse embryos up to the 8 cells stage, thus until the end of the maternal-embryo transition [18].

We show here that Bmi1-null mice present constitutive heterochromatin anomalies in neurons characterized by reduced chromocenters size and number, decreased accumulation of heterochromatin protein 1 (HP1) and Ring1b at genomic repeats, and activation of intergenic retro-elements and satellite repeats. Bmi1 is enriched at constitutive heterochromatin in both mouse and human cells and required for $H2A^{ub}$ deposition and $H3K9^{me3}$ loading at repeat-DNA sequences. BMI1 co-purifies with architectural heterochromatin proteins and histones $H2A^{ub}$ and $H3K9^{me3}$. Loss- and gain-of-function studies revealed that BMI1 and BRCA1 display functional redundancy for $H2A^{ub}$ deposition at repeat-DNA sequences.

MATERIALS AND METHODS

Animals

Mice were used in accordance with the Animal Care Committee of the Maisonneuve-Rosemont Hospital Research Center (Approval ID #2009-40; #2009-42; # 2011-23).

Neuronal cultures

Embryonic day 18.5 cortices were dissected in oxygenated HBSS. Following meninges removal, cortices were cut to ~1mm^3 pieces, and incubated at 37ºC for 15 min in 2 ml TrypleEx solution (Invitrogen). Afterwards, enzymatic solution was discarded, and cortex pieces dissociated in HBSS with a 1 ml tip (10 times up and down). After dissociation, cells were plated at 1.5 x 10^5 cells/well on poly-L-lysine-coated 6-well plates or 8-well cultures slides (BD Biosciences). Cells were maintained in normal medium composed of Neurobasal-A Medium (Invitrogen), Glutamax-I (Gibco), gentamycin (50 µg/ml; Gibco), B27 supplement (Gibco), NGF (50 ng/ml; Invitrogen) and BDNF (0.5 ng/ml; Invitrogen). Neurons were nucleofected with plasmid DNA using the Mouse Neuron Nucleofector Kit

according to manufacturer's instructions (Amaxa Biosystems).

Chromatin Immunoprecipitaion (ChIP) assay

ChIP was performed using the ChIP Assay kit (Upstate). Cells were homogenized at RT according to the manufacturer's protocol and sonicated on ice for 10 sec at 30% amplitude to shear the chromatin (Branson Digital Sonifier 450, Crystal Electronics, On. Canada). Sonicated materials were immunoprecipitated using 2 µg mouse anti-BMI1, mouse anti-Ubiquityl H2A clone E6C5, mouse anti-RING1B, and mouse anti-HP1 (Millipore), rabbit anti-H3K9me3, and rabbit anti-H3K27me3 (Abcam), rabbit anti-BRCA1 (SantaCruz), and rabbit anti-mouse IgG (Upstate) antibodies. Fragments were then amplified by real-time PCR in triplicates. Human primers sets used were as follow: MCBOX (F) 5'-AGGGAATGTCTTCCCATAAAAACT-3'; (R) 5'-GTCTACCTTTTATTTGAATTCCCG-3'; SATIII (F) 5'-AATCAACCCGAGTGCAATCNGAATGG-3'; (R) 5'-TCCATTCCATTCCTGTACTCGG-3'; SATa (F) 5'-AAGGTCAATGGCAGAAAAGAA-3'; (R) 5'-CAACGAAGGCCACAAGATGTC-3'; ACTIN (F) 5'-CCTCAATCTCGCTCTCGCTC-3'; (R) 5'-CTCTAAGGCTGCTCAATGTCA-3'; ß-GLOBIN (F) 5'-GGCTGTCATCACTTAGACCTC-3'; (R) 5'-GGTTGCTAGTGAACACAGTTG-3';5'. Mouse primers sets used were as follow: MajSAT 5′-GGCGAGAAAACTGAAAATCACG-3′, 5′-CTTGCCATATTCCACGTCCT-3′; MinSAT 5′- TTGGAAACGGGATTTGTAGA-3′, 5′-CGGTTTCCAACATATGTGTTTT-3′; LINE 5′-TGGCTTGTGCTGTAAGATCG-3′, 5′-TCTGTTGGTGGTCTTTTTGTC-3′; SINE1 5′-GAGCACACCCATGCACATAC-3′, 5′-AAAGGCATGCACCTCTACCACC-3′; Actin 5'-TCGATATCCACGTGACATCCA-3'; 5'-GCAGCATTTTTTTACCCCCTC-3'; HoxA7 5'-GTGGGCAAAGAGTGGATTTC-3'; 5'-CCCCGACAACCTCATACCTA-3'; β-major 5′-CAGTGAGTGGCACAGCATCC-3′; 5′-CAGTCAGGTGCACCATGATGT-3′. ChIP-qPCR data was analyzed according to the Percent Input method. First, the raw Ct of the diluted 1% input fraction is adjusted by subtracting 6.64 cycles (i.e. log2 of the dilution

factor 100). Subsequently, the percent input of each IP fraction is calculated according to this equation: $100*2^{(\text{Adjusted Input Ct-Ct(IP)})}$.

Real-time RT-PCR

Mouse cortices or human cells were diced and RNA was isolated using TRIzol reagent (Invitrogen). Reverse transcription (RT) was performed using 1 μg of total RNA and the MML-V reverse transcriptase (Invitrogen). Real-time PCR was carried in triplicates using Platinum SYBRGreen Supermix (Invitrogen) and Real-time PCR apparatus (ABI prism 7002).

Micrococcal nuclease and DNase sensitivity assays

One million (10^6) cells were harvested at the log phase growth and used in either nuclease sensitivity assay. Cells were permeabilized (0.02% l-α-lysolecithin, 150 mM sucrose, 35 mM HEPES, 5 mM KH_2PO_4, 5 mM $MgCl_2$, 0.5 mM $CaCl_2$) on ice for 90 s than washed in ice cold PBS. The cell pellet was resuspended in nuclease buffer (150 mM sucrose, 50 mM Tris–HCl (pH 7.5), 50 mM NaCl, 2 mM $CaCl_2$) on ice, and nucleases were added. Digestions were performed at 24°C. Reactions were stopped by adding digestion stop buffer (20 mM Tris.Cl (pH7.4), 0.2 M NaCl, 10 mM EDTA, 2% SDS) and 0,1 mg/ml RNaseA for 30 min at 37°C. DNA was extracted by phenol/chloroform and visualized on 0.8% native agarose gel/ethidium bromide.

Plasmid constructs and viruses

Sequence-specific oligonucleotides stretch shRNA designed to target the BMI-1 ORF (accession #: BC011652): were synthetized. Oligo#1 (nt 1061-1081) 5'-CCTAATACT TTCCAGATTGAT-3', and oligoScramble (nt 573-591) 5'- GGTACTTCATTGA TGCCAC-3' were used in this study. These sequences are followed by the loop sequence (TTCAAGAGA) and finally the reverse complements of the targeting sequences. The double stranded shRNA sequences were cloned downstream of the H1P promoter of the H1P-UbqC-HygroEGFP plasmid using Age1, SmaI, and XbaI cloning sites. The shRNA-expressing lentiviral plasmids were cotransfected with plasmids pCMVdR8.9 and pHCMV-G into 293FT packaging cells using Lipofectamin (Invitrogen) according to the

manufacturer's instructions. Viral containing media were collected, filtered, and concentrated by ultracentrifugation. Viral titers were measured by serial dilution on 293T cells followed by microscopic analysis 48 hr later. For viral transduction, lentiviral vectors were added to dissociated cells prior to plating. Hygromycin selection (150 μg/ml) was added 48 h later. shBRCA1 constructs (MISSION shRNA) are from Sigma, and siRING1B (FlexiTube siRNA) are from Qiagen.

Proteomics

293T cells were transfected with the EFv-CMV-GFP (GFP-293T) or EFv-BMI1-Myc-CMV-GFP (Myc-293T) plasmids. Protein extracts were subjected to immunoprecipitation using an anti-Myc antibody. Immunoprecipitates were resolved by SDS-PAGE and LC-MS analysis was performed.

BMI1 Overexpression

Full-length human *BMI1* cDNA (2611 base pairs) was cloned by RT-PCR from normal human retina RNA extracts. The DNA fragment was cloned into a lentiviral vector to generate the EF-1a-*BMI1*.CMV-GFP construct.

Fixation, sectioning, and immunolabeling

For fixation, tissues were immersed for 1 h at room temperature in 4% paraformaldehyde (PFA)/3% sucrose in 0.1 M phosphate buffer, pH 7.4. Samples were washed three times in PBS, cryoprotected in PBS/30% sucrose, and frozen in CRYOMATRIX embedding medium (CEM) (Thermo Shandon, Pittsburgh, PA). Otherwise, tissues were fixed in 10% buffered formalin and embedded in paraffin according to standard protocols. 5 to 7 μm thick sections were mounted on Super-Frost glass slides (Fisher Scientific) and processed for immunofluorescence or immunohistochemistry staining. For immunofluorescence labeling, sections were incubated overnight with primary antibody solutions at 4ºC in a humidified chamber. After three washes in PBS, sections were incubated with secondary antibodies for 1 h at room temperature. Slides were mounted on coverslips in DAPI-containing mounting medium (Vector Laboratories, CA). For immunohistochemistry labeling, formalin-fixed paraffin-embedded slices were analyzed by using the Vectastain®

ABC kit (Vector) according to the manufacturer instructions. Peroxidase substrates used are the Vector® VIP (Pink) (Vector), and DAB (brown) (Sigma). Observations were made under a fluorescence microscope (Leica DMRE, Leica Microsystems) and images were captured with a digital camera (Retiga EX; QIMAGING; with OpenLab, ver.3.1.1 software; Open-Lab, Canada). Antibodies used in this study were mouse anti-BMI1, mouse anti-Ubiquityl H2A clone E6C5, mouse anti-RING1B, and mouse anti-HP1 (Millipore), rabbit anti-H3K9Ac, rabbit anti-H3K9me3, and rabbit anti-H3K27me3 (Abcam). Secondary antibodies used were FITC-conjugated donkey anti-mouse and rhodamine-conjugated donkey anti-rabbit (Chemicon).

Electron microscopy

Tissues were fixed overnight in 3% glutaraldehyde. After fixation with 2% osmium tetraoxide for 3 h, tissues were dehydrated through a graded series of ethanol (30–100%) and propylene oxide, and were embedded in epoxy resin LX-112 (Ladd Research). Sections were cut at 0.1 μm and stained with uranyl acetate and lead citrate. An Hitachi H7600 transmission electron microscope was used to capture images.

Immunoprecipitation and Western blot

Cells were resuspended in the K solution (20mM sodium phosphate, 150mM KCl, 30mM sodium pyrophosphate 0,1% NP-40, 5mM EDTA, 10mM NaF, 0,1mM Na3VO4 into CompleteMini protease inhibitor cocktail solution (Roche Diagnostics)) and sonicated. Whole-cell extracts were immunoprecipitated with 2ug of IgG, BMI1 and p-ATM antibodies following Catch and Release v2.0 kit (Millipore) and used in Western blot experiments. For Western blot, cellular extracts were homogenized in the Complete Mini Protease inhibitor cocktail solution (Roche Diagnostics), followed by sonication. Protein material was quantified using the Bradford reagent. Proteins were resolved in 1x Laemelli reducing buffer by SDS-PAGE electrophoresis and transferred to a Nitrocellulose blotting membrane (Bio-Rad). Subsequently, membranes were blocked for 1h in 5% non-fat milk-1X TBS solution and incubated overnight with primary antibodies. Membranes were then washed 3 times in 1X TBS; 0.05% Tween solution and incubated for 1h with corresponding horseradish peroxidase-conjugated secondary antibodies. Membranes were

developed using the Immobilon Western (Millipore). Blots were quantified using the Image quant program.

Statistical analysis

Statistical differences were analyzed using Student's *t*-test for unpaired samples. Two way-ANOVA test was used for multiple comparisons with one control group. In all cases, the criterion for significance (*P* value) was set as mentioned in the figures.

RESULTS

Heterochromatin formation is perturbed in *Bmi1*-deficient neurons

In most eukaryotes, constitutive heterochromatin perturbations result in genomic instability and premature ageing/senescence, which are hallmarks of the *Bmi1*-null phenotype [19-25]. We performed immuno-histochemistry (IHC) on cortical sections from WT and *Bmi1*$^{-/-}$ mice at post-natal day 30 (P30) using antibodies against histone H3 tri-methylated at lysine 9 (H3K9^{me3}), a mark of constitutive heterochromatin, and histone H3 acetylated at lysine 9 (H3K9^{ac}), a mark of open chromatin. We observed reduced H3K9^{me3} labeling in *Bmi1*$^{-/-}$ neurons together with increased H3K9^{ac} labeling (Fig. 1a). Labeling for HP1 as well as for KAP1, HDAC1 and DEK1 was also reduced in *Bmi1*$^{-/-}$ neurons, suggesting heterochromatin anomalies (Fig. 1a and data not shown). Quantitative analysis revealed that the number of H3K9^{me3}-positive chromocenters was reduced in *Bmi1*$^{-/-}$ neurons, while neuron's nuclear diameter was increased (Fig. 1b). Consistently, electron-dense chromocenters were smaller and the nuclear matrix was generally irregular in *Bmi1*$^{-/-}$ neurons, as evaluated by transmission electron microscopy (Fig. 1c). Deficiency in constitutive heterochromatin formation can directly affect repeat-DNA sequences expression and indirectly perturb DNA methylation at imprinted genes, and Bmi1 was previously shown to form a complex with the DNA methyltransferase Dnmt1 and its co-factor Dmap [26]. Consistently, quantitative RT-PCR (qPCR) analysis of *Bmi1*$^{-/-}$ mouse cortices or cultured e18.5 neurons revealed increased expression of intergenic LINE elements and pericentric repeat-DNA sequences (Fig. 1d, e). Furthermore, analysis of our previously published micro-array data using e18.5 *Bmi1*$^{-/-}$

neurons revealed that the majority of the top 10 most up-regulated genes are imprinted genes (Fig. 1f) [10]. Because post-natal neurodegeneration may account for the observed heterochromatin anomalies in *Bmi1*$^{-/-}$ mice, we analyzed the cortex of WT and *Bmi1*$^{-/-}$ embryos at e18.5. We found that H3K9^{me3} and HP1 staining were reduced in *Bmi1*$^{-/-}$ neurons, while that of H3K9^{ac} was unaffected (Fig. 1g). Comparable anomalies were also observed in *Bmi1*$^{-/-}$ retinas at P30 where H3K9^{me3} levels and electron-dense chromatin were reduced in photoreceptor cells, while H3K9^{ac} levels were unaffected (Fig. 1h, i).

Bmi1 accumulates at satellite DNA and is required for H2Aub and H3K9me3 deposition in mouse neurons

The E3 ubiquitin ligase BRCA1 was shown to be required for pericentric heterochromatin formation, satellite repeat repression and genomic stability through ubiquitylation of H2A at heterochromatin [27], raising the possibility that Bmi1 mediates repression of repeat-DNA through H2A^{ub} deposition. To test this, we performed Chromatin Immuno-Precipitation experiments (ChIP) on cultured WT and *Bmi1*$^{-/-}$ e18.5 neurons. Bmi1 and Ring1b were found to accumulate at all genomic repeats analyzed as well as at *Hoxa7* locus (a known Bmi1-target gene) (Fig. 2). In contrast, while enrichment for H3K27^{me3} was observed at the *Hoxa7* locus in WT neurons and slightly reduced in *Bmi1*$^{-/-}$ neurons, H3K27^{me3} enrichment at repeat-DNA was negligible in both WT and *Bmi1*$^{-/-}$ neurons. Importantly, we found that *Bmi1*-deficiency resulted in depletion of Ring1b and HP1 at genomic repeats, but not of BRCA1. In some instances, BRCA1 enrichment was also increased in *Bmi1*$^{-/-}$ neurons (Fig. 2). Notably, enrichment for H2A^{ub} and H3K9^{me3} at genomic repeats was highly reduced in *Bmi1*$^{-/-}$ neurons when compared to WT, suggesting that deficient H2A^{ub} deposition could underlie the observed heterochromatin compaction defect (Fig. 2).

BMI1 is required for heterochromatin compaction in human cells

To test for conserved function across species, BMI1 was inactivated in human 293T cells using a small hairpin RNA (shBMI1) [28]. This resulted in increased expression of the BMI1 target gene *p16*^{Ink4a} and of McBox and SATIII repeats (Fig. 3a). Conversely, BMI1 over-expression resulted in reduction of *p16*^{Ink4a} and repeat-DNA sequences expression

(Fig. 3b). We performed ChIP experiments on shScramble and shBMI1 virus-infected cells. We found that BMI1 and RING1B accumulated at genomic repeats and the HOXC13 control locus in shScramble cells, and these were depleted in shBMI1 cells (Fig. 3c). BMI1 knockdown in human cells also led to reduce HP1 accumulation as well as $H3K9^{me3}$ and $H2A^{ub}$ deposition at all repeat-DNA sequences. This was accompanied by increased BRCA1 enrichment only at ALU sequences (Fig. 3c). Nuclease hypersensitivity is a classical phenotype of cells deficient in heterochromatin condensation [29]. Micrococcal nuclease (MNase) assays can be used to obtain information about the location of nucleosomes along DNA strands and chromatin compaction level [30-32]. We used native chromatin extracts isolated from control and shBMI1 293T cells in MNase and DNaseI experiments and found that cells knockdown for BMI1 were hypersensistive to both nucleases, indicating reduced heterochromatin compaction (Fig. 3d).

RING1B knockdown does not affect $H2A^{ub}$ deposition at constitutive heterochromatin

Considering that BMI1 is enriched together with RING1B and $H2A^{ub}$ at constitutive heterochromatin, we tested whether the BMI1 knockdown heterochromatin phenotype could be mimicked by RING1B knockdown in 293T cells (Supplementary Fig. 1a). We observed that while RING1B accumulation at pericentric and intergenic heterochromatin and at *HOXC13* was highly reduced in siRING1B-treated cells, $H2A^{ub}$ reduction was only detected at *HOXC13*. Likewise, RING1B knockdown did not significantly affect BMI1 and HP1 accumulation and $H3K9^{me3}$ deposition at all tested regions (Supplementary Fig. 1b). These results suggested a possible dissociation between constitutive heterochromatin and *HOXC13* for RING1B-dependent $H2A^{ub}$ deposition, and revealed that RING1B knockdown is not sufficient to reproduce the BMI1 knockdown heterochromatin phenotype.

BMI1 localization at constitutive heterochromatin is EZH2 and H3K27me3-independent

To investigate the possibility that BMI1 localization at constitutive heterochromatin was PRC2 and H3K27^{me3}-dependent, we performed ChIP experiments on 293T cells knockdown for EZH2 using a previously characterized lentiviral construct [28]. In control cells, EZH2 and H3K27^{me3} enrichment was negligible at pericentric and intergenic heterochromatin but robust at the PRC2-target loci *HOXC13* (Supplementary Fig. 2). In contrast, enrichment for BMI1 and H2A^{ub} was significant at both pericentric and intergenic heterochromatin and at *HOXC13* (Supplementary Fig. 2). In EZH2 knockdown cells, we observed reduced EZH2 and H3K27^{me3} enrichment at *HOXC13* but with no measurable effect on BMI1 or H2A^{ub} enrichment at constitutive heterochromatin and *HOXC13*, altogether indicating that BMI1 accumulation and H2A^{ub} deposition can be EZH2 and H3K27^{me3}-independent (Supplementary Fig. 2).

BMI1 co-purifies with architectural heterochromatin proteins and histone H3K9^{me3}

To identify novel BMI1-associated proteins, we infected 293T cells with a lentivirus expressing a Myc-tagged BMI1 fusion protein or a control virus expressing GFP. After immuno-precipitation (IP) with an anti-Myc antibody, samples were separated on a 1D gel and sequenced by LC-MS (Fig. 4a). In the BMI1-myc sample, we identified several unique peptides corresponding to proteins involved in heterochromatin organization, including DEK1, HP1a (also called CBX5) and Lamins (Fig. 4a) [29, 33-35]. To confirm these results, we performed IP experiments on control and BMI1 virus-infected cells. We observed that BMI1 co-precipitated with RING1B but not with EZH2 (Fig. 4b). Co-precipitation of BMI1 with KAP1, DEK1 and HP1 was also observed (Fig. 4b). Notably, while BMI1 was found to co-precipitate with histones H3K9^{me3}, H3 (total), H1 and H2A^{ub}, co-precipitation was not observed with histones H3K9^{me2}, H3K27^{me2} and H3K27^{me3} (Fig. 4b). To further investigate the relationship of BMI1 with H3K9^{me3}, we performed co-localization studies in 293T cells. This revealed that ~79 +/- 20% of the endogenous BMI1 signal co-localized with H3K9^{me3} (Fig. 4c). To test whether BMI1 knockdown could perturb the subnuclear distribution of heterochromatin proteins, we performed cellular fractionation experiments in control and shBMI1 virus-infected 293T cells [29]. In these assays, the SDS fraction is thought to contain chromatin-bound proteins and compacted heterochromatin. In controls cells, BMI1 was detected in the 450nM NaCl

and SDS fractions (Fig. 4d). Likewise, BRCA1 and H3K9^{me3} were only found in the 100nM-450nM NaCl and SDS fractions, while modest HP1 distribution was also observed in the nucleosol fraction (Fig. 4d). In shBMI1 cells, the distribution of HP1 and H3K9^{me3} was highly reduced in the SDS fraction and apparently displaced in other fractions, while distribution of H3 and BRCA1 was not affected (Fig. 4d). Taken together, these results revealed co-purification of BMI1 with architectural heterochromatin proteins and H3K9^{me3}, co-localization of BMI1 with H3K9^{me3}, and BMI1 requirement for HP1 and H3K9^{me3} distribution in the SDS-soluble nuclear fraction.

BMI1 and BRCA1 display redundancy in heterochromatinization

Since the PRC1 and BRCA1 display H2A^{ub} activity and that BRCA1 enrichment and distribution at heterochromatin is not affected upon BMI1 depletion, we tested whether BMI1 and BRCA1 displayed functional redundancy in heterochromatinization. To confirm previous findings, we first performed BRCA1 knockdown in 293T cells (Supplementary Fig. 3b). In control cells, we observed BRCA1 enrichment at pericentric and intergenic heterochromatin and weak accumulation at *HOXC13* (Supplementary Fig. 3a). In BRCA1 knockdown cells, HP1 accumulation as well as H2A^{ub} and H3K9^{me3} deposition were reduced by ~50% at pericentric and intergenic heterochromatin. Comparable reduction for these marks was also observed at *HOXC13* (Supplementary Fig. 3a). BRCA1 knockdown was also accompanied by increased expression of repeat-DNA sequences (Supplementary Fig. 3c), thus confirming previous findings [27]. Notably, BMI1 and RING1B enrichment was increased at all tested regions in BRCA1 knockdown cells (Supplementary Fig. 3a), suggesting that BMI1 and BRCA1 are mutually independent and/or compete for accumulation at heterochromatin. To test for possible redundancy, stably infected shBMI1 cells were transfected with an shBRCA1 plasmid, generating double knockdown (DKN) cells. Notably, while H3K9^{me3} enrichment was reduced by 55-70% in DKN cells at all tested chromatin regions, enrichment for HP1 and H2Aub was further reduced by 80-90% in DKN cells (Fig. 5a), thus revealing an additive effect. In DKN cells, these chromatin modifications also correlated with an additive effect on *ALU* and *Sata* expression, while no additive effect was observed for *SatIII* and *McBox* expression (Fig. 5b). To test whether BMI1 could compensate for BRCA1

deficiency, we over-expressed BMI1 in control and shBRCA1-treated cells. In control cells, we found that BMI1 over-expression could not displace endogenous BRCA1 enrichment on the chromatin at all tested regions (Fig. 6a). However, accumulation of both endogenous BMI1 (shBRCA1 cells) and transgenic BMI1 (shBRCA1 + BMI1-Myc cells) proteins at pericentric and intergenic heterochromatin, as well as at *HOXC13*, was enhanced following BRCA1 knockdown (Fig. 6a). A similar but less dramatic trend was also observed for RING1B. Most notably, while BMI1 over-expression could increase $H2A^{ub}$ and $H3K9^{me3}$ deposition as well as HP1 accumulation at all tested regions in control cells, it could also rescue the corresponding heterochromatin anomalies in shBRCA1 cells (Fig. 6a). Importantly, BMI1 over-expression in shBRCA1 cells resulted in normalization of *ALU*, *McBox*, *Sata* and *SatIII* expression (Fig. 6b), altogether suggesting that BMI1 over-expression can rescue the BRCA1-deficient heterochromatin phenotype

DISCUSSION

We showed here that *Bmi1*-deficiency in mouse neurons and BMI1 knockdown in human cells result in anomalies in constitutive heterochromatin compaction. These anomalies were accompanied by transcriptional activation of intergenic retro-elements and pericentromeric satellite repeats. Using ChIP analysis, we observed that loss of BMI1 function was associated with reduced $H2A^{ub}$ and $H3K9^{me3}$ deposition at constitutive heterochromatin, and that knockdown of RING1B was not sufficient to reproduce this phenotype. Using ChIP, IP and microscopy analyses, we found that BMI1 accumulates at constitutive heterochromatin, co-purifies with architectural heterochromatin proteins and histones $H2A^{ub}$ and $H3K9^{me3}$, and co-localizes with $H3K9^{me3}$. In contrast, EZH2 and $H3K27^{me3}$ were not enriched at constitutive heterochromatin, did not co-purify with BMI1, and BMI1 accumulation and $H2A^{ub}$ deposition were *EZH2* and $H3K27^{me3}$-independent. Using gain- and loss-of-function studies, we showed that BMI1 and BRCA1 were mutually independent for accumulation at constitutive heterochromatin and displayed functional redundancy for $H2A^{ub}$ deposition and heterochromatinization.

We provided substantial evidences that BMI1 deficiency results in defective heterochromatin formation. Notably, this phenotype was also associated with increased nuclear diameter and an irregular nuclear lamina (see Fig. 1). These anomalies are particularly interesting considering our identification of LaminA/C, Lamin B2 and Importin as putative BMI1-co-purifying proteins and the recent demonstration that loss of heterochromatin foci can result in disruption of the nuclear lamina [35]. It is also notable that RING1B knockdown could not mimic the BMI1-deficient phenotype. More particularly, while $H2A^{ub}$ levels were reduced at *HOXC13* in RING1B knockdown cells, this was not accompanied by a corresponding reduction in HP1 and $H3K9^{me3}$ levels, as observed in BMI1 knockdown cells. Furthermore, there was not apparent effect on $H2A^{ub}$ levels at constitutive heterochromatin. This finding leaves us open with many explanations, the most likely one being functional compensation by RING1a for $H2A^{ub}$ deposition, as shown in other context [17, 36-38].

Using ChIP analysis, we found BMI1 enrichment at pericentric and intergenic heterochromatin (all data being normalized to one repeat sequence using the input data) in mouse and human cells. This was also confirmed by BMI1 co-purification and co-localization with $H3K9^{me3}$. Considering that there is about 10 000 pericentric repetitive DNA sequences in the mouse genome, and that 40% of the human genome is constituted of intergenic retro-elements, our results argue that a large fraction of the BMI1 protein pool is bound to constitutive heterochromatin. Consistently, previous findings revealed that BMI1 localizes at pericentric heterochromatin and electron-dense heterochromatin in human cells [14, 16]. Likewise, our cell fractionation assay revealed that a large portion of the BMI1 protein pool is bound to the SDS chromatin fraction, which is predicted to correspond to constitutive heterochromatin. Interestingly, we also observed that: 1) BMI1 did not co-purify with EZH2 or $H3K27^{me3}$, 2) EZH2 and $H3K27^{me3}$ were not enriched at constitutive heterochromatin, and 3) BMI1 accumulation at constitutive heterochromatin and *HOXC13* was *EZH2* and $H3K27^{me3}$-independent. These results are in agreement with recent findings, implying that previous models proposing a strict hierarchy in PRC activity may be only applicable to specific loci [39].

How BMI1- and BRCA1-mediated $H2A^{ub}$ deposition at repetitive DNA sequences can translate into heterochromatinization (i.e. $H3K9^{me3}$ loading and

heterochromatin compaction) is an intriguing issue. One possibility is that $H2A^{ub}$ induces allosteric changes in the histone H3 lysine tri-methyltransferases SUV39H1/2 to promote their activity, such as proposed for $H2B^{ub}$ and H3K4 methylation [40, 41]. This would be consistent with our findings that BMI1 co-purifies with architectural heterochromatin proteins, and with previous observations that PRC1 components can interact with SUV39H1 [15]. Alternatively, BMI1 may directly or indirectly regulate the transcription of H3 lysine methyltransferases or demethylases, thus also operating in trans. We also showed that co-inactivation of BMI1 and BRCA1 induces more severe $H2A^{ub}$, $H3K9^{me3}$ and HP1 depletion at constitutive heterochromatin than single BMI1 or BRCA1 deficiencies, and that BMI1 over-expression could rescue the BRCA1-deficient heterochromatin phenotype. These results suggest that BMI1 and BRCA1 are functionally redundant for $H2A^{ub}$ deposition at constitutive heterochromatin. The observation that BMI1 and BRCA1 proteins accumulation is mutually independent and that BMI1 levels are increased in BRCA1-deficient cells (and reciprocally) also indicate that both proteins possibly bind to the same substrate to catalyze $H2A^{ub}$ deposition.

In conclusion, we showed that BMI1 is associated with constitutive heterochromatin and required for heterochromatin formation and maintenance in mouse and human cells. Since BMI1 is highly expressed in several cancers, it will be of prime interest to investigate the function of BMI1 on cancer cell's heterochromatin structure. At the opposite, BMI1 deficiency is associated with premature aging, genomic instability and DNA damage accumulation [42-44], raising the possibility that the heterochromatin de-compaction phenotype we unraveled here could account for some of these effects.

ACKNOWLEDGMENTS

We are grateful to S. Breault for technical assistance with electron microscopy and to Dr. F. Rodier for critical reading of the manuscript. This work was supported by a grant from the Natural Science and Engineering Research Council of Canada. J. E. H. is supported by a fellowship from the University of Montreal Molecular Biology Program. V.P. is supported by a fellowship from the Natural Science and Engineering Research Council of Canada. G.B. is supported by a Senior fellowship from the Fonds de Recherche en Santé du Québec.

REFERENCES

1. Fodor, B.D., Shukeir, N., Reuter, G. & Jenuwein, T. Mammalian Su(var) genes in chromatin control. *Annu. Rev. Cell Dev. Biol.* **26**, 471-501 (2010).

2. Matsui, T.*, et al.* Proviral silencing in embryonic stem cells requires the histone methyltransferase ESET. *Nature* **464**, 927-931 (2010).

3. Rowe, H.M.*, et al.* KAP1 controls endogenous retroviruses in embryonic stem cells. *Nature* **463**, 237-240 (2010).

4. Kondo, Y.*, et al.* Downregulation of histone H3 lysine 9 methyltransferase G9a induces centrosome disruption and chromosome instability in cancer cells. *PLoS One* **3**, e2037 (2008).

5. Sparmann, A. & van Lohuizen, M. Polycomb silencers control cell fate, development and cancer. *Nat Rev Cancer* **6**, 846-856 (2006).

6. Levine, S.S.*, et al.* The core of the polycomb repressive complex is compositionally and functionally conserved in flies and humans. *Mol. Cell. Biol.* **22**, 6070-6078 (2002).

7. Dellino, G.I.*, et al.* Polycomb silencing blocks transcription initiation. *Mol. Cell* **13**, 887-893 (2004).

8. Kuzmichev, A., Nishioka, K., Erdjument-Bromage, H., Tempst, P. & Reinberg, D. Histone methyltransferase activity associated with a human multiprotein complex containing the Enhancer of Zeste protein. *Genes Dev.* **16**, 2893-2905 (2002).

9. Wang, H.*, et al.* Role of histone H2A ubiquitination in Polycomb silencing. *Nature* **431**, 873-878 (2004).

10. Chatoo, W., *et al.* The polycomb group gene Bmi1 regulates antioxidant defenses in neurons by repressing p53 pro-oxidant activity. *J. Neurosci.* **29**, 529-542 (2009).

11. Jacobs, J.J., Kieboom, K., Marino, S., DePinho, R.A. & van Lohuizen, M. The oncogene and Polycomb-group gene bmi-1 regulates cell proliferation and senescence through the ink4a locus. *Nature* **397**, 164-168 (1999).

12. Molofsky, A.V., *et al.* Bmi-1 dependence distinguishes neural stem cell self-renewal from progenitor proliferation. *Nature* **425**, 962-967 (2003).

13. Hernandez-Munoz, I., Taghavi, P., Kuijl, C., Neefjes, J. & van Lohuizen, M. Association of BMI1 with polycomb bodies is dynamic and requires PRC2/EZH2 and the maintenance DNA methyltransferase DNMT1. *Mol. Cell. Biol.* **25**, 11047-11058 (2005).

14. Saurin, A.J., *et al.* The human polycomb group complex associates with pericentromeric heterochromatin to form a novel nuclear domain. *J. Cell Biol.* **142**, 887-898 (1998).

15. Sewalt, R.G., *et al.* Selective interactions between vertebrate polycomb homologs and the SUV39H1 histone lysine methyltransferase suggest that histone H3-K9 methylation contributes to chromosomal targeting of Polycomb group proteins. *Mol. Cell. Biol.* **22**, 5539-5553 (2002).

16. Smigova, J., Juda, P., Cmarko, D. & Raska, I. Fine structure of the "PcG body" in human U-2 OS cells established by correlative light-electron microscopy. *Nucleus* **2**, 219-228 (2011).

17. Leeb, M., *et al.* Polycomb complexes act redundantly to repress genomic repeats and genes. *Genes Dev.* **24**, 265-276 (2010).

18. Puschendorf, M., *et al.* PRC1 and Suv39h specify parental asymmetry at constitutive heterochromatin in early mouse embryos. *Nat. Genet.* **40**, 411-420 (2008).

19. Blander, G. & Guarente, L. The Sir2 family of protein deacetylases. *Annu. Rev. Biochem.* **73**, 417-435 (2004).

20. Oberdoerffer, P., *et al.* SIRT1 redistribution on chromatin promotes genomic stability but alters gene expression during aging. *Cell* **135**, 907-918 (2008).

21. Wang, R.H., *et al.* Impaired DNA damage response, genome instability, and tumorigenesis in SIRT1 mutant mice. *Cancer Cell* **14**, 312-323 (2008).

22. Larson, K., *et al.* Heterochromatin formation promotes longevity and represses ribosomal RNA synthesis. *PLoS Genet* **8**, e1002473 (2012).

23. Pegoraro, G., *et al.* Ageing-related chromatin defects through loss of the NURD complex. *Nat Cell Biol* **11**, 1261-1267 (2009).

24. Peng, J.C. & Karpen, G.H. Heterochromatic genome stability requires regulators of histone H3 K9 methylation. *PLoS Genet* **5**, e1000435 (2009).

25. Peters, A.H., *et al.* Loss of the Suv39h histone methyltransferases impairs mammalian heterochromatin and genome stability. *Cell* **107**, 323-337 (2001).

26. Negishi, M., *et al.* Bmi1 cooperates with Dnmt1-associated protein 1 in gene silencing. *Biochem. Biophys. Res. Commun.* **353**, 992-998 (2007).

27. Zhu, Q., *et al.* BRCA1 tumour suppression occurs via heterochromatin-mediated silencing. *Nature* **477**, 179-184 (2011).

28. Abdouh, M., *et al.* BMI1 sustains human glioblastoma multiforme stem cell renewal. *J. Neurosci.* **29**, 8884-8896 (2009).

29. Kappes, F., *et al.* The DEK oncoprotein is a Su(var) that is essential to heterochromatin integrity. *Genes Dev.* **25**, 673-678 (2011).

30. Hewish, D.R. & Burgoyne, L.A. Chromatin sub-structure. The digestion of chromatin DNA at regularly spaced sites by a nuclear deoxyribonuclease. *Biochem. Biophys. Res. Commun.* **52**, 504-510 (1973).

31. Kornberg, R.D., LaPointe, J.W. & Lorch, Y. Preparation of nucleosomes and chromatin. *Methods Enzymol.* **170**, 3-14 (1989).

32. Wu, C. The 5' ends of Drosophila heat shock genes in chromatin are hypersensitive to DNase I. *Nature* **286**, 854-860 (1980).

33. Tadeu, A.M., *et al.* CENP-V is required for centromere organization, chromosome alignment and cytokinesis. *EMBO J.* **27**, 2510-2522 (2008).

34. Shumaker, D.K., *et al.* Mutant nuclear lamin A leads to progressive alterations of epigenetic control in premature aging. *Proc. Natl. Acad. Sci. U. S. A.* **103**, 8703-8708 (2006).

35. Pinheiro, I., *et al.* Prdm3 and Prdm16 are H3K9me1 Methyltransferases Required for Mammalian Heterochromatin Integrity. *Cell* **150**, 948-960 (2012).

36. Buchwald, G., *et al.* Structure and E3-ligase activity of the Ring-Ring complex of polycomb proteins Bmi1 and Ring1b. *EMBO J.* **25**, 2465-2474 (2006).

37. de Napoles, M., *et al.* Polycomb group proteins Ring1A/B link ubiquitylation of histone H2A to heritable gene silencing and X inactivation. *Dev Cell* **7**, 663-676 (2004).

38. Roman-Trufero, M.*, et al.* Maintenance of undifferentiated state and self-renewal of embryonic neural stem cells by Polycomb protein Ring1B. *Stem Cells* **27**, 1559-1570 (2009).

39. Tavares, L.*, et al.* RYBP-PRC1 complexes mediate H2A ubiquitylation at polycomb target sites independently of PRC2 and H3K27me3. *Cell* **148**, 664-678 (2012).

40. Kim, J.*, et al.* The n-SET Domain of Set1 Regulates H2B Ubiquitylation-Dependent H3K4 Methylation. *Mol. Cell* **49**, 1121-1133 (2013).

41. Wu, L.*, et al.* ASH2L Regulates Ubiquitylation Signaling to MLL: trans-Regulation of H3 K4 Methylation in Higher Eukaryotes. *Mol. Cell* **49**, 1108-1120 (2013).

42. Chagraoui, J., Hebert, J., Girard, S. & Sauvageau, G. An anticlastogenic function for the Polycomb Group gene Bmi1. *Proc. Natl. Acad. Sci. U. S. A.* **108**, 5284-5289 (2011).

43. Facchino, S., Abdouh, M., Chatoo, W. & Bernier, G. BMI1 confers radioresistance to normal and cancerous neural stem cells through recruitment of the DNA damage response machinery. *J. Neurosci.* **30**, 10096-10111 (2010).

44. Ismail, I.H., Andrin, C., McDonald, D. & Hendzel, M.J. BMI1-mediated histone ubiquitylation promotes DNA double-strand break repair. *J. Cell Biol.* **191**, 45-60 (2010).

FIGURE LEGENDS

Figure 1. Heterochromatin compaction defects in *Bmi1*-deficient neuronal cells

(a) Paraffin-embedded brain sections from P30 WT and *Bmi1*$^{-/-}$ mice were analyzed by immuno-histochemistry (IHC). Labeled cells are neurons located in the upper cortical layers of the cerebral cortex. Scale bar, 10 μm. (b) Quantification of the total number and number of large H3K9^{me3}-positive chromocentres. Note that neuron's nuclear diameter is increased in *Bmi1*$^{-/-}$ mice. Where n = 3 brains for each genotype. *P < 0.05, **P < 0.01. (c) Transmission electron microscopy analysis of cortical neurons in P30 WT and *Bmi1*$^{-/-}$ mice. Note the reduction in electron-dense chromocenters in *Bmi1*$^{-/-}$ neurons. (d) Whole cortices or (e) e18.5 neurons from WT and *Bmi1*$^{-/-}$ mice were analyzed by qPCR for satellite repeats and intergenic retro-elements expression. *P16*^{Ink4a} was used as positive control. Note the up-regulation of minor and major satellite repeats in *Bmi1*$^{-/-}$ neurons. Where n = 3 independent samples for each genotype. *P < 0.05, **P < 0.01. (f) Analysis of DNA micro-array data revealed up-regulation of several imprinted genes in e18.5 *Bmi1*$^{-/-}$ neurons relative to WT. (g) Paraffin-embedded brain sections from e18.5 WT and *Bmi1*$^{-/-}$ embryos were analyzed by IHC. Most labeled cells are cortical neurons. Scale bar, 50 μm. (h) Immuno-fluorescence analysis of frozen retinal sections from P30 WT and *Bmi1*$^{-/-}$ mice. The outer nuclear layer of the retina, which contains the cell body of photoreceptors, is shown. (i) Photoreceptors from P30 WT and *Bmi1*$^{-/-}$ mice were visualized by transmission electron microscopy. Note the reduction in electron-dense chromocenters in *Bmi1*$^{-/-}$ photoreceptors.

Figure 2. Bmi1 accumulates at repeat-DNA sequences and is required for H2Aub and H3K9me3 deposition

WT and *Bmi1*$^{-/-}$ neurons were analyzed by ChIP for proteins enrichment at satellite repeats, intergenic retro-elements and *HoxA7* (positive control gene). Note the accumulation of Bmi1 and Ring1b at all repeat-DNA sequences. While HP1 accumulation and H2Aub and H3K9me3 deposition were reduced in *Bmi1*$^{-/-}$ neurons at all tested loci, Brca1 accumulation was either unaffected (Minor and Major satellites) or increased (Line, Sine and IAP

). Note the near absent accumulation of Brca1 at *HoxA7* in both WT and *Bmi1*$^{-/-}$ neurons.

Figure 3. Bmi1 is required for heterochromatin compaction in human cells

(a, b) 293T cells were infected with shScramble or shBMI1 viruses (a) or with viruses expressing either GFP or the BMI1-myc fusion protein and GFP (b). (b) Gene expression was analyzed by qPCR, and where n = 3 independent cultures. *P < 0.05, **P < 0.01. (c) 293T cells knockdown for BMI1 were analyzed by ChIP for proteins enrichment at satellite repeats, intergenic retro-elements and *HoxC13* (positive control). (d) 293T cells were infected with shScramble or shBMI1 viruses and treated or not with MNase (0.4U at 24°C for different time periods) or DNaseI at the indicated concentrations for 20 minutes at 24°C. Note the nuclease hypersensitivity phenotype of shBMI1-treated cells.

Figure 4. BMI1 co-purifies with architectural heterochromatin proteins and H3K9^{me3}

(a, b) 293T cells were infected with EFv-CMV-GFP or EFv-BMI1-Myc-CMV-GFP viruses. Protein extracts were subjected to IP using an anti-Myc antibody, and immunoprecipitates were resolved by SDS-PAGE and analyzed either by LC-MS/MS (a) or Western blot (b). (a) Note the co-purification of BMI1 with several heterochromatin proteins and with Lamins. (b) Note the preferential co-purification of BMI1 with histone H3K9^{me3} (*). (c) 293T cells were labeled with BMI1 and H3K9^{me3} antibodies, counterstained with DAPI, and analyzed by quantitative confocal microscopy. Note the co-localization of BMI1 with H3K9^{me3}-positive chromocenters. (d) 293T cells were infected with shScramble or shBMI1 viruses and cell's compartments were fractionated. Note HP1 and H3K9^{me3} reduction (*) in the SDS fraction of shBMI1-treated cells.

Figure 5. BRCA1 and BMI1 display redundant activities for H2A^{ub} deposition at heterochromatin

(a, b) 293T cells were infected with shScramble or shBMI1 viruses. After selection with hygromycin, cells were transfected or not with an shBRCA1-encoding plasmid, (a) and analyzed by ChIP. Note the severe reduction in H2A^{ub} and H3K9^{me3} deposition and HP1 accumulation at all tested loci in shBMI1/shBRCA1 cells. (b) Cells were analyzed by

qPCR. Note the combined effect of shBMI1/shBRCA1 on ALU expression (when compared to shBMI1 or shBRCA1 alone).

Figure 6. BMI1 over-expression can rescue BRCA1-knockdown heterochromatic phenotype

(a, b) 293T cells stably expressing BMI1-myc or not were transfected with shScramble or shBRCA1 plasmids and analyzed by ChIP (a), and q-PCR (b). (a) Note the enrichment for both endogenous and exogenous BMI1 in shBRCA1-treated cells at all tested loci. Note also that BMI1-myc over-expression can prevent the reduction in $H2A^{ub}$ and $H3K9^{me3}$ deposition and HP1 accumulation in shBRCA1-treated cells at all repeat-DNA sequences. (b) BMI1-myc over-expression also normalizes repeat-DNA sequences expression in shBRCA1-treated cells.

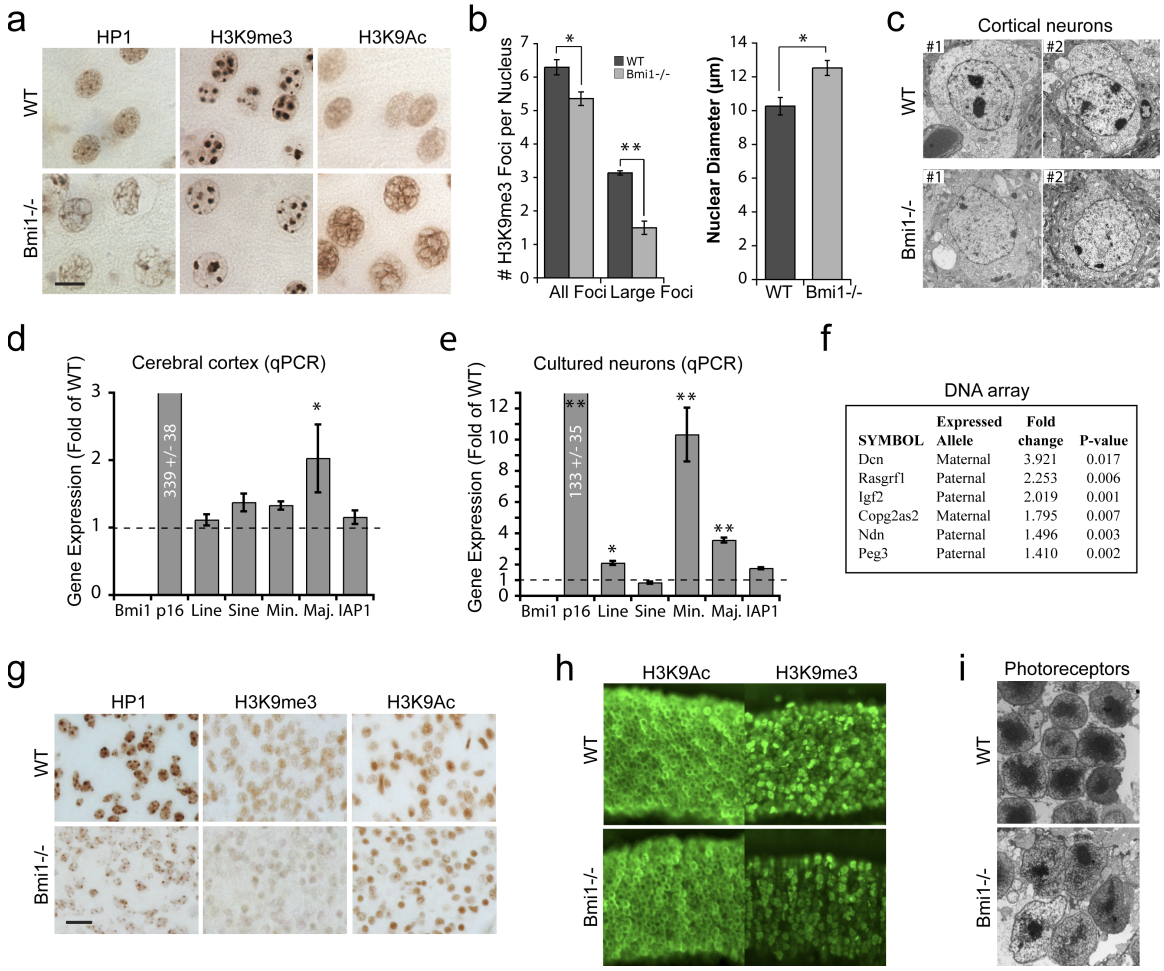

SYMBOL	Expressed Allele	Fold change	P-value
Dcn	Maternal	3.921	0.017
Rasgrf1	Paternal	2.253	0.006
Igf2	Paternal	2.019	0.001
Copg2as2	Maternal	1.795	0.007
Ndn	Paternal	1.496	0.003
Peg3	Paternal	1.410	0.002

Figure 1

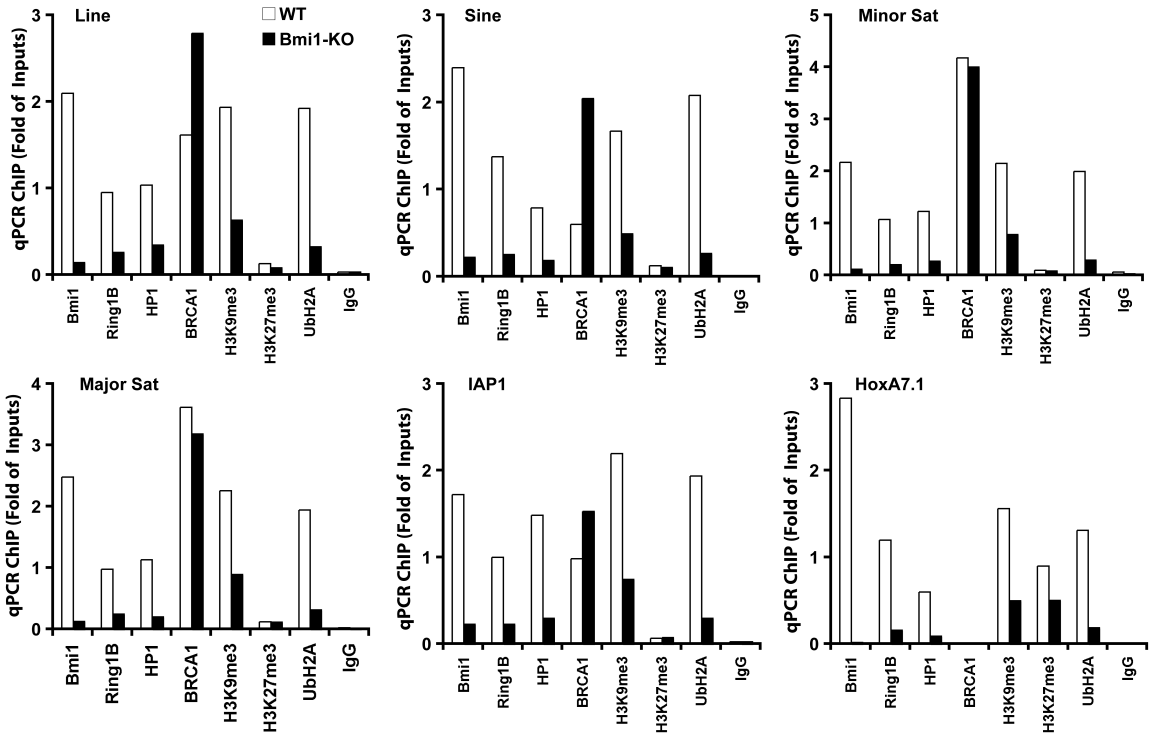
Line
WT
Bmi1-KO
Sine
Minor Sat
Major Sat
IAP1
HoxA7.1
qPCR ChIP (Fold of Inputs)
Bmi1
Ring1B
HP1
BRCA1
H3K9me3
H3K27me3
UbH2A
IgG

Figure 2

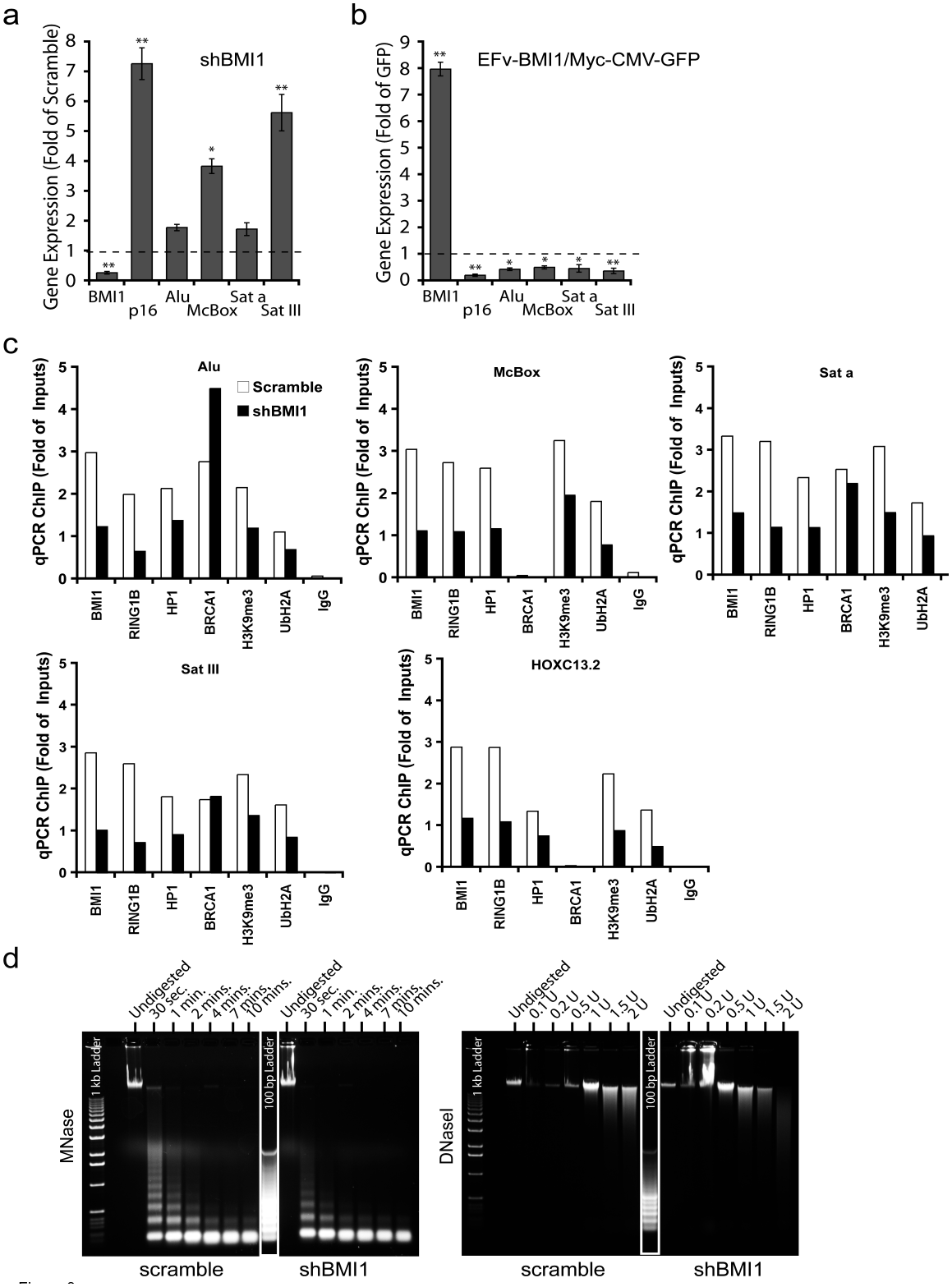
a
shBMI1
Gene Expression (Fold of Scramble)
BMI1
p16
Alu
McBox
Sat a
Sat III
b
EFv-BMI1/Myc-CMV-GFP
Gene Expression (Fold of GFP)
c
Alu
McBox
Sat a
Sat III
HOXC13.2
Scramble
shBMI1
qPCR ChIP (Fold of Inputs)
BMI1
RING1B
HP1
BRCA1
H3K9me3
UbH2A
IgG
d
MNase
DNaseI
Undigested
30 sec.
1 min.
2 mins.
4 mins.
7 mins.
10 mins.
0.1 U
0.2 U
0.5 U
1 U
1.5 U
2 U
1 kb Ladder
100 bp Ladder
scramble
shBMI1

Figure 3

a

Protein Name	NCBI Accession	Molecular Weight(Da)	Identification Probability	% Sequence Coverage	# Unique Peptides
H1x	NP_006017	22,469.90	100%	17.40%	3
CBX5	CAG33699	22,207.60	99.80%	12.60%	2
LMNB2	NP_116126	67,671.70	100%	15.30%	8
LMNA (Lamin-A/C)	CAI15523	74,053.50	100%	12.30%	8
BAF (Barrier-to-autointegration factor)	NP001137457	10,040.70	100%	42.70%	3
DEK	NP_003463	42,657.90	100%	13.60%	4
BAZ1A (Bromodomain adjacent to zinc finger domain protein 1A)	AAH20636	178,689	99.80%	2.19%	2
NUP93 (nucleoporin)	NP_055484	93,367.10	99.80%	3.17%	2
KPNB1 (karyopherin (importin) beta 1)	NP_002256.2	97,167.40	100%	8.11%	5
KPNA2 (karyopherin alpha 2 (importin alpha 1))	NP_002257	57,844.50	99.80%	7.56%	2
B3KRS5_HUMAN cDNA FLJ34837 fis, clone NT2NE2010632, highly simila		55,347.50	99.80%	5.94%	2
CENPV (Centromere protein V)	NP_859067	29,928.20	100%	18.20%	3
BAZ1B	AAH65029	170,889	100%	2.36%	3

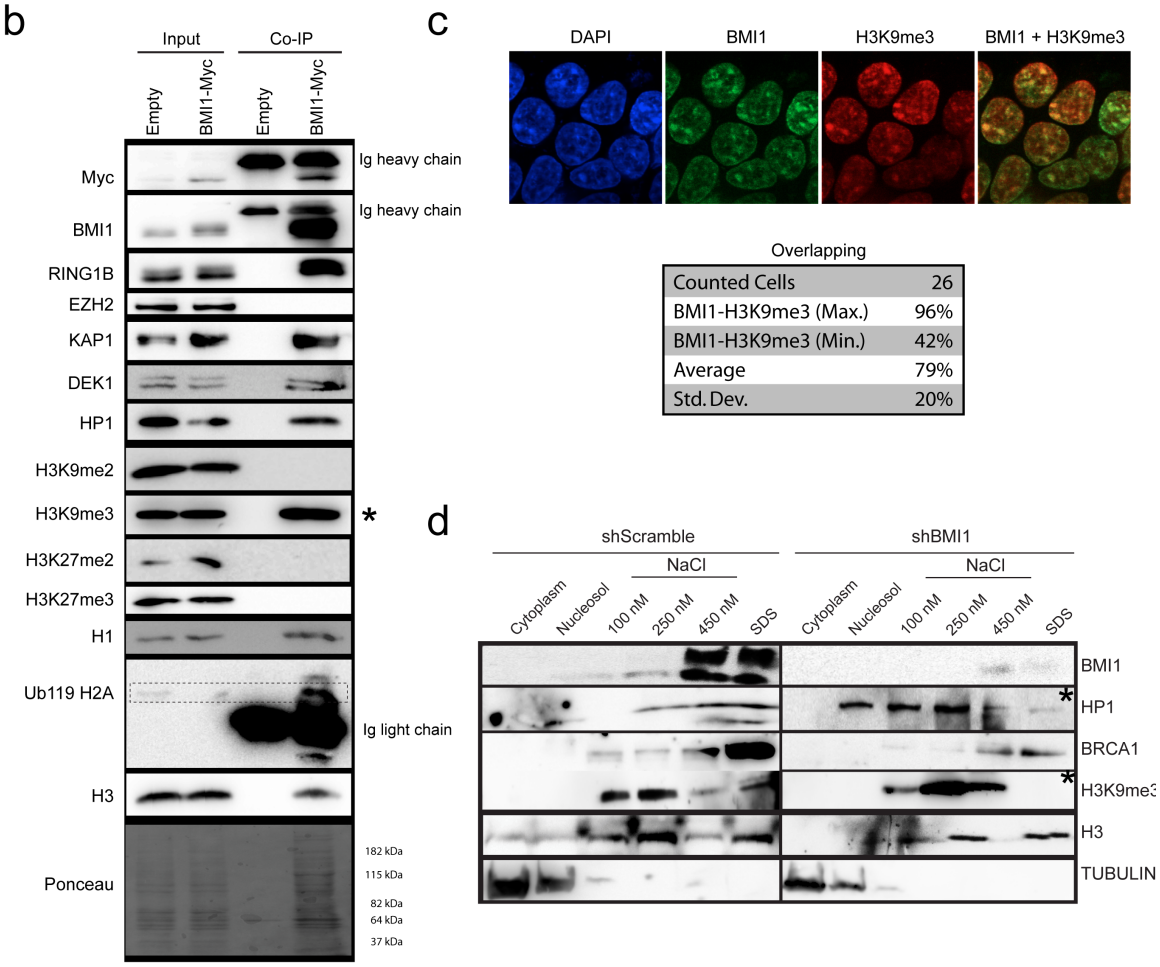

Figure 4

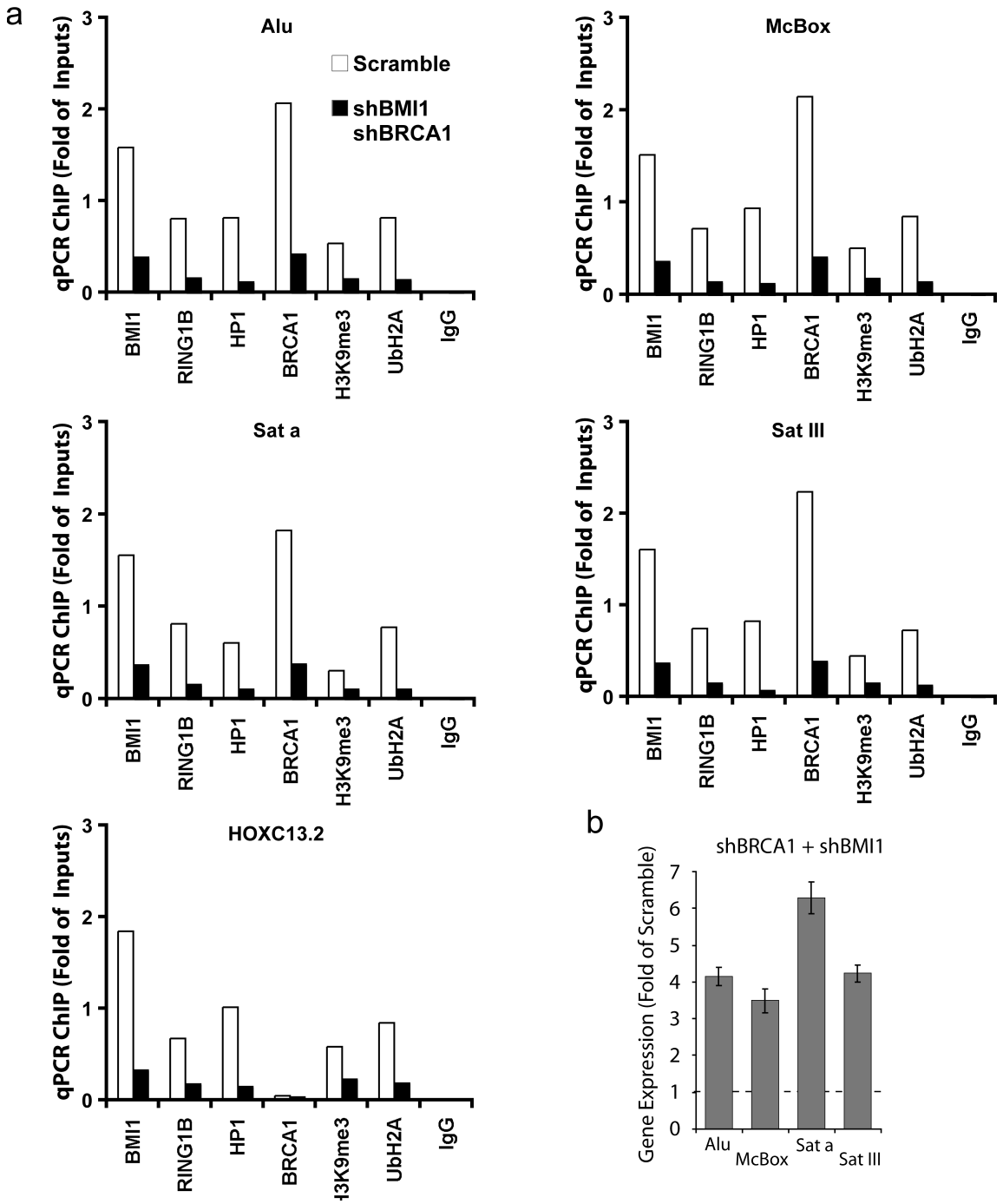
a
Alu
Scramble
shBMI1
shBRCA1
McBox
Sat a
Sat III
HOXC13.2
qPCR ChIP (Fold of Inputs)
BMI1
RING1B
HP1
BRCA1
H3K9me3
UbH2A
IgG
b
shBRCA1 + shBMI1
Gene Expression (Fold of Scramble)
Alu
McBox
Sat a
Sat III

Figure 5

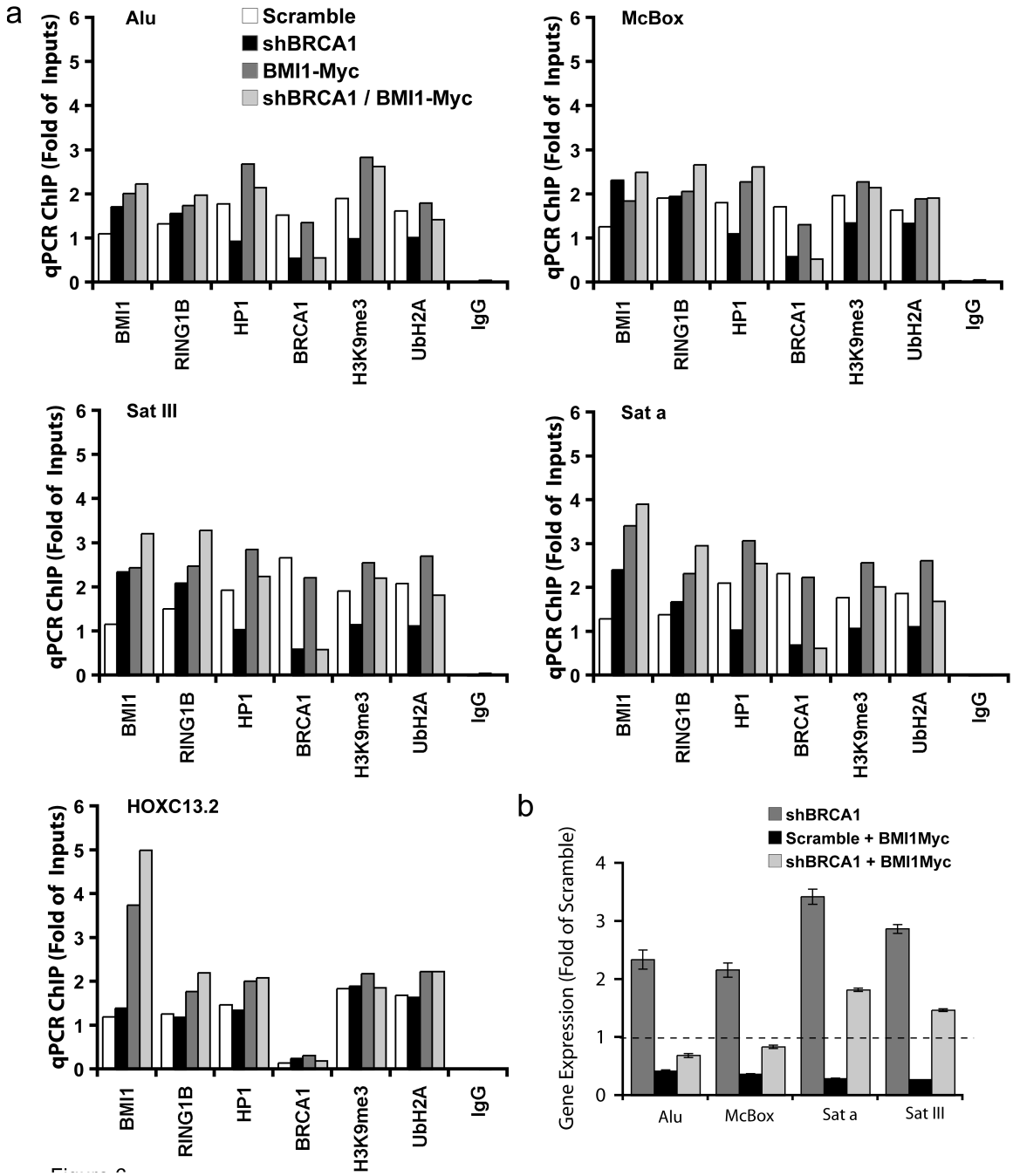
a
Alu
Scramble
shBRCA1
BMI1-Myc
shBRCA1 / BMI1-Myc
McBox
Sat III
Sat a
HOXC13.2
qPCR ChIP (Fold of Inputs)
BMI1
RING1B
HP1
BRCA1
H3K9me3
UbH2A
IgG
b
shBRCA1
Scramble + BMI1Myc
shBRCA1 + BMI1Myc
Gene Expression (Fold of Scramble)
Alu
McBox
Sat a
Sat III

Figure 6

CHAPTER 3:

Chapter 3 is the article reporting that aged *Bmi1*$^{+/-}$ mice develop a neurological disorder resembling LOAD. Moreover, this study reveals that *Bmi1* is required for the genomic stability of constitutive heterochromatin in neurons and that loss of *Bmi1* triggers activation of DNA damage response at repetitive DNA sequences.

I am first author on this article. I contributed majorly to conception of the study and I performed 90% of the experiments as well as the writing of the manuscript.

CHAPTER 3

ARTICLE

BMI1 deficiency and heterochromatic genome instability in late-onset Alzheimer's disease

Jida El Hajjar[1], Mohamed Abdouh[1], Wassim Chatoo[1], Nicolas Tetreault[1], Stéphane Lefrançois[2], Josée Ferreira[3], Yiu Chung Tse[4,5], Tak Pan Wong[4,5], and Gilbert Bernier[1, 6]

(Manuscript in revision at *Nature neuroscience*)

[1] Stem Cell and Developmental Biology Laboratory

[2] Cellular Trafficking Laboratory

[3] Department of Pathology, Maisonneuve-Rosemont Hospital, 5415 Boul. l'Assomption, Montreal, Canada, H1T 2M4

[4] Department of Psychiatry, McGill University, Montreal, Canada

[5]Douglas Mental Health University Institute, Montreal, Canada

[6] Department of Ophthalmology, University of Montreal, Montreal, Canada

ABSTRACT

Late-onset or sporadic Alzheimer's disease (LOAD) is the most prevalent form of dementia, but its origin remains poorly understood. The Bmi1 protein is part of the Polycomb Repressive Complex 1, which catalyzes histone H2A ubiquitylation (H2Aub) for repression of senescence-associated and developmental genes. We show here that Bmi1+/- mice develop normally but present with age a neurological disorder resembling LOAD. This phenotype was preceded by a reduction in H2Aub and H3K9me3 levels, neuronal heterochromatin de-compaction and DNA damage response (DDR). BMI1 deficiency, reduced H2Aub and H3K9me3 levels, heterochromatin de-compaction, and DDR were characteristic of LOAD but not of elderly control or familial Alzheimer's disease brains. In Bmi1+/- mice and LOAD patients, DNA damage preferentially accumulated at heterochromatin. Consistently, Bmi1 co-localized with H3K9me3 and was enriched at heterochromatin together with H2Aub. We conclude that BMI1 deficiency and heterochromatic genome instability are hallmarks of LOAD.

INTRODUCTION

Alzheimer's disease (AD) is characterized by progressive memory and behavioral impairment owing to degeneration of limbic and cortical areas of the brain. Pathological hallmarks are the presence of amyloid plaques, neurofibrillary phospho-TAU tangles and synaptic dysfunction [1]. Early-onset (familial) AD (EOAD) has been linked to mutations in *AMYLOID PRECURSOR PROTEIN*, *PRESENILIN1/2*, while the E4 allele of *APOLIPOPROTEIN* or allelic variants of *SORL1* represent risk factors for EOAD and late-onset (sporadic) AD (LOAD) [2, 3]. Despite these findings, the etiology of LOAD, which account for ~95% of AD cases, remains poorly understood [4]. The probability to develop LOAD increases dramatically with age, suggesting that aging-related mechanisms may account for disease progression or origin [5].

Nucleosomes are the basic building unit of chromatin and are comprised of 147 bp of DNA wrapped around a histone octamer [6]. Euchromatin defines "open" chromatin regions mostly containing actively transcribed genes. In contrast, heterochromatin defines "closed" chromatin regions either containing protein-encoding genes (the facultative heterochromatin) or not (the constitutive heterochromatin) [6]. Constitutive heterochromatin encompasses a large part of the mammalian genome, is localized at intergenic, pericentric, centric and telomeric regions of chromosomes, is comprised of repetitive DNA sequences, and generally enriched for histone H3 trimethylated at lysine 9 ($H3K9^{me3}$).

Bmi1 is a component of the Polycomb Repressive Complex 1, which promotes chromatin compaction and gene repression through its E3-mono-ubiquitin ligase activity mediated by Ring1a/b on histone H2A at lysine 119 ($H2A^{ub}$) [7, 8]. *Bmi1*$^{-/-}$ mice present reduced post-natal growth and lifespan together with cerebellar degeneration [9]. *Bmi1*-deficient cells undergo premature senescence owing in part to up-regulation of the *Ink4a* locus [10]. The Bmi1 protein is also recruited to DNA break sites where it promotes DNA damage response (DDR) and repair [11, 12]. We previoulsy showed that Bmi1 is required to prevent brain aging and p53-mediated repression of antioxidant response genes in neurons [13].

We show here that while mice lacking one Bmi1 allele develop normally, they display an age-dependent brain pathology resembling LOAD. Analysis of disease progression revealed that it was preceded by structural and molecular alterations of the neuron's constitutive heterochromatin. These alterations were associated with preferential DDR at constitutive heterochromatin. Bmi1 co-localized with $H3K9^{me3}$ in wild type (WT) neurons, and Bmi1 and $H2A^{ub}$ were enriched at $H3K9^{me3}$-associated heterochromatin in neuronal extracts. Deficient BMI1 expression, heterochromatin anomalies and DDR at heterochromatin were found in LOAD but not in elderly control or EOAD brains. Our results suggest that Bmi1 is required for neuronal heterochromatin compaction and stability in mice, and that deficient BMI1 expression and heterochromatic genome instability are characteristics of LOAD.

MATERIALS AND METHODS

Human samples

Paraffin-embedded human brains were obtained from the department of pathology of Maisonneuve-Rosemont Hospital. Post-mortem human cortices were provided by the Douglas Hospital Brain Bank and used accordingly to the Maisonneuve-Rosemont Hospital Ethic Committee. All samples were confirmed by histopathological analysis as non-demented controls or "classical" EOAD or LOAD cases (see Supplementary table 1).

Animals

Mice of the C57BL/6 strain were used in accordance with the Animal Care Committee of the Maisonneuve-Rosemont Hospital Research Center (Approval ID #2009-40; #2009-42; # 2011-23). For behavioral and LTP studies, mice were randomized using numbers to avoid bias. Behavioral studies were performed in the morning during the light cycle.

Antibodies

Rabbit anti-p53 (Santa Cruz Biotechnology), rabbit anti-p-JNK (Invitrogen), mouse anti-synaptophysin (Sigma), mouse anti-amyloid clone DE2B4 (Abcam), rabbit anti-amyloid

clone FCA3542 (Calbiochem), mouse anti-p-TAU clone AT-8 (Thermo scientific), mouse anti-p-TAU clone PHF1 (a gift from Dr. Davies, Albert Einstein College of Medicine), rabbit anti-BACE1 (Covance), mouse anti-NeuN (Chemicon), rabbit anti-cleaved caspase-3 (Cell Signaling), mouse anti-Bmi1 clone F6 (Millipore), mouse anti-Bmi1 (Abcam), mouse anti-p-ATM (Novus), rabbit anti-p-ATR (Santa Cruz Biotechnology), rabbit anti-H3K9me3 (Abcam), mouse anti-H2Aub clone E6C5 (Millipore), mouse anti-HP1 (Millipore), mouse anti-β-actin (Sigma), mouse anti-tubulin (Sigma), mouse anti-H3 (Upstate), and rabbit anti-mouse IgG (Upstate).

Amyloid fractions

Cortices were minced and homogenized in a 10ml TBS 1x/protease inhibitor cocktail solution (Roche Diagnostics), using a tissue grinder. The homogenates were sonicated and ultra-centrifuged at 175,000g for 1h at 4°C. The supernatants were collected as the soluble cellular fraction. The dense pellet was re-homogenized in a 10ml TBS 1x/Triton 1%/ protease inhibitor cocktail solution, followed by sonication and centrifugation at 100,000g for 1h at 4°C. The supernatants were recuperated as the insoluble cellular fraction.

Immunohistochemistry

For paraffin fixation, tissues were immersed for 1 h at room temperature in Formalin or 4% paraformaldehyde/3% sucrose in 0.1 M phosphate buffer, pH 7.4. Samples were washed three times in PBS, cryo-protected in PBS/30% sucrose, and embedded in paraffin according to standard protocols. 5 to 8 µm thick sections were mounted on Super-Frost glass slides (Fisher Scientific) and processed for immunohistochemistry staining. Paraffin-embedded slices were analyzed by using the Vectastain® ABC kit (Vector) according to the manufacturer instructions. Peroxidase substrates used are the Vector® VIP (Violet) (Vector), and DAB (brown) (Sigma). Observations were made using the Zeiss imager Z2 microscope and images were captured with a digital camera. Pyramidal neurons from the frontal cortex were used to quantify the number of chromocenter/neuron. When required, neuronal cell identity was determined by the morphology (using phase contrast imaging), the large nuclear diameter (when compared

to astrocytes), and the presence of chromocenters and of a large nucleolus.

Western Blot

Total cortical extracts were homogenized in the Complete Mini Protease inhibitor cocktail solution (Roche Diagnostics), followed by sonication. Protein material was quantified using the Bradford reagent. Proteins were resolved in 1x Laemelli reducing buffer by SDS-PAGE electrophoresis and transferred to a Nitrocellulose blotting membrane (Bio-Rad). Subsequently, membranes were blocked for 1h in 5% non-fat milk-1X TBS solution and incubated overnight with primary antibodies. Membranes were then washed 3 times in 1X TBS; 0.05% Tween solution and incubated for 1h with corresponding horseradish peroxidase-conjugated secondary antibodies. Membranes were developed using the Immobilon Western (Millipore). Blots were quantified using the Image quant program.

Neuronal cultures

After dissociation of e18.5 cortices, cells were plated at 1,5 x 10^5 cells/well on poly-L-lysine-coated 8-well cultures slides (BD Biosciences). Cells were maintained in normal medium composed of Neurobasal-A Medium (Invitrogen), Glutamax-I (Gibco), gentamycin (50 μg/ml; Gibco), B27 supplement (Gibco), nerve growth factor (50 ng/ml; Invitrogen) and BDNF (0,5 ng/ml; Invitrogen). For inhibitory assays, we added 2 μM of DMSO, 2 μM of ATM/ATR inhibitor (CGK733; Millipore) or 10 μM of ATM inhibitor (KU55933; KuDOS Pharmaceuticals) to the cell culture medium for 16 hours. NAC was added daily at 5mM into the culture medium for 7 days.

Chromatin Immunoprecipitaion (ChIP) assay

ChIP was performed using the ChIP Assay kit (Upstate). Briefly, 50 mg of cortical tissue was frozen for 1 hour and than homogenized at RT according to the manufacturer's protocol. The tissue was sonicated on ice for 10 sec at 30% amplitude to shear the chromatin (Branson Digital Sonifier 450, Crystal Electronics, On. Canada). Sonicated materials were immunoprecipitated using designated antibodies. Fragments were then amplified by real-time PCR in triplicates. Human primers sets used were as follow:

MCBOX (F) 5'-AGGGAATGTCTTCCCATAAAAACT-3'; (R) 5'-GTCTACCTTTTATTTGAATTCCCG-3'; SATIII (F) 5'-AATCAACCCGAGTGCAATCNGAATGG-3'; (R) 5'-TCCATTCCATTCCTGTACTCGG-3'; SATa (F) 5'-AAGGTCAATGGCAGAAAAGAA-3'; (R) 5'-CAACGAAGGCCACAAGATGTC-3'; ACTIN (F) 5'-CCTCAATCTCGCTCTCGCTC-3'; (R) 5'-CTCTAAGGCTGCTCAATGTCA-3'; ß-GLOBIN (F) 5'-GGCTGTCATCACTTAGACCTC-3'; (R) 5'-GGTTGCTAGTGAACACAGTTG-3';5'. Mouse primers sets used were as follow: MajSAT 5′-GGCGAGAAAACTGAAAATCACG-3′, 5′-CTTGCCATATTCCACGTCCT-3′; MinSAT 5′- TTGGAAACGGGATTTGTAGA-3′, 5′-CGGTTTCCAACATATGTGTTTT-3′; LINE 5′-TGGCTTGTGCTGTAAGATCG-3′, 5′-TCTGTTGGTGGTCTTTTTGTC-3′; SINE1 5′-GAGCACACCCATGCACATAC-3′, 5′-AAAGGCATGCACCTCTACCACC-3′; Actin 5'-TCGATATCCACGTGACATCCA-3'; 5'-GCAGCATTTTTTTACCCCCTC-3'; HoxA7 5'-GTGGGCAAAGAGTGGATTTC-3';5'-CCCCGACAACCTCATACCTA-3';β-major 5′-CAGTGAGTGGCACAGCATCC-3′; 5′-CAGTCAGGTGCACCATGATGT-3′. ChIP-qPCR data was analyzed according to the Percent Input method. First, the raw Ct of the diluted 1% input fraction is adjusted by subtracting 6.64 cycles (i.e. log2 of the dilution factor 100). Subsequently, the percent input of each IP fraction is calculated according to this equation: $100*2^{(\text{Adjusted Input Ct-Ct(IP)})}$.

Real-time RT-PCR

Mouse cortices were diced and RNA was isolated using TRIzol reagent (Invitrogen). Reverse transcription (RT) was performed using 1 µg of total RNA and the MML-V reverse transcriptase (Invitrogen). Real-time PCR was carried in triplicates using Platinum SYBRGreen Supermix (Invitrogen) and Real-time PCR apparatus (ABI prism 7002). Primer sets used were as described [13].

Statistical analysis

Statistical differences were analyzed using Student's *t*-test for unpaired samples. Two way-ANOVA test was used for multiple comparisons with one control group. In all cases,

the criterion for significance (*P* value) was set as mentioned in the figures. Significance was assessed using an unpaired two-sided Student's t-test in figures 1-4 and 6 and 7, as these all represent comparisons of independent samples of equal size and variance following a normal distribution. For figures 5 and 8, where several groups were compared, significance was assessed by ANOVA and adjusted for multiple comparisons using the Bonferroni correction.

RESULTS

Bmi1$^{+/-}$ mice display aging features and neurological symptoms

Alopecia and weight loss are common characteristics of premature aging in mice and we previously reported that *Bmi1*$^{+/-}$ mice presented reduced median and maximal lifespan [13]. We observed that *Bmi1*$^{+/-}$ mice between the ages of 15-20 months (defined here as old mice) exhibited alopecia and reduced body size when compared to age-match WT littermates (Fig. 1a, b). These features were not present in 3- and 12-month old *Bmi1*$^{+/-}$ mice (Fig. 1a, b). We performed the paw-clasping test to verify if alopecia-affected *Bmi1*$^{+/-}$ mice presented pathological reflexes. Instead of limb extension as in WT mice, *Bmi1*$^{+/-}$ mice displayed an irregular clasping behavior characterized by the dragging of the fore paws towards the trunk and asymmetry in limb position (Fig. 1c), thus suggestive of a neurological syndrome. The Bmi1 gene operates as a central regulator of the p19^{Arf}/p53 and p16^{Ink4a}/pRb axes, which promote apoptosis and senescence [10]. Although senescence is thought not to occur in neurons, increased SA β-galactosidase activity and expression of the senescence-associated genes *p19*^{Arf} and *p16*^{Ink4} have been described in cortical neurons of aged *p73*$^{+/-}$ mice and *Bmi1*$^{-/-}$ pups [13, 14]. To test for neuronal senescence, we compared the cortex of 24-month old (defined here as very old) WT and 15-month old *Bmi1*$^{+/-}$ mice for SA β -galactosidase activity. Very old WT mice were used to compensate for possible premature aging in *Bmi1*$^{+/-}$ mice. Yet, robust SA β-galactosidase staining was observed in pyramidal neurons (layers 2 and 3 of the frontal cortex) of *Bmi1*$^{+/-}$ mice when compared to WT, together with a 2-fold increase in the number of SA b-galactosidase-positive neurons (Fig. 1d, e). Expression of *p16*^{Ink4} is

considered as a biomarker of aging [15]. Consistently, we observed increased $p16^{Ink4}$ (~25 fold) and $p19^{Arf}$ (~5 fold) expression in $Bmi1^{+/-}$ mice compared to WT (Fig. 1f), suggesting that old $Bmi1^{+/-}$ mice display premature brain aging.

$Bmi1^{+/-}$ mice show altered spatial memory and reduced long-term potentiation

To test if cognitive functions were perturbed, we examined healthy 15-months old WT and $Bmi1^{+/-}$ littermates for spatial learning and memory aptitude. For the Morris water navigation task, mice were trained for 4 days (traning) and then evaluated on their capacity to remember the platform location (probe test). $Bmi1^{+/-}$ mice performed poorly in this assay during both the training period and probe test, as demonstrated by the increased time (latency) required to reach the platform (Fig. 2a, b). Although the swimming speed of $Bmi1^{+/-}$ mice was reduced (0.25 m/s for WT and 0.20 m/s for $Bmi1^{+/-}$), it was sufficiently close to that of WT mice to exclude this variable as the cause of the highly increased latency (Fig. 2a). $Bmi1^{+/-}$ mice also exhibited an anxious phenotype as demonstrated by an increased thigmotactic behavior while performing the task (Fig. 2a). The Barnes maze test is based on mice aversion to open enlightened spaces. $Bmi1^{+/-}$ mice were more prone to visiting non-target holes while searching for the hole with the escape box and the latency of escape was also increased (Fig. 2c). These results suggested that otherwise healthy $Bmi1^{+/-}$ mice present impaired spatial memory formation and increased anxiety.

Using the same animals, we tested if impairment of spatial memory formation was related to an impairment of long-term potentiation (LTP), a cellular model for spatial memory formation [16]. LTP of the Schaffer collateral pathway was induced in the CA1 region of the hippocampus in both WT and $Bmi1^{+/-}$ mice. We found that inducing LTP (100 Hz, 100 pulses) enhanced fEPSP slope in WT mice at 60 minutes after tetanus (Percent potentiation: 48.9 ± 5.2%, data from 6 slices and 3 mice). Compared with fEPSP recorded before tetanus (baseline), WT slices displayed significant potentiation (P = 0.036; paired Student's t-test) (Fig. 2d, e). Slices from $Bmi1^{+/-}$ mice exhibited weaker potentiation than WT (11.7 ± 11.2%, data from 6 slices, 4 mice; $Bmi1^{+/-}$ vs. WT: P = 0.045, Student's t-test) and failed to show significant potentiation when compared to baseline at 60 minutes after tetanus (P = 0.357; paired Student's t-test) (Fig. 2f). Our

findings suggested that *Bmi1* hemi-deficiency significantly impaired LTP formation, and LTP deficits have been observed in transgenic mouse models of AD that exhibit spatial memory impairment [17, 18].

Bmi1$^{+/-}$ mice present neuropathological features resembling AD

We previously showed that most neuronal anomalies present in *Bmi1*$^{-/-}$ mice were mediated by p53 activity [13]. We therefore analyzed p53 expression and found that when compared to old WT, p53 levels were increased in the brain of old *Bmi1*$^{+/-}$ mice, suggesting the presence of a brain pathology (Fig. 3a). Hallmarks of AD are accumulation of p-TAU in neuron's perikarya, extra-cellular amyloid plaque formation, reduced synaptophysin immunoreactivity and neuronal loss. By immunoblot using antibodies that recognize p-TAU at Ser202 (AT-8) or Ser396 (PHF1), we observed the presence of p-TAU accumulation in *Bmi1*$^{+/-}$ cortices (Fig. 3a). By immunohistochemistry (IHC), we observed p-TAU immunoreactivity in the neuron's perikarya of old WT and *Bmi1*$^{+/-}$ mice. However, large p-TAU deposits in "ghost-like" neurons and strong immunoreactivity in track fibers of the cortical white matter were only observed in *Bmi1*$^{+/-}$ mice (Fig. 3b). These pathological features correlated with increased p-JNK and reduced synaptophysin levels (Fig. 3a). Accumulation of p-JNK and p-TAU (S202) was not observed in very old WT mice (Fig. 3c). Cleavage of APP by the β -secretase BACE1 is the first step in the sequential production of β-amyloid, and BACE1 levels are increased in sporadic AD [19]. Notably, we observed increased BACE1 levels in *Bmi1*$^{+/-}$ cortices (Fig. 3a). Soluble amyloid oligomeres of ~10-12kda are believed to perturb synaptic and mitochondrial functions in AD and these were shown to accumulate in the neuronal cytoplasm of AD patients and of transgenic mice carrying the *APP*$^{E693\text{-}deleted}$ mutation [20, 21]. By immunoblot using the FCA3542 antibody, which recognizes the mouse and human 1-42 amyloid peptide, a 10-12kda band was revealed in 15-month old *Bmi1*$^{+/-}$ mice, but not in old WT mice (Fig. 3d-input 20%). After immunoprecipitation using a mouse monoclonal antibody (DE2B4) that recognizes the mouse and human amyloid peptide, the presence of the 10-12kda band was also observed with FCA3542 in 15-month old *Bmi1*$^{+/-}$ mice and 6-month old APP transgenic mice carrying the AD-related Swe/Iowa/Nevada mutations (*APP*^{TG}), but not in old WT mice (Fig. 3d). By IHC on

cortical sections, we observed intra-neuronal immunoreactivity for β-amyloid in old *Bmi1*$^{+/-}$ mice, but not in WT littermates (Fig. 3e). Amyloid accumulation was also not observed in very old WT mice (Fig. 3f). To evaluate the possibility of neuronal loss, we calculated the total number of cortical neurons per section in the frontal cortex using a pan-neuronal marker (NeuN). When compared to WT littermates, old *Bmi1*$^{+/-}$ mice displayed a ~20% reduction in NeuN-positive neurons (Fig. 3g). To measure cell death, we quantified the number of neurons positive for activated caspase-3 in the frontal cortex. This revealed a ~2 fold increase in the frequency of apoptotic neurons in old *Bmi1*$^{+/-}$ mice (Fig. 3h), altogether suggesting ongoing neurodegeneration resembling AD in *Bmi1*$^{+/-}$ mice.

Cortical neurons of *Bmi1*$^{+/-}$ mice present heterochromatin anomalies and a DDR involving the ATM and ATR kinases

In most eukaryotes, constitutive heterochromatin perturbations result in genomic instability and premature aging or reduced lifespan [22-27]. Hence, we reasoned that the pathological brain aging phenotype observed in *Bmi1*$^{+/-}$ mice could result from heterochromatin alterations. To test this, we performed immunoblot analysis on old WT and *Bmi1*$^{+/-}$ cortices using antibodies against histone H2A^{ub}, the main target of Bmi1/Ring1b activity, and histone H3K9^{me3}, which marks constitutive heterochromatin. As expected, H2A^{ub} levels were reduced in *Bmi1*$^{+/-}$ mice when compared to WT. Most notably, we also observed reduced H3K9^{me3} levels (Fig. 4a, b). Of note, Bmi1 levels in the brain of old *Bmi1*$^{+/-}$ mice were also below the 50% reduction expected from deleting one Bmi1 allele (Fig. 4a, b). In mammalian cells, a core of proteins is involved in constitutive heterochromatin formation. This involves tri-methylation of H3K9$^{me1/2}$ by the SUV39h1/2 methyltransferases, which form a complex with heterochromatin protein 1 (HP1) [6, 27]. To test for an abnormal heterochromatin structure, we performed IHC on cortical sections using antibodies against H3K9^{me3} and HP1. We observed that in contrast to WT neurons, where 2-3 large chromocenters were present, *Bmi1*$^{+/-}$ neurons had smaller and more numerous chromocenters, suggesting heterochromatin de-nucleation (Fig. 4c-e). One prediction of heterochromatin de-nucleation is activation of a DDR, owing to genomic instability. The *Ataxia Telengectasia Mutated* (ATM) and *Ataxia Telengectasia*

and RAD-3 Related (ATR) kinases work at the apex of the DDR, operate as sensors of chromatin and DNA damage, and are activated by phosphorylation and auto-phosphorylation at specific residues [28]. By immunoblot analysis, we observed increased activation of phospho-ATM at Serine 1981 (p-ATM) and phospho-ATR at Serine 428 (p-ATR) in the cortices of old *Bmi1*$^{+/-}$ mice when compared to WT (Fig. 4f). By IHC, we also observed accumulation of the histone variant γH2AX, a mark of DNA damage, in cortical neurons of old *Bmi1*$^{+/-}$ mice, suggesting a primarily neuronal DDR (Fig. 4g) [29]. To test if the observed heterochromatin anomalies preceded apparition of other pathological marks, we performed immunoblot analysis on cortices from 90-day old WT and *Bmi1*$^{+/-}$ mice. This revealed that p53, p-ATM, p-ATR, γH2AX, p-JNK, p-TAU and amyloid were not yet detectable in young *Bmi1*$^{+/-}$ mice (Supplementary Fig. 1a). In contrast, H2A^{ub} and H3K9^{me3} levels were reduced by ~50% in these mice (Fig. 4h, i). Furthermore, neuron's chromocenters were smaller and more numerous than in WT (Supplementary Fig. 1b, c). These findings revealed that heterochromatin anomalies in *Bmi1*$^{+/-}$ mice are present before the appearance of other pathological marks.

Bmi1 is enriched at heterochromatin in WT mice and required to prevent DNA damage accumulation at heterochromatin in *Bmi1*$^{+/-}$ mice

To test where Bmi1 and DDR proteins were localized on the genome, we performed chromatin immuno-precipitation (ChIP) experiments using Bmi1, H2A^{ub}, H3K9^{me3}, p-ATR, gH2AX and IgG antibodies on old WT and *Bmi1*$^{+/-}$ mice. As positive control for Bmi1 enrichment, we analyzed the *Hoxa7* locus (a known target of Bmi1), while the *b-globin* locus was used as negative control [13]. We found that Bmi1 was highly enriched together with H3K9^{me3} and H2A^{ub} at pericentric (Minor and Major satellite repeats) and intergenic (LINE) constitutive heterochromatin in WT cortices (Fig. 5a). In contrast, Bmi1, H3K9^{me3} and H2A^{ub} enrichment was highly reduced in *Bmi1*$^{+/-}$ cortices (Fig. 5a). We also found that p-ATR and gH2AX enrichment was nearly absent for all tested regions in WT cortices (Fig. 5b). In contrast, while there was no enrichment for gH2AX and p-ATR at euchromatin (*b-actin*), silent facultative heterochromatin (*b-globin*), or bivalent facultative heterochromatin (*Hoxa7*) in *Bmi1*$^{+/-}$ cortices, important accumulation (up to 100 fold difference relative to WT) was found at constitutive heterochromatin (Fig.

5b, c). These findings suggested that Bmi1 and $H2A^{ub}$ are highly enriched at constitutive heterochromatin in WT mouse brains and that DDR in *Bmi1*$^{+/-}$ mouse brains predominantly occurs at constitutive heterochromatin.

Bmi1 is required for proper $H3K9^{me3}$ distribution and co-localizes with $H3K9^{me3}$ in neurons

We performed confocal microscopy imaging analyses on cortical sections from 45-day old WT and *Bmi1*$^{+/-}$ mice to further investigate heterochromatin anomalies. We observed reduced and fragmented $H3K9^{me3}$ immunostaining in *Bmi1*$^{+/-}$ pyramidal neurons (Fig. 6a). DAPI staining was also fragmented, but to a lesser extend (Fig. 6a). While $H3K9^{me3}$ and DAPI signals co-localized in WT neurons, their co-localization was poor in *Bmi1*$^{+/-}$ neurons (Fig. 6a). Quantitative analysis of the data revealed that $H3K9^{me3}$ distribution in WT neurons was very close to a bell curve (normal distribution), while that of *Bmi1*$^{+/-}$ neurons resembled an imperfect bell curve, and where maximal $H3K9^{me3}$ intensity was reduced (Fig. 6b, c). DAPI staining distribution was also affected in *Bmi1*$^{+/-}$ neurons, and where the bell curve was fragmented and compressed (Fig. 6b, c). To confirm Bmi1 enrichment at heterochromatin, we performed IF analyses on cortical sections from WT mice. We observed co-expression of Bmi1 and $H3K9^{me3}$ in the nuclei of pyramidal neurons, and where 90-96% of the Bmi1 signal co-localized with $H3K9^{me3}$ (Fig. 6d).

Heterochromatin anomalies are present at the onset of neurogenesis

To evaluate when heterochromatin anomalies could be first detected, we performed ChIP analysis on cultured embryonic day 18.5 (e18.5) cortical neurons. This method yields a nearly pure neuronal cell population after 7 days *in vitro* [13]. We found enrichment for Bmi1, $H2A^{ub}$ and $H3K9^{me3}$ at the chromatin of *Minor* and *Major satellite repeats* as well as *LINE* intergenic retro-element in WT neurons, and this was significantly reduced in *Bmi1*$^{+/-}$ neurons (Supplementary Fig. 2a). Importantly, Bmi1 also accumulated at the chromatin of its target gene, *Hoxa7*, but not at the chromatin of *b-globin* (Supplementary Fig. 2a). These results established that heterochromatin anomalies in *Bmi1*$^{+/-}$ mice are present at the onset of neurogenesis, and confirmed Bmi1 and $H2A^{ub}$ enrichment at heterochromatin in neurons.

The ATM/ATR kinases operate upstream of p53 and p-TAU

The Chk1 and Chk2 kinases can target TAU for phosphorylation at specific residues [30]. Likewise, ATM and ATR can target p53 for phosphorylation and stabilization [31, 32]. To test if we could establish a cause an effect relationship between DDR and the neuronal pathology, we analyzed cultures of e18.5 neurons. Using antibodies against p-ATM and p-Chk1 (a downstream target of ATR), we found that DDR was not detectable in WT or *Bmi1*$^{+/-}$ neurons. In contrast, it was readily observed in *Bmi1*-null neurons, suggesting a gene dosage effect (Supplementary Fig. 2b). Notably, p-TAU accumulation was also observed in *Bmi1*-null neurons, but not in WT or *Bmi1*$^{+/-}$ neurons (Supplementary Fig. 2b). Neurons were exposed to a pharmaceutical inhibitor of ATM and ATR (ATM/ATRi) for 16 hours and this could effectively prevent p-ATM and p-Chk1 as well as p-TAU accumulation in *Bmi1*$^{-/-}$ neurons (Supplementary Fig. 2b). Using a competitive pharmaceutical inhibitor of ATM (ATMi) at a concentration showed to block ATM autophosphorylation [11], we found that p53 accumulation in *Bmi1*-null neurons could not be prevented (Supplementary Fig. 2b). In contrast, exposing *Bmi1*-null neurons to ATM/ATRi largely prevented p53 accumulation (Supplementary Fig. 2b), suggesting that the DDR machinery operates upstream of p53 and p-TAU in the neuropathological cascade.

BMI1 deficiency, heterochromatin alterations and DDR in LOAD brains

Considering the similarities between the *Bmi1*$^{+/-}$ mouse phenotype and AD, we investigated BMI1 expression in AD. The hippocampus is a brain region where severe neurodegeneration occurs in AD. By immunoblot analysis, we observed comparable BMI1 expression in the hippocampus of control brains (n = 3 brains, median age of 59 year) and EOAD brains (n = 4 brains, median age of 61 year) (Fig. 7a, b, and Supplementary Table 1). In contrast, while BMI1 expression was present in the hippocampus of all elderly control brains (n = 3 brains, median age of 87 year), it was nearly absent in LOAD brains (n = 5 brains, median age of 82 year) (Fig. 7c, e, data not shown, and Supplementary Table 1). Since the hippocampus is highly affected in AD, we analyzed BMI1 expression in the frontal cortex, which is affected later and less severely.

Because BMI1 expression could only be detected in elderly control brains in regular immunoblot assays (n = 12 samples with two experiments, data not shown), blots were incubated with the BMI1 antibody for 3 days in order to increase sensitivity. This revealed the presence of a BMI1 triplet representing different phosphorylated forms of BMI1 (Fig. 7d) [33, 34]. While BMI1 expression was detected in all control brains (n = 6 brains, median age of 87 year), it was nearly absent in LOAD brains (n = 6 brains, median age of 87 year) (Fig. 7d, e, and Supplementary Table 1). BMI1 mRNA levels were also reduced by ~90% in LOAD samples when compared to elderly controls (not shown). Histone H2A is the main target of BMI1/RING1a/b activity [7, 8], and we found that *Bmi1* hemi-deficiency is associated with reduced $H3K9^{me3}$ levels in mice. Notably, $H2A^{ub}$ and $H3K9^{me3}$ levels were significantly reduced in LOAD brains (Fig. 7c-e). In contrast, $H2A^{ub}$ and $H3K9^{me3}$ levels were normal in EOAD brains (Fig. 7a, b), and in elderly control brains (Fig. 7c-e). To test for genomic instability, we analyzed the expression of DDR proteins. We observed accumulation of p-ATM, p-ATR and p-CHK1 in all LOAD brains, but not in elderly control brains (Fig. 7d). In contrast, p-ATM, p-ATR or p-CHK1 accumulation in EOAD and young control brains was not observed, with the exception of one EOAD sample presenting p-ATM accumulation (Fig. 7a). To investigate whether the LOAD chromatin phenotype was neuronal, we performed IHC on frontal cortex sections. We observed pyramidal neurons expressing BMI1 and NeuN in control brains, while neuronal BMI1 expression was reduced or absent in LOAD brains (Fig. 7f, and Supplementary Table 1). Likewise, large nuclei corresponding to that of pyramidal neurons had reduced or absent (~38% of all neurons) $H3K9^{me3}$ nuclear staining and neuron's chromocenters were smaller and more numerous in LOAD brains when compared to elderly controls (Fig. 7g-i). Furthermore, p-ATM accumulation in LOAD brains was found primarily in neurons (Fig. 7j).

BMI1 is enriched at heterochromatin in healthy brains and DDR occurs at heterochromatin in LOAD brains

To establish whether BMI1 was also enriched at heterochromatin in the human brain, we performed ChIP experiments on human frontal cortex samples. The *b-GLOBIN* locus was used as negative control and the *HOXC13* locus as positive control for BMI1 binding to

chromatin [35]. We observed BMI1 and H3K9^{me3} enrichment at pericentric heterochromatin in control brains, while BMI1 and H3K9^{me3} were depleted in LOAD brains (Fig. 8a). We also tested for DDR localization on the genome by ChIP. When compared to controls, there was predominant enrichment for p-ATR and gH2AX in LOAD at constitutive heterochromatin (*SATIII*, *SATA* and *McBOX*), but not facultative heterochromatin (*HOXC13* and *b-GLOBIN*) or euchromatin (*ACTIN*) (Figure 8b, c). There was also a (non-significant) trend for p-ATM enrichment at constitutive heterochromatin in LOAD (Fig. 8b, c). These findings suggested predominant accumulation of DDR proteins at H3K9^{me3}-dependent constitutive heterochromatin in LOAD brains.

DISCUSSION

We demonstrated here that: 1) *Bmi1*$^{+/-}$ mice develop a behavioral, physiological, neuropathological and molecular phenotype resembling LOAD; 2) heterochromatin anomalies in *Bmi1*$^{+/-}$ neurons precede other pathological marks; 3) DDR in *Bmi1*$^{-/-}$ neurons works upstream of p53 and p-TAU and occurs at H3K9^{me3}-associated heterochromatin; 4) Bmi1 co-localizes with H3K9^{me3} in neurons; 5) Bmi1 and H2A^{ub} are enriched at H3K9^{me3}-associated heterochromatin in mouse brains; 6) BMI1 expression is deficient in LOAD brains, together with that of H2A^{ub} and H3K9^{me3}; 7) BMI1 is enriched at H3K9^{me3}-associated heterochromatin in human brains; 8) DDR also occurs at constitutive heterochromatin in LOAD brains. These results reveal striking molecular similarities between the *Bmi1*$^{+/-}$ mouse and LOAD phenotypes. They also provide evidences that Bmi1 is enriched at constitutive heterochromatin and required for heterochromatic genome stability. Most unexpectedly, they suggest that deficient BMI1 expression and heterochromatic genome instability are hallmarks of LOAD.

The heterochromatin island hypothesis of aging stipulates that epigenome instability at the constitutive heterochromatin is a driving force of cellular aging [36, 37]. Notably, perturbations of the nuclear matrix or inactivation of chromatin remodeling proteins, such as those of the NURD complex, result in DDR and cellular senescence that are preceded by heterochromatin alterations [25]. Furthermore, modifications of constitutive heterochromatin in response to an acute stress can result in epigenome instability and

perturbation of gene expression program, which are hallmarks of cellular aging [22]. In mice, deletion of the SUV39h1/h2 methyltransferases leads to reduced viability, loss of H3K9^{me3} and genomic instability [27]. In *Drosophila*, perturbation of H3K9^{me2} levels through inactivation of Su(var)3-9 results in genomic instability and DDR at heterochromatin [26]. We showed here that heterochromatin alterations in *Bmi1*$^{+/-}$ mice precede the other pathological marks and are present at the time of neurogenesis. Notably, this correlated with DDR at constitutive heterochromatin. The p53 protein is a critical mediator of neuronal cell death in multiple neurodegenerative disorders [38-40]. Similarly, p-TAU mediates amyloid dependent and independent neurodegeneration and synaptic dysfunction [41-43]. Using *Bmi1*-null neurons, we showed that a causal relationship could be established between DDR and accumulation of p53 and p-TAU, suggesting that persistent DDR in neurons is sufficient to cause neurodegeneration. Hence, over-expression of Chk1 or Chk2 can exacerbate TAU toxicity in a *Drosophila* model of neurodegeneration through phosphorylation of human TAU at Ser262 [44]. Likewise, JNK activation may promote TAU hyper-phosphorylation [14]. Taken together, these observations suggest that a sequential neuropathological cascade operates in *Bmi1*$^{+/-}$ mice and where deficient heterochromatin compaction initiates the disease process.

There is overlooked evidence for PRC1 proteins localization, including BMI1, at pericentric heterochromatin in human cells [45]. We have found that Bmi1 hemi-deficiency results in molecular alterations at constitutive heterochromatin characterized by reduced H2A^{ub} and H3K9^{me3} deposition. This correlated with Bmi1 and H2A^{ub} accumulation at constitutive heterochromatin and co-localization with H3K9^{me3} in neurons. By performing ChIP, we also established that BMI1 accumulates at H3K9^{me3}–associated heterochromatin in healthy human brains, and that BMI1 and H3K9^{me3} were reduced at heterochromatin in LOAD brains. Taken together, these results suggest that Bmi1 promotes heterochromatin formation by catalyzing H2A^{ub} deposition at genomic repetitive sequences. Interestingly, a similar mechanism was proposed for BRCA1-mediated heterochromatinization [46]. How Bmi1/Ring1b-mediated H2A^{ub} deposition at heterochromatin translates into H3K9^{me3} deposition and heterochromatin spreading remains an open question. Furthermore, whether confounding mechanisms are also

involved in the heterochromatin de-compaction phenotype observed in *Bmi1*$^{+/-}$ mice remains to be investigated.

We have found that enrichment for p-ATR and γH2AX in LOAD brains occurs preferentially at constitutive heterochromatin. The relatively weak accumulation of p-ATM in LOAD brains as observed by ChIP (in contrast with immunoblot) suggests that a portion of the p-ATM pool is not chromatin-bound. This is consistent with p-ATM accumulation in both cytosolic and nuclear neuronal compartments (see Fig. 7). Why loss of heterochromatin compaction in LOAD brains and *Bmi1*$^{+/-}$ mouse brains is associated with DNA damage accumulation is unknown. It is possible that repetitive DNA sequences are intrinsically unstable upon loss of H3K9^{me3}, and thus prone to *de novo* DNA damage formation [26]. It is also possible that the efficiency of DNA repair is reduced upon BMI1 deficiency or that recognition of the H3K9^{me3} mark is important to activate the process of DNA repair [11, 12, 47].

There are mounting evidences supporting the possibility that epigenetic modifications are involved in LOAD [48, 49]. Particularly, it was showed that genome-wide reductions in DNA methylation are characteristic of LOAD [50]. We found deficient BMI1 expression, loss of heterochromatin compaction and reduced histone H2A^{ub} and H3K9^{me3} levels in all LOAD samples tested. These anomalies were not present in elderly controls or EOAD samples, thus excluding brain aging or neurodegeneration as the primary cause. The molecular dichotomy observed between EOAD and LOAD further suggests that they represent distinct pathological entities [4]. Why BMI1 expression is reduced in LOAD and whether this is a cause or a consequence of the human disease remains to be investigated.

ACKNOWLEDGMENTS

We are grateful to D. Cécyre and J. Prud'homme for the human brain samples, and J. Rochford for help with the behavioral analysis (Douglas Hospital Research Center). We thank Drs F. Rodier, R. Kothary, G. Ferbeyre and D. Picketts for critical reading of the manuscript. This work was supported by a grant from the Natural Science and Engineering Research Council of Canada. J. E. H. is supported by a fellowship from the University of Montreal Molecular Biology Program and G.B. is supported by a fellowship from the from the Fonds de Recherche en Santé du Québec. The authors declare no competing financial interests.

REFERENCES

1. Blennow, K., de Leon, M.J. & Zetterberg, H. Alzheimer's disease. *Lancet* 368, 387-403 (2006).

2. Campion, D.*, et al.* Early-onset autosomal dominant Alzheimer disease: prevalence, genetic heterogeneity, and mutation spectrum. *Am. J. Hum. Genet.* 65, 664-670 (1999).

3. Rogaeva, E.*, et al.* The neuronal sortilin-related receptor SORL1 is genetically associated with Alzheimer disease. *Nat. Genet.* 39, 168-177 (2007).

4. Pimplikar, S.W. Reassessing the amyloid cascade hypothesis of Alzheimer's disease. *Int. J. Biochem. Cell Biol.* 41, 1261-1268 (2009).

5. Savva, G.M.*, et al.* Age, neuropathology, and dementia. *N. Engl. J. Med.* 360, 2302-2309 (2009).

6. Fodor, B.D., Shukeir, N., Reuter, G. & Jenuwein, T. Mammalian Su(var) genes in chromatin control. *Annu. Rev. Cell Dev. Biol.* 26, 471-501 (2010).

7. Buchwald, G.*, et al.* Structure and E3-ligase activity of the Ring-Ring complex of polycomb proteins Bmi1 and Ring1b. *EMBO J.* 25, 2465-2474 (2006).

8. Li, Z.*, et al.* Structure of a Bmi-1-Ring1B polycomb group ubiquitin ligase complex. *J. Biol. Chem.* 281, 20643-20649 (2006).

9. van der Lugt, N.M.*, et al.* Posterior transformation, neurological abnormalities, and severe hematopoietic defects in mice with a targeted deletion of the bmi-1 proto-oncogene. *Genes Dev.* 8, 757-769 (1994).

10. Jacobs, J.J., Kieboom, K., Marino, S., DePinho, R.A. & van Lohuizen, M. The oncogene and Polycomb-group gene bmi-1 regulates cell proliferation and senescence through the ink4a locus. *Nature* 397, 164-168 (1999).

11. Facchino, S., Abdouh, M., Chatoo, W. & Bernier, G. BMI1 confers radioresistance to normal and cancerous neural stem cells through recruitment of the DNA damage response machinery. *J. Neurosci.* 30, 10096-10111 (2010).

12. Ismail, I.H., Andrin, C., McDonald, D. & Hendzel, M.J. BMI1-mediated histone ubiquitylation promotes DNA double-strand break repair. *J. Cell Biol.* 191, 45-60 (2010).

13. Chatoo, W.*, et al.* The polycomb group gene Bmi1 regulates antioxidant defenses in neurons by repressing p53 pro-oxidant activity. *J. Neurosci.* 29, 529-542 (2009).

14. Wetzel, M.K.*, et al.* p73 regulates neurodegeneration and phospho-tau accumulation during aging and Alzheimer's disease. *Neuron* 59, 708-721 (2008).

15. Krishnamurthy, J.*, et al.* Ink4a/Arf expression is a biomarker of aging. *J. Clin. Invest.* 114, 1299-1307 (2004).

16. Bliss, T.V. & Collingridge, G.L. A synaptic model of memory: long-term potentiation in the hippocampus. *Nature* 361, 31-39 (1993).

17. Chapman, P.F.*, et al.* Impaired synaptic plasticity and learning in aged amyloid precursor protein transgenic mice. *Nat. Neurosci.* 2, 271-276 (1999).

18. Nalbantoglu, J.*, et al.* Impaired learning and LTP in mice expressing the carboxy terminus of the Alzheimer amyloid precursor protein. *Nature* 387, 500-505 (1997).

19. Li, R.*, et al.* Amyloid beta peptide load is correlated with increased beta-secretase activity in sporadic Alzheimer's disease patients. *Proc. Natl. Acad. Sci. U. S. A.* 101, 3632-3637 (2004).

20. Tomiyama, T.*, et al.* A mouse model of amyloid beta oligomers: their contribution to synaptic alteration, abnormal tau phosphorylation, glial activation, and neuronal loss in vivo. *J. Neurosci.* 30, 4845-4856 (2010).

21. Tomiyama, T.*, et al.* A new amyloid beta variant favoring oligomerization in Alzheimer's-type dementia. *Ann. Neurol.* 63, 377-387 (2008).

22. Oberdoerffer, P.*, et al.* SIRT1 redistribution on chromatin promotes genomic stability but alters gene expression during aging. *Cell* 135, 907-918 (2008).

23. Wang, R.H.*, et al.* Impaired DNA damage response, genome instability, and tumorigenesis in SIRT1 mutant mice. *Cancer Cell* 14, 312-323 (2008).

24. Larson, K.*, et al.* Heterochromatin formation promotes longevity and represses ribosomal RNA synthesis. *PLoS Genet* 8, e1002473 (2012).

25. Pegoraro, G.*, et al.* Ageing-related chromatin defects through loss of the NURD complex. *Nat Cell Biol* 11, 1261-1267 (2009).

26. Peng, J.C. & Karpen, G.H. Heterochromatic genome stability requires regulators of histone H3 K9 methylation. *PLoS Genet* 5, e1000435 (2009).

27. Peters, A.H.*, et al.* Loss of the Suv39h histone methyltransferases impairs mammalian heterochromatin and genome stability. *Cell* 107, 323-337 (2001).

28. Smith, J., Tho, L.M., Xu, N. & Gillespie, D.A. The ATM-Chk2 and ATR-Chk1 pathways in DNA damage signaling and cancer. *Adv. Cancer Res.* 108, 73-112 (2010).

29. Rogakou, E.P., Pilch, D.R., Orr, A.H., Ivanova, V.S. & Bonner, W.M. DNA double-stranded breaks induce histone H2AX phosphorylation on serine 139. *J. Biol. Chem.* 273, 5858-5868 (1998).

30. Mendoza, J.*, et al.* Global Analysis of Phosphorylation of Tau by the Checkpoint Kinases Chk1 and Chk2 in vitro. *J Proteome Res* (2013).

31. Keramaris, E., Hirao, A., Slack, R.S., Mak, T.W. & Park, D.S. Ataxia telangiectasia-mutated protein can regulate p53 and neuronal death independent of Chk2 in response to DNA damage. *J. Biol. Chem.* 278, 37782-37789 (2003).

32. Lakin, N.D., Hann, B.C. & Jackson, S.P. The ataxia-telangiectasia related protein ATR mediates DNA-dependent phosphorylation of p53. *Oncogene* 18, 3989-3995 (1999).

33. Kim, J., Hwangbo, J. & Wong, P.K. p38 MAPK-Mediated Bmi-1 down-regulation and defective proliferation in ATM-deficient neural stem cells can be restored by Akt activation. *PLoS One* 6, e16615 (2011).

34. Voncken, J.W.*, et al.* Chromatin-association of the Polycomb group protein BMI1 is cell cycle-regulated and correlates with its phosphorylation status. *J. Cell Sci.* 112 (Pt 24), 4627-4639 (1999).

35. Abdouh, M.*, et al.* BMI1 sustains human glioblastoma multiforme stem cell renewal. *J. Neurosci.* 29, 8884-8896 (2009).

36. Imai, S. & Kitano, H. Heterochromatin islands and their dynamic reorganization: a hypothesis for three distinctive features of cellular aging. *Exp. Gerontol.* 33, 555-570 (1998).

37. Villeponteau, B. The heterochromatin loss model of aging. *Exp. Gerontol.* 32, 383-394 (1997).

38. Bae, B.I.*, et al.* p53 mediates cellular dysfunction and behavioral abnormalities in Huntington's disease. *Neuron* 47, 29-41 (2005).

39. Chatoo, W., Abdouh, M. & Bernier, G. P53 pro-oxidant activity in the central nervous system: implication in aging and neurodegenerative diseases. *Antioxid Redox Signal* (2011).

40. Culmsee, C. & Mattson, M.P. p53 in neuronal apoptosis. *Biochem. Biophys. Res. Commun.* 331, 761-777 (2005).

41. Ballatore, C., Lee, V.M. & Trojanowski, J.Q. Tau-mediated neurodegeneration in Alzheimer's disease and related disorders. *Nat Rev Neurosci* 8, 663-672 (2007).

42. Hoover, B.R.*, et al.* Tau mislocalization to dendritic spines mediates synaptic dysfunction independently of neurodegeneration. *Neuron* 68, 1067-1081 (2010).

43. Ittner, L.M.*, et al.* Dendritic function of tau mediates amyloid-beta toxicity in Alzheimer's disease mouse models. *Cell* 142, 387-397 (2010).

44. Iijima-Ando, K., Zhao, L., Gatt, A., Shenton, C. & Iijima, K. A DNA damage-activated checkpoint kinase phosphorylates tau and enhances tau-induced neurodegeneration. *Hum. Mol. Genet.* 19, 1930-1938 (2010).

45. Saurin, A.J.*, et al.* The human polycomb group complex associates with pericentromeric heterochromatin to form a novel nuclear domain. *J. Cell Biol.* 142, 887-898 (1998).

46. Zhu, Q.*, et al.* BRCA1 tumour suppression occurs via heterochromatin-mediated silencing. *Nature* 477, 179-184 (2011).

47. Sun, Y.*, et al.* Histone H3 methylation links DNA damage detection to activation of the tumour suppressor Tip60. *Nat Cell Biol* 11, 1376-1382 (2009).

48. Bihaqi, S.W., Schumacher, A., Maloney, B., Lahiri, D.K. & Zawia, N.H. Do epigenetic pathways initiate late onset Alzheimer disease (LOAD): towards a new paradigm. *Curr Alzheimer Res* 9, 574-588 (2012).

49. Wang, S.C., Oelze, B. & Schumacher, A. Age-specific epigenetic drift in late-onset Alzheimer's disease. *PLoS One* 3, e2698 (2008).

50. Mastroeni, D.*, et al.* Epigenetic changes in Alzheimer's disease: decrements in DNA methylation. *Neurobiol. Aging* 31, 2025-2037 (2010).

FIGURE LEGENDS

Figure 1. *Bmi1*$^{+/-}$ mice present neurological symptoms

(a) Photographs of 3-month old and old WT and *Bmi1*$^{+/-}$ mice. Note that old *Bmi1*$^{+/-}$ mice (n = 5) are smaller and exhibit hair loss (alopecia) compared to WT littermates (n = 5). (b) Quantification representing the mean weight of 3-month (n = 6), 1-yr (n = 6) and old (n = 6) WT and *Bmi1*$^{+/-}$ mice, and where n = the number of mice/genotype. (c) Photographs showing the paw clasping reflex of old WT (n = 5) and *Bmi1*$^{+/-}$ mice (n = 5). Note that the *Bmi1*$^{+/-}$ mouse pulls its fore limbs into its body rather than spreading them away from its trunk, and present asymmetry in the hind limbs' position. (d) Analysis of SA b-galactosidase activity in the cortices of 24 month-old (24 M) WT and 15 month-old (15 M) *Bmi1*$^{+/-}$ mice. Scale bar: 20μm. (e) Quantification of the number of SA b-galactosidase positive neurons/cortical section (n = 6), where n = number of brain sections/mouse. (f) Quantitative PCR analysis of *p16*^{Ink4a} and p19^{Arf} expression in the cortices of age-match 16 month-old WT (n = 3) and *Bmi1*$^{+/-}$ (n = 3) mice. All values are mean ± SEM. (*) P<0.05; (**)<0.01; Student's t-test.

Figure 2. *Bmi1*$^{+/-}$ mice display spatial memory deficit and reduced LTP

(a-c) Healthy 15-month old WT (n = 5) and *Bmi1*$^{+/-}$ (n = 5) male mice were tested for behavioral changes associated with spatial memory formation deficit. (a) Results of Morris water maze probe test, showing mean swim speed, time spent in the target quadrant searching for the hidden platform, and mean time to reach the target platform (latency). (b) Charts representing mean latency and mean thigmotaxis of Morris water maze 4-day trials of WT and *Bmi1*$^{+/-}$ mice. (c) Histograms representative of Barnes maze test results including mean total errors and mean latency to reach the target probe. (d) LTP in 15-month old WT and *Bmi1*$^{+/-}$ mice. Scatter plots revealed changes in the slope of field excitatory postsynaptic potential (fEPSP) recorded from the hippocampal CA1 region of WT and *Bmi1*$^{+/-}$ mice. LTP was induced by tetanus (100 Hz, 100 stimulation). Dotted line represents the baseline. (e) Representative traces of fEPSP recorded before (baseline) and 60 min after tetanus. Dotted lines represent baselines. (f) Histogram of fEPSP slope at 60 min after LTP induction. Normalized fEPSP slopes, recorded between

55-60 min after tetanus, were averaged for calculating percent potentiation. All values are mean ± SEM. (*) P< 0.05; (**) P< 0.01; Student's t-test.

Figure 3. *Bmi1*$^{+/-}$ mice present AD-like neurodegeneration

(a) Western blot analysis of cortical extracts from 15-month old WT (n = 6) and *Bmi1*$^{+/-}$ (n = 6) mice, where n = the number of independent samples analyzed. (b) IHC for p-TAU (PHF1) on cortical sections of 20-month old WT (n = 3) and *Bmi1*$^{+/-}$ mice (n = 3), where n = the number of independent animals. (i) Low magnification. Scale bar: 20µm. Higher magnifications in (ii) revealed p-TAU deposits on ghost-like neurons and in (iii) p-TAU immunoreactivity in track fibers of the cortical white matter of *Bmi1*$^{+/-}$ mice. Scale bar: 8µm. (c) Western blot analysis of cortical extracts from 24-month old WT (n = 3 mice) and 15-month old *Bmi1*$^{+/-}$ mice (n = 1 mouse), with 2 independent experiments. (d) Western blot (input) and IP (using DE2B4) of the soluble cellular fraction of 15-month old WT (n = 3) and *Bmi1*$^{+/-}$ (n = 3) cortices, and from a 6-month old *APP*^{TG} mouse, all revealed with the FCA3542 antibody, with 2 independent experiments. (e) IHC on brain sections from 20 month-old WT (n = 3 mice) and *Bmi1*$^{+/-}$ (n = 3 mice) mice to analyze the expression of b-amyloid oligomers (DE2B4). Top images scale bar is 20µm; Lower images scale bar is 8µm. (f) Western blot analysis of cortical extracts from 24-month old WT (n = 3 mice), 15-month old *Bmi1*$^{+/-}$ (n = 1) and 12-month old *APP*^{TG} (n = 1) mice with the FCA3542 antibody, with 2 independent experiments. H3: histone H3. (g) Quantification of the number of NeuN+ cortical neurons in the frontal cortex of age-match old WT (n = 5 mice) and *Bmi1*$^{+/-}$ (n = 5 mice) using IHC. (h) Quantification of the number of neurons positive for activated caspase-3 in the frontal cortex of age-match old WT (n = 5 mice) and *Bmi1*$^{+/-}$ (n = 5 mice) mice. All values are mean ± SEM. (*) P<0.05; Student's t-test.

Figure 4. Heterochromatin anomalies are present in cortical neurons of *Bmi1*$^{+/-}$ mice

(a) Western blot analysis of cortical extracts from old WT (n = 6) and *Bmi1*$^{+/-}$ (n = 6) mice, where n = the number of independent animals. (b) Quantification of data presented in (a). (c, e) IHC was performed on cortical sections from old WT (n = 3) and *Bmi1*$^{+/-}$ (n

= 3) mice to reveal the expression of constitutive heterochromatin markers. Scale bar: 20µm. Scale bar in the inset: 8µm. (d) Quantification of the number of H3K9^{me3} foci per nucleus in (c), and where 6 sections/sample were count. (f) Western blot analysis of cortical extracts from old WT (n = 3) and *Bmi1*$^{+/-}$ (n = 3) mice using antibodies against p-ATM and p-ATR. (g) IHC for gH2AX on cortical sections of old WT (n = 2) and *Bmi1*$^{+/-}$ (n = 2) mice. (h) Western blot on cortical extracts of 3-month old WT (n = 3) and *Bmi1*$^{+/-}$ (n = 3) mice. (i) Quantification of results obtained in (h). Scale bar: 20µm. All values are mean ± SEM. (*) P<0.05; (**)<0.01; Student's t-test.

Figure 5. BMI1 is enriched at heterochromatin and required to prevent DNA damage accumulation at pericentric and intergenic heterochromatin in *Bmi1*$^{+/-}$ mouse brains

(a) ChIP analyses were performed on frontal cortex homogenates from 15-month old WT (n = 3) and *Bmi1*$^{+/-}$ (n = 3) mice. Quantitative PCR was performed in triplicate for each DNA sequence. All data are presented as fold of input. Bmi1 and H2A^{ub} reduction ($p < 0.05$), and p-ATR and gH2AX accumulation ($p < 0.01$) in *Bmi1*$^{+/-}$ mice are significant (Two-way ANOVA analysis). (b) Fold differences for gH2AX and p-ATR accumulation in *Bmi1*$^{+/-}$ mice were measured relative to WT levels for each DNA sequence.

Figure 6. Bmi1 is required for normal H3K9^{me3} distribution and co-localizes with H3K9^{me3} in cortical neurons

(a) Cortical slices from 45-day old mice were labeled with an H3K9^{me3} antibody, mounted with DAPI and analyzed by confocal microscopy, where n = 2 for the number of experiments. Areas showed are located in layers 2-3 of the frontal cortex. In WT mice, large pyramidal neurons are strongly labeled by the H3K9^{me3} antibody. Note the co-localization of H3K9^{me3} with DAPI. In *Bmi1*$^{+/-}$ samples, large pyramidal neurons are weakly labeled by the H3K9^{me3} antibody and the H3K9me3 signal is fragmented. Note the poor co-localization of H3K9^{me3} with DAPI. (b, c) Quantification of the images showed in (a) revealing the normal distribution of the H3K9^{me3} signal in WT (b), but near bimodal (i) H3K9^{me3} distribution in the *Bmi1*$^{+/-}$ samples (c). Likewise, DAPI signal in the *Bmi1*$^{+/-}$ samples is compressed, enlarged and fragmented (ii). Note also the reduced

maximal intensity of the H3K9^{me3} signal in the *Bmi1*$^{+/-}$ samples (iii). (d) Cortical slices from 45-day old WT mice were labeled with Bmi1 and H3K9^{me3} antibodies, mounted with DAPI and analyzed by confocal microscopy, where n = 2 for the number of experiments. About 90-96% of the Bmi1 signal was found to co-localize with H3K9^{me3}.

Figure 7. BMI1 deficiency, neuronal heterochromatin loss and DDR in LOAD brains

(a) Immunoblot on hippocampal extracts from young control and EOAD patients. (b) Quantification of the results in (a) relative to "healthy" controls. (c) Immunoblot on hippocampal extracts of aged control and LOAD patients. (d) Immunoblot on frontal cortex extracts from control and LOAD patients. (e) Quantification of the results in (c, d) relative to "healthy" controls. (f) IHC staining for BMI1 (black arrows) and NeuN (red arrows) on frontal cortex sections of age-match control and LOAD samples. Note the lipofuscin deposition (blue arrows). Scale bar: 8μm. (g) IHC staining for H3K9^{me3} on frontal cortex sections of "healthy" control and LOAD brains: (i) reduced peri-nucleolar heterochromatin in LOAD (arrows), (ii) chromocenters de-condensation in LOAD, and (iii) loss of H3K9^{me3} immunoreactivity in LOAD neurons. Scale bar: 5μm. (h) Quantification of the number of H3K9^{me3} foci/H3K9^{me3}-positive neuron. H3K9^{me3}-negative neurons were excluded from the analysis. (i) Quantification of the number of H3K9^{me3}-negative neurons, which were not found in aged controls. 6 full-fields at 630 magnification/sample were counted, with n = 6 independent samples. (j) IHC staining for p-ATM on frontal cortex sections of "healthy" control and LOAD patients. p-ATM is predominant in LOAD neurons and accumulates in both cytosolic (blue arrowhead) and nuclear (black arrowhead) compartments. All values are mean ± SEM. (*) P<0.05; (**)<0.01; (***)<0.001; Student's t-test.

Figure 8. DNA damage accumulates at constitutive heterochromatin in LOAD brains

(a, b) ChIP experiments were performed on frontal cortex extracts of age-match "healthy" control (n = 6 independent samples) and LOAD patients (n = 6 independent samples). All data are represented as *fold of input*. (a) BMI1 is enriched at constitutive heterochromatin

(McBOX, SATIII and SATA) together with H3K9^{me3} in control samples. BMI1 was also found at HOXC13. Note loss of BMI1 and H3K9^{me3} enrichment in LOAD samples. (b) Both p-ATR and gH2AX showed preferential enrichment at constitutive heterochromatin, but not elsewhere, in LOAD samples when compared to control samples. (c) Fold differences between "healthy" control and LOAD samples for p-ATM, p-ATR and gH2AX accumulation. Differences were more notable for p-ATR and gH2AX (bold numbers). All values are mean ± SEM. (*) $P<0.05$; (**)<0.01; Two way-ANOVA test was performed for multiple gene analysis and Student's t-test for single gene analysis.

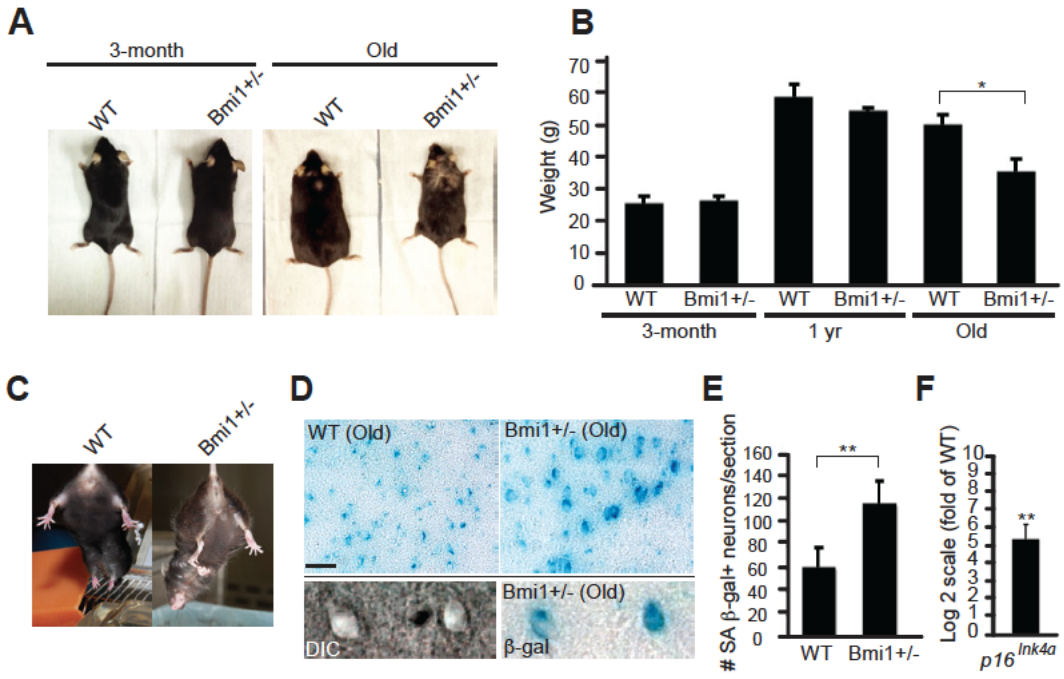
A
3-month
Old
WT
Bmi1+/-
WT
Bmi1+/-
B
Weight (g)
70
60
50
40
30
20
10
0
*
WT
Bmi1+/-
WT
Bmi1+/-
WT
Bmi1+/-
3-month
1 yr
Old
C
WT
Bmi1+/-
D
WT (Old)
Bmi1+/- (Old)
DIC
Bmi1+/- (Old)
β-gal
E
SA β-gal+ neurons/section
160
140
120
100
80
60
40
20
0
**
WT
Bmi1+/-
F
Log 2 scale (fold of WT)
10
9
8
7
6
5
4
3
2
1
0
**
p16Ink4a

Figure 1

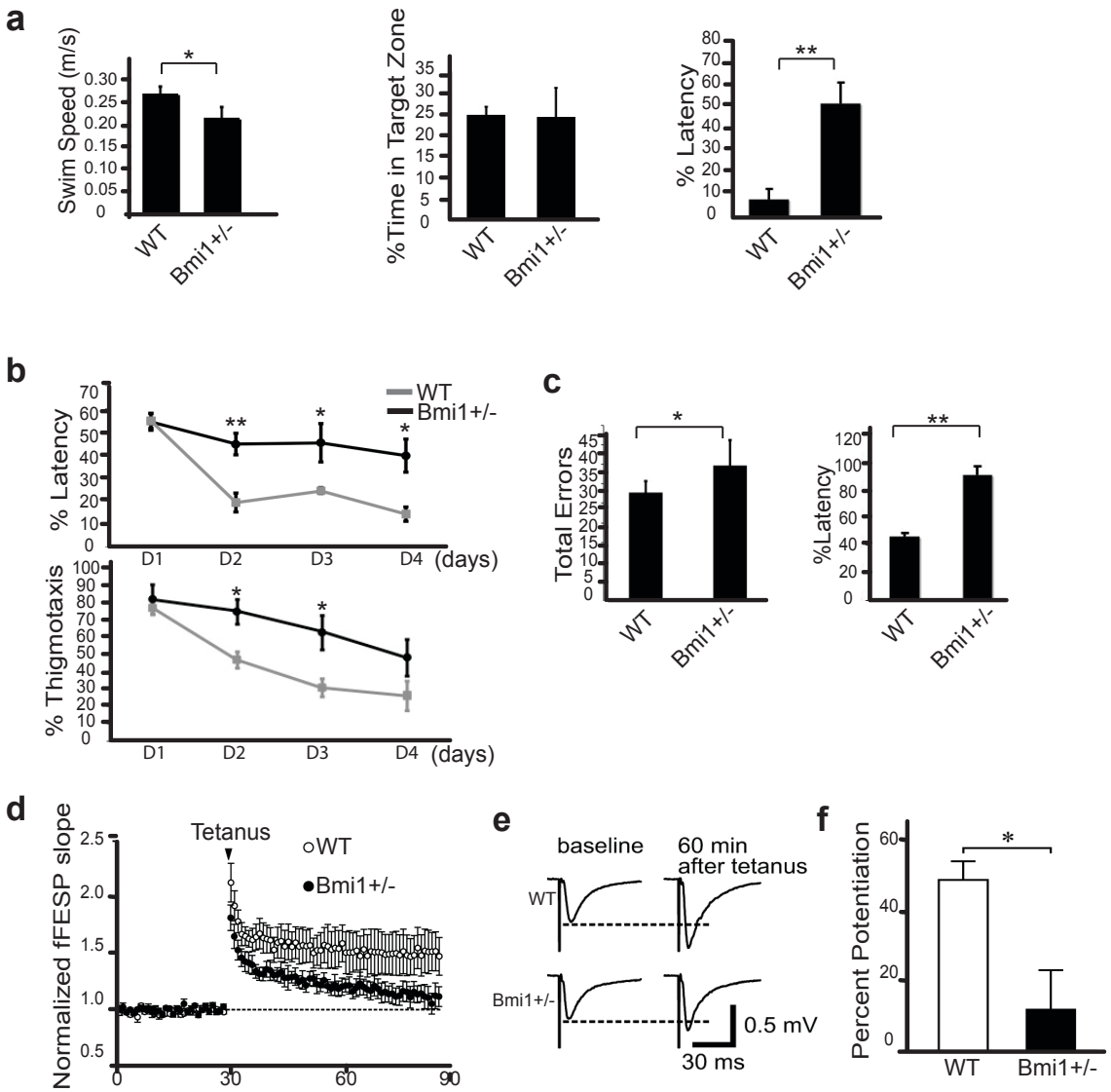
a
Swim Speed (m/s)
0.30
0.25
0.20
0.15
0.10
0.05
0
*
WT
Bmi1+/-
%Time in Target Zone
35
30
25
20
15
10
5
0
WT
Bmi1+/-
% Latency
80
70
60
50
40
30
20
10
0
**
WT
Bmi1+/-
b
% Latency
70
60
50
40
30
20
10
0
WT
Bmi1+/-
**
*
*
D1
D2
D3
D4
(days)
% Thigmotaxis
100
90
80
70
60
50
40
30
20
10
0
*
*
D1
D2
D3
D4
(days)
c
Total Errors
45
40
35
30
25
20
15
10
5
0
*
WT
Bmi1+/-
%Latency
120
100
80
60
40
20
0
**
WT
Bmi1+/-
d
Normalized fFESP slope
2.5
2.0
1.5
1.0
0.5
Tetanus
○WT
●Bmi1+/-
0
30
60
90
e
baseline
60 min
after tetanus
WT
Bmi1+/-
0.5 mV
30 ms
f
Percent Potentiation
60
40
20
0
*
WT
Bmi1+/-

Figure 2

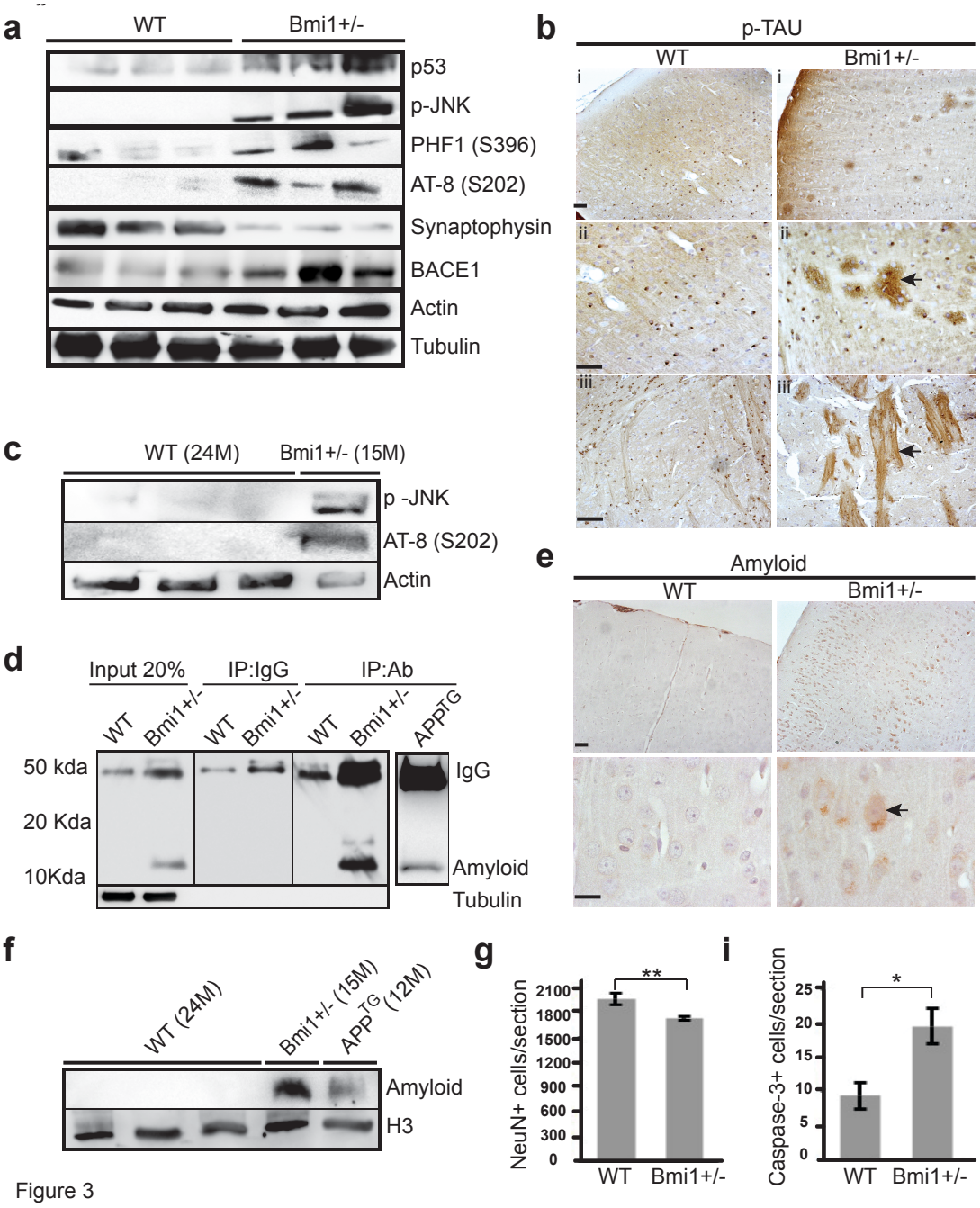

Figure 3

Figure 3

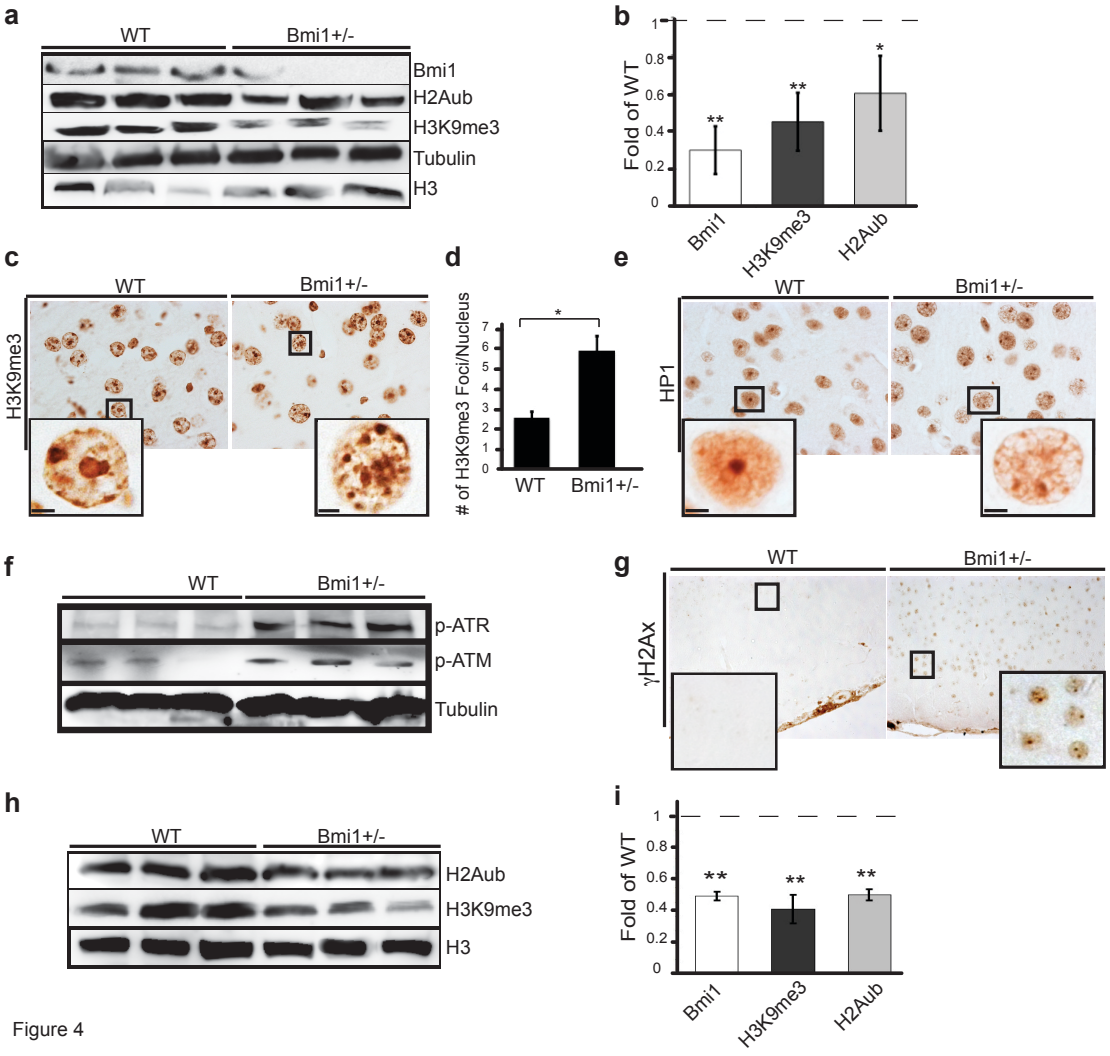

Figure 4

Figure 4

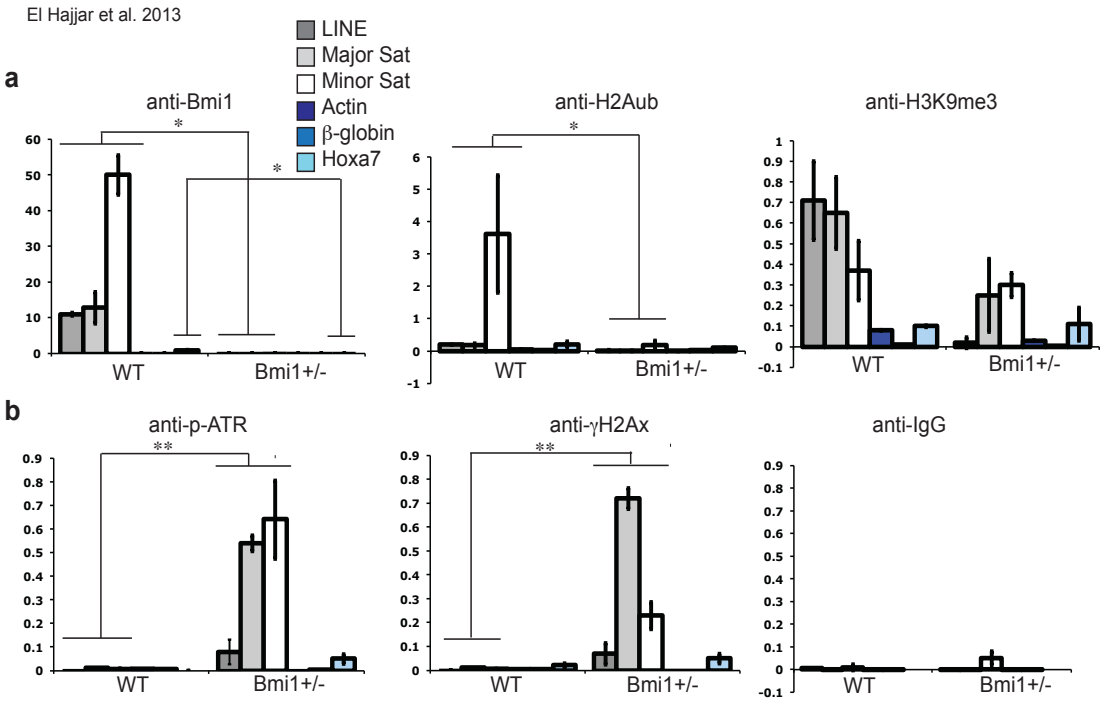

c

	Fold of WT					
	LINE	*Major Sat*	*Minor Sat*	*Actin*	*β-globin*	*Hoxa7*
p-ATR	18.6	40.9	101.8	1.1	1.0	2.3
γ-H2Ax	14.8	53.0	40.2	0.2	0.7	2.4

Figure 5

Figure 5

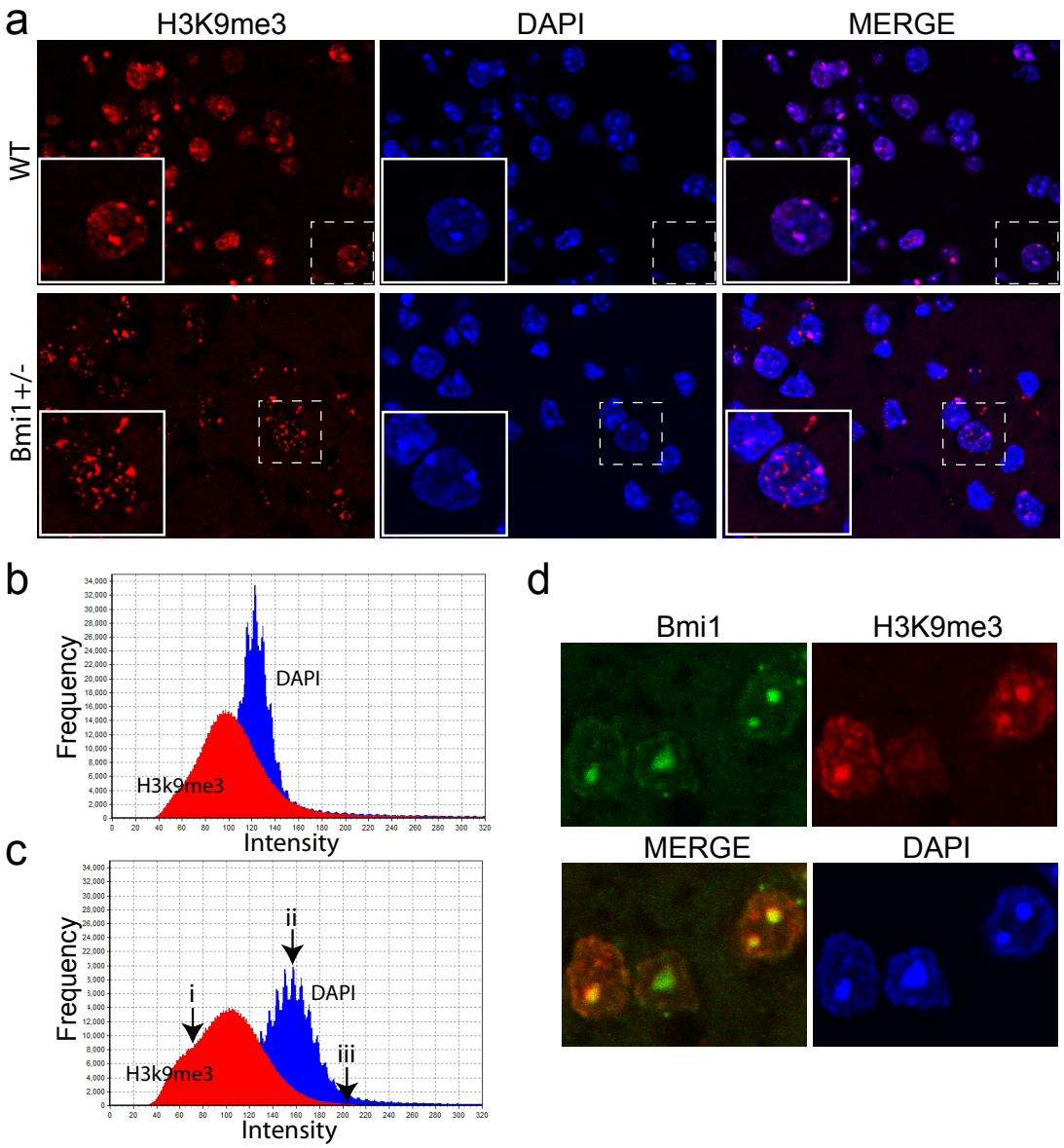
a
H3K9me3
DAPI
MERGE
WT
Bmi1+/-
b
Frequency
DAPI
H3k9me3
Intensity
c
Frequency
i
ii
iii
DAPI
H3k9me3
Intensity
d
Bmi1
H3K9me3
MERGE
DAPI

Figure 6

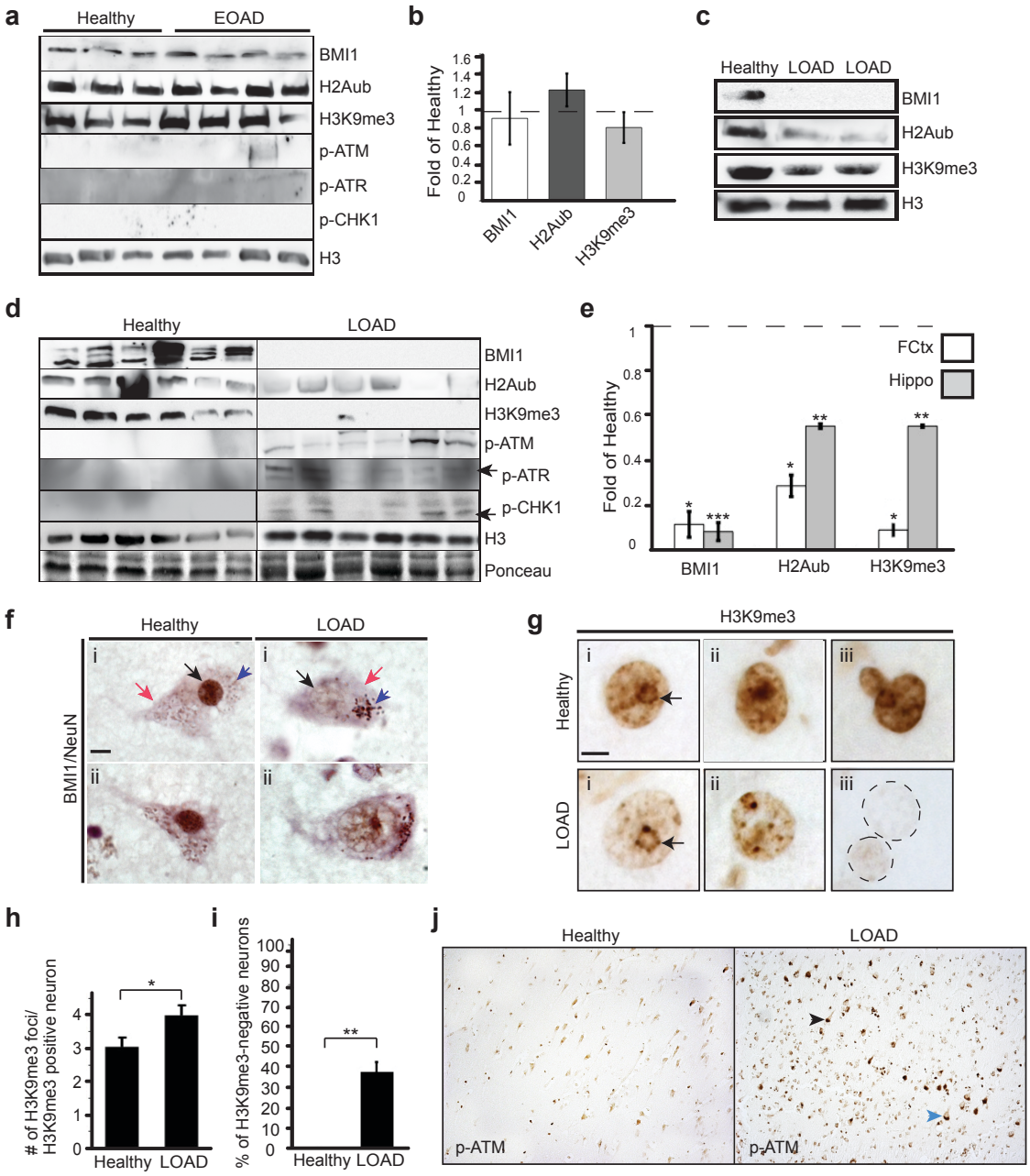
a
Healthy
EOAD
BMI1
H2Aub
H3K9me3
p-ATM
p-ATR
p-CHK1
H3
b
Fold of Healthy
BMI1
H2Aub
H3K9me3
c
Healthy LOAD LOAD
BMI1
H2Aub
H3K9me3
H3
d
Healthy
LOAD
BMI1
H2Aub
H3K9me3
p-ATM
p-ATR
p-CHK1
H3
Ponceau
e
FCtx
Hippo
Fold of Healthy
BMI1
H2Aub
H3K9me3
f
Healthy
LOAD
BMI1/NeuN
g
H3K9me3
Healthy
LOAD
h
# of H3K9me3 foci/ H3K9me3 positive neuron
Healthy LOAD
i
% of H3K9me3-negative neurons
Healthy LOAD
j
Healthy
LOAD
p-ATM
p-ATM

Figure 7

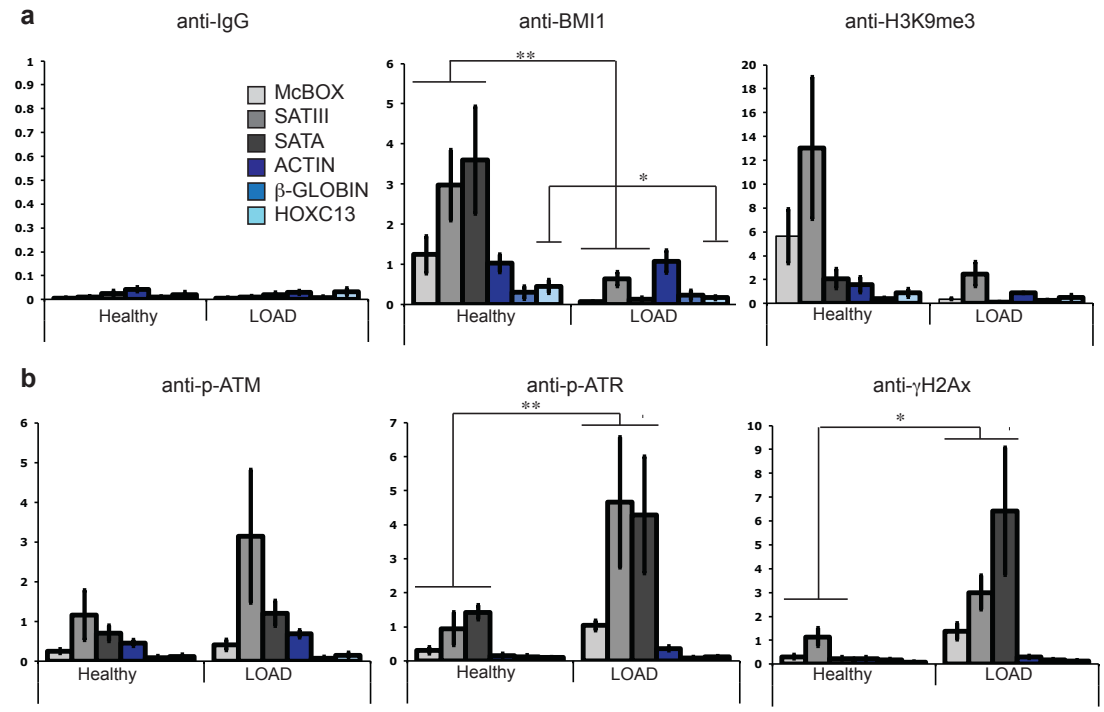

c

Fold of Healthy

	McBOX	SATIII	SATA	ACTIN	β-GLOBIN	HOXC13
p-ATM	1.6	2.7	1.7	1.5	0.9	1.2
p-ATR	**3.3**	**4.9**	**2.9**	2.2	0.7	1.2
γ-H2Ax	**4.4**	**2.6**	**27.0**	1.2	1	1

Figure 8

Figure 8

SUPPLEMENTARY FIGURE LEGENDS:

Supplementary Figure 1. Heterochromatin anomalies in *Bmi1*$^{+/-}$ mice are present before the apparition of neuropathological marks

(A)Western blot on cortical extracts from 3-month old WT (n=3) and *Bmi1*$^{+/-}$ (n=3) mice, and one old *Bmi1*$^{+/-}$ mouse (positive control). We used PHF1 for p-TAU and FCA3542 for amyloid. (B) IHC for H3K9^{me3} on cortical sections of 3-month old WT (n=3) and *Bmi1*$^{+/-}$ (n=3) mice, Scale bar: 20µm, Scale bar in the inset: 8 µm. (C) Quantification of the total number of H3K9^{me3} foci per nucleus, as measured using IHC data obtained in (B) in neuronal layers 2 and 3 of the frontal cortex. All values are mean ±SEM. (*) P<0.05; Student's t-test.

Supplementary Figure 2. *Bmi1* is required for heterochromatin formation and genomic stability in embryonic cortical neurons.

ChIP analysis on 18.5 embryonic day WT (n=3) and *Bmi1*$^{+/-}$ (n=3) cortical neurons to evaluate the levels of H2A^{ub} and H3K9^{me3} at the HoxA7, IAP1 (Interstitial A particles), and satellite repeats (Minor and Major Sat) loci. Quantitative PCR was performed in triplicate for each DNA sequence. All data are present as fold of input. Two-way ANOVA analysis exposed a highly significant decrease of *Bmi1* (P<0.001), H2A^{ub} (P<0.0001), and H3K9^{me3} (p<0.0001) accumulation at heterochromatin domains in *Bmi1*$^{+/-}$ neurons. (B) and (C) Immunoblot were performed on embryonic moue cortical neurons cultured for 7days in vitro. (B) DMSO or ATM/ATRi were added to the cultures 16 hours prior to protein extraction. ATM/ATRi prevent p-ATM, p-CHK1 and p-TAU accumulation in *Bmi1*$^{-/-}$ neurons. (C) ATM/ATRi, but not ATMi, also largely prevented p53 accumulation in *Bmi1*$^{-/-}$ neurons. Numbers 1 and 2 in (C) represent two *Bmi1*$^{-/-}$ independent neuronal samples.

Supplementary Table 1. Human brain samples used in the study

The Douglas hospital (DH) provided all western blot samples. The identification number (Id) of each sample is included but donor names are not known. The Hopital

Maisonneuve Rosemont (HMR) provided the IHC samples. The Id of each sample is included but donors are also anonymous.

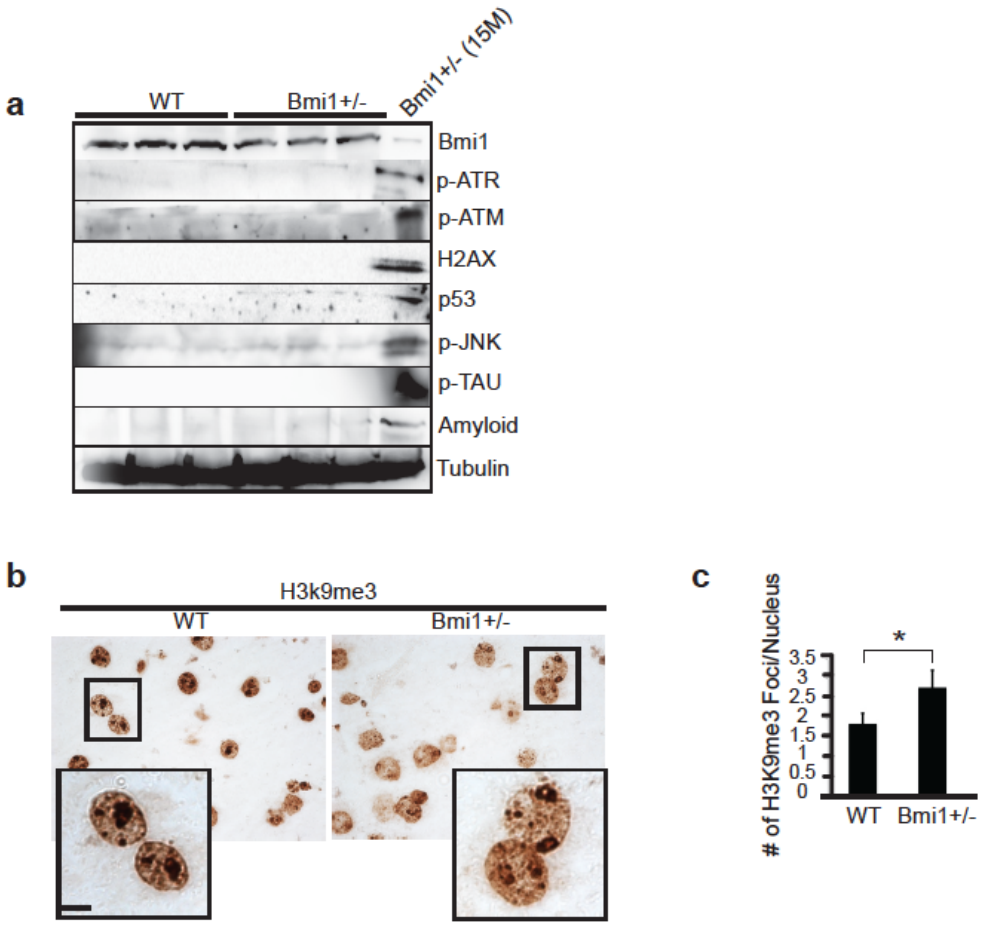

Supplementary Figure 1

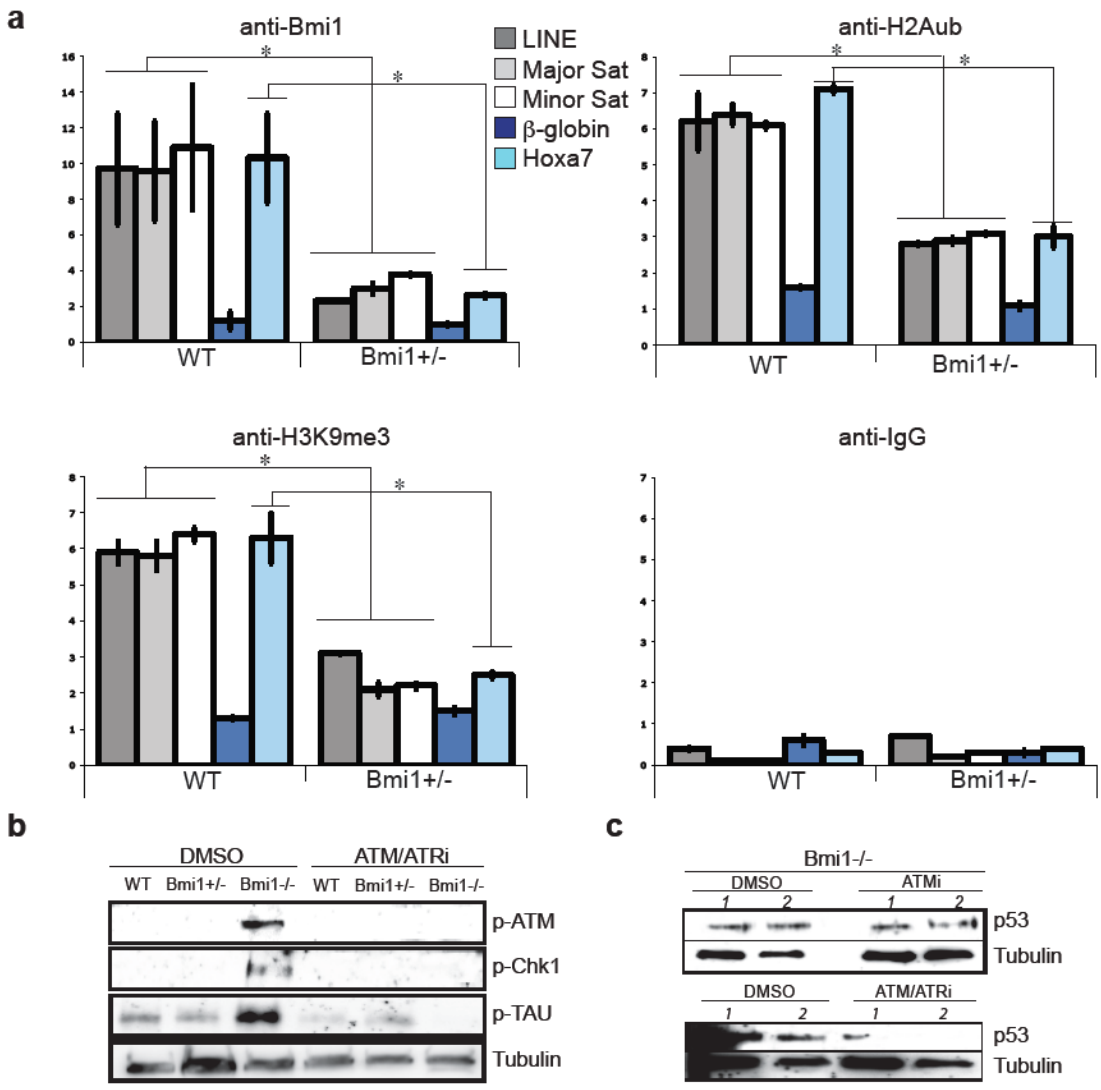

Supplementary Figure 2

Western Blot samples

Hippocampus	DH-Id # of samples	Sex	Age (yrs)	Median Age (yrs)
Young Healthy	1388	M	57	59
	1705	M	61	
	1722	M	59	
EOAD	1214	M	64	61.3
	410	M	63	
	1201	M	63	
	1147	F	55	
Old Healthy	626	F	87	86.7
	1582	M	85	
	1585	M	88	
LOAD	1427	F	82	82.2
	1129	M	88	
	1065	M	76	
	588	M	82	
	450	F	83	

Frontal Cortex	DH-Id # of samples	Sex	Age (yrs)	Median Age (yrs)
Old Healthy	428	M	89	87.3
	488	F	86	
	616	F	86	
	727	M	87	
	881	M	85	
	1487	F	91	
LOAD	999	F	87	87.2
	1018	M	88	
	1073	M	85	
	1127	M	88	
	1157	F	85	
	1599	F	90	

IHC samples

Frontal Cortex	HMR-Id # of samples	Sex	Age (yrs)	Median Age (yrs)
Old Healthy	12c00024	M	90	81.3
	10c00052	M	72	
	10c00020	M	82	
LOAD	10c00088	M	75	81.6
	10c00042	M	89	
	10c00030	M	81	

Supplementary Table 1

CHAPTER 4:

In chapter 4, I discuss my results and correlate them with similar findings in the literature. In order to examine thoroughly the impact of the findings, I divided the chapter into three sections. In section 1, I explore the role of Bmi1 in the progression of Alzheimer's disease. In section 2, I comment on the novel and important function of Bmi1 in the formation of constitutive heterochromatin. In the third section, I relate the three parameters i.e. Bmi1, AD, and constitutive heterochromatin together and suggest a new concept involving abnormal constitutive heterochromatin organization with development of neurodegeneration. And finally, I discuss about future perspectives.

CHAPTER 4

DISCUSSION: SECTION 1

Bmi1 and Alzheimer's disease

4.1. Bmi1 haploinsufficiency instigates neurodegeneration

Aged *Bmi1*$^{+/-}$ mice display reduced median and maximal lifespan as well as enhanced onset of numerous ageing features at 15 month-old. These features include apparition of lens cataracts, alopecia, reduced body size, abnormal paw-clasping reflex, increased senescence-associated β-galactosidase activity, and significant upregulation of *p16* expression. *Bmi1* is highly expressed in neurons and has been previously described as an "anti-progeroid" gene since mice lacking *Bmi1* manifest an ageing phenotype similar to that of old *Bmi1*$^{+/-}$ mice, which appears however at very early stages when mice are approximately one-month old [1]. These findings indicate that *Bmi1* activity is dosage sensitive, which may affect its molecular interactions and the stoichiometry of the protein complexes it constitutes. The observations that stem cell characteristics and cancer incidence in *Bmi1*$^{+/-}$ mice are similar but not as significant as those observed in *Bmi1*$^{-/-}$ mice also support the notion of *Bmi1*'s dosage sensitive function [2]. We previously demonstrated that *Bmi1* expression decreases in the brain with advancing age [3]. One explanation for the enhanced ageing phenotype observed in *Bmi1*$^{+/-}$ mice is that the remaining *Bmi1* allele of these mice displays decreased expression in the brain with ageing, which makes them eventually behave as *Bmi1*$^{-/-}$ mice but at later stages. This concept is similar to loss of heterozygosity of tumor suppressor genes in carcinogenesis where any hit affecting the remaining allele leads to its inactivation and favours cancer development. Therefore, *Bmi1* could act as an ageing suppressor gene; however, loss of expression of the residual allele will promote ageing development.

As mentioned in Chapter I, *Bmi1* is the main repressor of the Ink4a/Arf locus that mediates the senescence pathway via *p16* protein. Importantly, Ink4a/Arf locus upregulation is not only observed in senescing cultured cell lines, but is also detected in tissues of ageing animals and its expression correlated with enhanced SA-β-galactosidase activity [4]. We observed increased sensitivity for SA-β-galactosidase assay as well significant upregulation of *p16* expression in cortical neurons of 15-month old *Bmi1*$^{+/-}$ mice when compared to those of 24-month old WT mice. This senescent phenotype could be caused by direct de-repression of the Ink4a/Arf locus in the neurons of *Bmi1*$^{+/-}$ mice.

Ageing is the main risk factor for progression of late-onset Alzheimer's disease so we investigated if *Bmi1*$^{+/-}$ mice show any symptoms resembling AD. Spatial learning and memory formation are perturbed in mouse models of Alzheimer's disease and interestingly *Bmi1*$^{+/-}$ mice were also impaired in this context exemplified by their poor performance in Morris water maze test and Barnes maze assay as well as by the significant reduction in LTP. These results imply a defective synaptic function and correlates with the observed severe decrease in the expression of synaptophysin in the cortices of these mice. Synaptophysin is a presynaptic vesicle that highly contributes to LTP formation and loss of its expression correlates with the cognitive decline in AD [5]. Accordingly, Cao et al. recently reported synaptophysin downregulation in one-month old *Bmi1*$^{-/-}$ mice cortices [6]. The severe synaptophysin reduction in *Bmi1*$^{+/-}$ mice could be explained by the degeneration of synapses due to expression of toxic proteins such as amyloid peptides in the neurons [7]. Another possibility is due to oxidative stress accumulation. Old *Bmi1*$^{+/-}$ mice present elevated oxidative stress levels and evidence revealed that ROS can mediate synaptic degeneration (Our unpublished data)[6, 8]. Finally, microarray analysis exposed that *Bmi1* regulates proteins involved in axonal guidance and neurite growth; hence loss of *Bmi1* may initiate malformation of synapses [9].

Our results reveal that *Bmi1*$^{+/-}$ mice present increased p53 activation, tau phosphorylation, and Aß expression. p53 protein is significantly elevated in brains of AD patients compared to healthy elderly controls [10]. Evidence of the pivotal role of p53 in neurodegeneration is provided by data from both *in vitro* and *in vivo* studies. Increased p53 immunoreactivity associated with neuronal death was observed in several models of brain injuries. Conversely, p53 inhibition prevents death in cultured neurons exposed to DNA-damaging agents and amyloid peptides [11]. DNA damage, oxidative stress and Arf are potent activators of p53 protein. Using cultured *Bmi1*-deficient neurons, we demonstrated that p53 activation in our model was neither due to increased oxidative stress nor de-repression of Ink4A/Arf locus, but due to activation of DDR kinases ATM and ATR (Annexe I, Figure 1), suggesting that DNA damage accumulation in *Bmi1* mutant neurons promotes p53 activation.

Surprisingly, Tau phosphorylation was also abrogated after treatment of *Bmi1*$^{-/-}$ neurons with inhibitors of ATM and ATR. Tau phosphorylation in our model could be caused by p53 upregulation. One study reported that p53 could induce Tau phosphorylation *in vitro* [10]. Other mechanistic possibility includes DDR kinases. Mendoza et al. demonstrated that the DNA-damage checkpoint kinases Chk1 and Chk2, which operate downstream of ATR and ATM respectively, phosphorylate tau protein at an AD-related site and enhance tau toxicity [12]. Moreover, tau can also be phosphorylated by the stress-activated JNK kinase, which is also upregulated in *Bmi1*$^{+/-}$ mice [13]. Thus, there are several possible ways in which *Bmi1* may be regulating Tau phosphorylation downstream of DNA damage and it will be interesting to dissect to the contribution of each.

Remarkably, the JNK pathway is also involved in oxidative stress-induced upregulation of ß-site APP cleaving enzyme 1 (BACE1), which expression is elevated in LOAD brains [14,15]. The lipid peroxidation metabolite 4-Hydroxynonenal induces BACE1 expression, linking JNK and ROS to Aβ metabolism [16]. We observed increased accumulation of amyloid-ß peptides, which correlated with BACE1 upregulation, in the cortices of *Bmi1*$^{+/-}$ mice. *Bmi1* mutation triggers ROS generation as well as elevated lipid peroxidation levels due to p53-mediated repression of antioxidant genes in the brain [1]. We detected that upon deletion of p53 in *Bmi1*$^{-/-}$ mice, amyloid accumulation is mitigated in the brain (Our unpublished data). Therefore, BACE1 upregulation and amyloid deposition in our model could involve directly p53 pro-oxidant activity in neurons. On the other hand, since *Bmi1* operates as a transcriptional silencer, it could also repress directly the expression of BACE1. The multifaceted ways in which *Bmi1* affects amyloid accumulation, like other AD hallmarks, has yet to be scrutinized but the convergence of p53, ROS and JNK to BACE1 suggests that this enzyme may be an important mediator.

Of note, some pathological marks such as p-TAU (S396) and SA b-galactosidase activity, although less abundant, were also detected in the brains of old WT mice. This finding correlates with a report showing that brains of some aged normal individuals display neurodegenerative hallmarks such as S396-tau neurofibrillary tangles [17].

Nonetheless, p-TAU (S202), p-JNK and amyloid expression were not yet observed in 24-month old WT mice but were present in 15-month *Bmi1*$^{+/-}$ mice, indicating that these features are associated with pathological AD-like ageing and not with physiological ageing. Better characterization of hallmarks of AD vs normal ageing is important not only for proper identification of Alzheimer's patients, but also in order to develop proper strategies for targeting the causative dysfunctional pathways.

A critical question that remains unresolved in all currently available animal models of AD, is how well do they model the disease where there are no mutations in either APP or tau. Therefore, development of animal models mimicking the neuropathology of AD that are not based upon overexpression of mutant human proteins, as this does not reflect LOAD, is significantly needed. In our study, we describe a novel mouse model for LOAD pathology and we show that mice heterozygous for *Bmi1* manifest, with advancing age, AD-like phenotypic features. Surprisingly, we also found that 6 month-old mice, which are both transgenic for APP and heterozygous for *Bmi1*, acquire a higher level of tau phosphorylation and amyloid burden indicating a synergistic interaction between APP and *Bmi1* in contributing to AD pathology (Annexe I, Figure 2). In conclusion, *Bmi1*$^{+/-}$ mouse model can greatly serve in AD research providing new insight in understanding the neuropathology that is different from the classical amyloid hypothesis and hence promoting novel ways of targeting therapies.

CHAPTER 4

DISCUSSION: SECTION 2

Bmi1 and constitutive heterochromatin

4.2. BMI1 is enriched at constitutive heterochromatin and its function is redundant with BRCA-1 mediated heterochromatinization

PRC1 complex is enriched at facultative heterochromatin and is recruited by the PRC2-mediated H3K27^{me3} repressive mark [18]. Our *in vitro* studies demonstrate that the PRC1 member BMI1 is also enriched at constitutive pericentric and intergenic heterochromatin where it colocalizes with the repressive H3K9^{me3} mark and its accumulation was independent of PRC2-mediated H3K27^{me3}, indicating a novel way for BMI1 to target chromatin that is different from the classical polycomb recruitment process. Consistently, our cell -fractionation assay revealed that a large portion of the BMI1 protein pool is bound to the SDS chromatin fraction, which is predicted to correspond to constitutive heterochromatin. Moreover, our ChIP analyses on cortices of WT mice as well as on brains of healthy individuals confirmed the enrichment of *Bmi1* at constitutive heterochromatin domains *in vivo*. Furthermore, our findings indicate that *Bmi1*-mediated repression through H2A ubiquitylation is required for maintenance of constitutive heterochromatic regions. Though little evidence in the literature hints at localization of PcG proteins such as *Bmi1* at constitutive heterochromatin, a few studies support our findings. Bernstein et al. showed that not all PcG chromodomain proteins bind preferentially to H3K27^{me3}; instead some display greater affinity to H3K9^{me3} [19]. Inactivation of PcG proteins *Ring1b* and *eed* in mouse embryonic cells resulted in reactivation of major satellite repeats [20]. Saurin et al. reported that BMI1 is localized at pericentromeric chromatin in human cells and suggested that the preferential 1qh association of BMI1 is mediated by specific protein interaction with a repeated sequence motif occurring in chromosome 1-specific α-satellite DNA [21]. Van Lohuizen group found that the DNA methylase DNMT1 is required for BMI1 recruitment to pericentric regions, since its downregulation led to diffuse distribution of the BMI1 fluorescence throughout the nucleus [22]. This finding corroborates a study analyzing genome-wide *Bmi1*-mediated H2A^{ub} localization and showing that enrichment of H2A^{ub} is not limited to regions containing the PRC2-H3K27^{me3} mark but is linked instead to DNA methylation patterns [23].

The question raised is how *Bmi1*-mediated $H2A^{ub}$ deposition at constitutive heterochromatin translates into $H3K9^{me3}$ deposition and heterochromatin spreading. Studies defined the mechanism by which $H2B^{ub}$, a mark associated with active transcription, regulates other histone modifications including trimethylation of K4 and K79 of histone H3 by the histone methyltransferases COMPASS and Dot1, respectively [24]. This *trans*-histone crosstalk is unidirectional meaning that defects in the histone methylation of H3 have no reciprocal effect on the upstream ubiquitylation event [24]. One study revealed *trans*-histone crosstalk between $H2A^{ub}$ and H3 methylation. The authors found that H2A ubiquitylation inhibited H3K4 trimethylation through MLL3 methylase and suggested that $H2A^{ub}$ might change the substrate specificity of MLL3 [25]. According to the crystal structure of the nucleosome, the C terminus of H2A and the N terminus of H3 are close together and form the entrance for the DNA [26]. Hence, one mechanistic insight is that $H2A^{ub}$ induces allosteric changes and enhances the affinity of the histone 3 substrate to H3K9 methylases such as Su(VAR) proteins. Another mechanism may involve p53 activity. A recent report by Mungamuri et al. revealed that p53 downregulates the H3K9 methylase SUV39H1 leading to heterochromatin reorganization [28]. On the other hand, Zhen et al. found that p53 directly induces the expression of the H3K9 demethylase JMJD2b through promoter binding [29]. Our preliminary data demonstrate that $Bmi1^{-/-};p53^{-/-}$ neurons show a rescue of the disrupted heterochromatin phenotype (Unpublished data). Further delineation of this pathway is imminent. Other mechanistic possibility involves the RNAi pathway. As discussed earlier, the RNAi process is required for nucleation and spreading of constitutive heterochromatin by SUV39H1-HP1 pathway. Evidence also includes RNA interference pathway for polycomb targeting to chromatin [30]. Findings from Bishof group show that lncRNAs are required for BMI1/RING1B mediated gene silencing (Unpublished data). Therefore, the RNA interference pathway may bridge *Bmi1*-mediated $H2A^{ub}$ with SUV39H1-HP1 system to methylate H3K9, thus providing more binding site for HP1 to spread heterochromatin formation.

On the other hand, *Bmi1*-mediated $H2A^{ub}$ deposition can also promote heterochromatin compaction independent of $H3K9^{me3}$. Crystallography analysis of the nucleosome core revealed that the C-terminal tail of $H2A^{ub}$ could reach the linker histone

H1, which is associated with high-ordered structure of chromatin and nucleosomal compaction. Moreover, immunoprecipitation of nucleosomes containing WT or its ubiquitination mutant, K119R, revealed that H1 preferentially associated with WT H2A, suggesting that ubiquitination of H2A facilitates interaction with H1 promoting heterochromatin condensation [24]. One last possibility involves the positive charge domain of interacting polycomb proteins such as the chromodomain protein M33 [31]. RYBP is an $H2A^{ub}$-binding protein that interacts with RING1A/B and M33/CBX2, functioning as a potential link between $H2A^{ub}$ and condensation of nucleosomes. Therefore, from all these observations, we can suggest four mechanisms to delineate the role of *Bmi1* in constitutive heterochromatin formation in our model: 1) *Bmi1/Ring1b* recruitment at constitutive heterochromatin is DNMT1-dependent promoting H2A ubiquitylation favouring increased affinity of H3K9 substrate to HMTases. 2) *Bmi1* represses the protein p53, which mediates heterochromatin reorganization and demethylation of H3K9 either via downregulation of HMTase or upregulation of histone demethylase. 3) *Bmi1/Ring1b* is targeted to constitutive heterochromatin via the RNAi pathway, which will also target H3K9 methyltransferases leading to constitutive heterochromatin initiation and spreading. And 4) *Bmi1/Ring1b*-mediated nucleosomal condensation at constitutive heterochromatin could be directly involving the conserved positive domains of interacting polycomb proteins and/or facilitating the binding of linker histone H1.

Similarly to BMI1, BRCA1 protein also catalyzes H2A ubiquitylation and was reported to mediate heterochromatinization in mouse neurons. Comparably to *Bmi1* heterozygous mice, absence of *Brca1* full-length isoform causes p53-mediated accelerated ageing in adult mice, including decreased lifespan, reduced body fat deposition, osteoporosis, and skin atrophy [32]. All these findings propose that *Bmi1* and *Brca1* promote similar effects. We report that co-inactivation of BMI1 and BRCA1 in human cells triggers a more rigorous depletion of $H2A^{ub}$, $H3K9^{me3}$ and HP1 at constitutive heterochromatin than single BMI1 or BRCA1 deficiencies, and that BMI1 overexpression could rescue the BRCA1-deficient heterochromatin phenotype. These observations suggest that BMI1 and BRCA1 are functionally redundant for $H2A^{ub}$ deposition at constitutive heterochromatin. The observation that BMI1 and BRCA1 proteins accumulation is mutually independent

and that BMI1 levels are increased in BRCA1-deficient cells (and reciprocally), also suggest that both proteins possibly bind to the same substrate to catalyze $H2A^{ub}$ deposition.

In conclusion, we provided substantial data demonstrating that BMI1 is associated with constitutive heterochromatin and that it is essential for heterochromatin maintenance in mouse and human cells. BMI1 also displayed functional redundancy with BRCA1 in heterochromatinization and was sufficient to rescue the BRCA1-deficient heterochromatin phenotype.

CHAPTER 4

DISCUSSION: SECTION 3

BMI1, constitutive heterochromatin, and Alzheimer's disease

4.3. Significant reduction in *Bmi1* expression, perturbed constitutive heterochromatin, and increased genomic instability at repetitive sequences in *Bmi1*$^{+/-}$ and LOAD, but not EOAD, brains

In light of recent studies, epigenetic modification has emerged as one of the possible pathogenic mechanisms of AD [33,34]. DNA methylation is associated with H3K9^{me3}, is tightly linked to heterochromatinization, is catalyzed by DNA methyltransferases (Dnmts), and recruits proteins known as methyl–binding domain proteins (MBDs) that are associated with chromatin compaction [35]. Immunohistochemical studies in the entorhinal cortex of AD patients revealed genome-wide reduction in the DNA methylation marker 5-methylcytosine (5-mC) and decreased expression of variety of proteins involved in the process of DNA methylation, such as Dnmt1 and methyl-CpG–binding protein 2 (MeCP2). The group analyzed monozygotic twins and demonstrated substantial DNA hypomethylation in the neocortex of an LOAD twin compared to his non-AD identical twin pair, strengthening the role of gene-environment interactions and epigenetics in AD progression [36]. Consistent with these findings, a recent study by Chouliaras et al. also showed a global robust decrease in 5-mC levels in the hippocampus of AD brains, which is the region of the brain associated with memory [37]. An emerging literature has established that the expression of certain transposable elements, such as some LINE, SINE and LTR transposons, is elevated in the brain of individuals affected with several neurodegenerative disorders including the rett syndrome, amyotrophic lateral sclerosis (ALS), aged-related macular degeneration, and sporadic Creutzfeldt-Jakob disease [38]. As mentioned earlier, transposable elements are highly abundant mobile genetic elements that can insert into new genomic locations, presenting a massive endogenous reservoir of genomic instability and cellular toxicity. The effects of these parasitic genetic elements are normally stifled by potent cellular mechanisms involving small interfering RNAs that act via the RNA induced silencing complex (RISC). Indeed, mutations in *Drosophila Argonaute 2* (*Ago2*) resulted in exacerbated transposon expression in the brain, progressive and age-dependent memory impairment, and reduced lifespan [39]. Moreover, DICER-1 loss promotes Alu RNA

toxicity in age related macular degeneration [40]. Overall, these findings indicate that transposon de-repression may contribute to age-dependent loss of neuronal function.

Bmi1$^{+/-}$ mice cortices and LOAD hippocampi and frontal cortices present significant *Bmi1* and H2A^{ub} downregulation as well as perturbed constitutive heterochromatin de-compaction characterized by severe reduction or nearly absence of H3K9^{me3} in neurons. One mechanism to explain this phenomenon is the fact that folate metabolism is required for the production of S-adenosyl-methyonine (SAM), the universal donor for DNA and histone methylation reactions. Interestingly, perturbations of the folate metabolism and SAM levels are common features in LOAD [41]. In *Caenorhabditis elegans* embryos, inhibition of SAM-synthetase results in preferential reduction of H3K9^{me3}, heterochromatin de-repression and release from the nuclear periphery [42]. PcG proteins have been reported to play a role in SAM production, as the PRC1 protein CBX4 was shown to sumoylate cystathionine β-synthase (CBS), an enzyme involved in the conversion of homocysteine to cysteine. Sumoylation of CBS inhibited its enzymatic activity resulting in altered homocysteine to cysteine conversion, which is an important step in the synthesis of SAM [43]. In mammals, SAM is generated by the methionine adenosyltransferase isozyme MATIIa, which interacts in the nucleus with multiple chromatin remodeling complexes, including NURD and Polycomb Repressive Complex1 (RING1A/RING1B) [44]. Remarkably, the MATIIa-deficient heterochromatin phenotype cannot be rescued by SAM supplementation, indicating that interaction between MATIIa, chromatin and histone methyltransferases is required for H3K9 trimethylation and H3K9^{me3} loading [45]. Therefore it would be interesting to analyze if folate or SAM supplementation would mitigate the loss-of-*Bmi1* phenotype or if *Bmi1* is physically required, like MATIIa, in order to rescue the phenotype. This is pertinent in terms of evaluation if folate can be used as a treatment for LOAD or if it is useless in LOAD characterized by BMI1 deficiency.

Since the main role of constitutive heterochromatin is to repress transcription, the observed heterochromatin decondensation in *Bmi1*$^{+/-}$ and LOAD brains may affect gene expression patterns and hence affect the integrity of the transcriptome. Heterochromatin maintenance is essential for silencing ribosomal RNA transcription; hence it would be intriguing to link the heterochromatin status, ribosomal RNA synthesis, and Alzheimer's

disease by taking into account the energy metabolism. That is, ribosomal RNA transcription is a rate-limiting step in protein synthesis and hence increased RNA transcription would promote growth and accelerate ageing.

Abundant reports suggested that constitutive heterochromatin is refractory to DNA damage; however, this notion was revisited by Chiolo *et al*. who demonstrated that γH2A and p-ATR foci are formed in heterochromatin upon DSBs [46]. Two reports revealed that disrupted heterochromatin induces the rate of spontaneous DSBs, leads to the expansion of DNA repeat arrays, and is correlated with genomic instability as well as reduced viability. In their model, *Drosophila* flies lacking the Su(var)3-9 H3K9 methyltransferase present reduced lifespan, muscle degeneration, and significantly elevated frequencies of spontaneous DNA damage in heterochromatin that occur in both somatic and germ-line cells. DNA repair proteins and mitotic checkpoints were also activated in mutant flies. Similar phenotype was also observed in flies that are deficient of RNA interference pathway component Dcr2, indicating that H3K9 methylation and RNAi processes are essential for heterochromatin stability [47]. Concomitantly, deletion of SUV39h1/h2 methyltransferases in mice also leads to reduced viability, loss of $H3K9^{me3}$ and genomic instability [48]. Knockdown of the chromatin remodeling complex NoRC, which is known to silence heterochromatic structures at centromeres and telomeres, leads to relaxation of heterochromatin and enhanced chromosomal instability [49]. Haider et al. recently reported that satellite repeat elements were significantly hypomethylated and upregulated in end-stage cardiomyopathic hearts relative to healthy normal controls. They suggest that satellite overexpression correlates with the widespread DNA damage observed in post-mitotic cardiomyocytes, highlighting that SAT expression may be a potential link between genomic damage and heart failure disease progression [50]. Consistent with all these findings, we show that $Bmi1^{+/-}$ mice cortices and LOAD brains show enrichment of DDR machinery, i.e. p-ATR and γH2AX, preferentially at constitutive heterochromatin domains. The relatively weak accumulation of p-ATM in LOAD brains as detected by ChIP, which is contradictory to immunoblot and immunohistochemistry results, suggests that a portion of the p-ATM pool is not chromatin-bound. This is consistent with p-ATM accumulation in both cytosolic and

nuclear neuronal compartments in *Bmi1*$^{+/-}$ cortices and LOAD brains (Annexe I Figure 3 and Figure 6E) [51].

The question is how the loss of heterochromatin compaction in LOAD and *Bmi1*$^{+/-}$ mice triggers DNA damage accumulation. 1) First possibility is that repetitive DNA sequences are intrinsically unstable upon loss of heterochromatin compaction and thus prone to *de novo* DNA damage formation. *De novo* mutations arise spontaneously and have recently been identified as contributors to neurodevelopmental disorders such as autism spectrum disorders, schizophrenia and mental retardation [52]. 2) Another explanation could involve the repetitive sequences of constitutive heterochromatin, where loss of chromatin condensation can lead to abnormal recombination of such sequences and thus genome rearrangement. 3) It is also probable that the efficacy of DNA repair is reduced upon BMI1 deficiency or that recognition of H3K9^{me3} mark and HP1 is important to activate the process of DNA repair in constitutive heterochromatin [53]. Indeed, several studies correlate HP1 with efficient DNA repair activity at heterochromatin sites [54]. 4) Another mechanism could involve the RNA interference pathway. Francia *et al*. identified that small RNA produced by DICER and DROSHA, two RNases type III enzymes that process non-coding RNA, are required to activate DDR and efficiently repair DNA at the damaged sites of heterochromatin. The DICER- and DROSHA-dependent small RNA products have the sequence of the damaged locus, and can restore DDR in RNase-treated cells [55]. These findings are highly important since they directly link RNAi-mediated heterochromatin formation with DNA repair. 5) Finally, it could be that the repair of damaged lesions at heterochromatin is not efficient. In fact, several studies reported that DNA repair at constitutive heterochromatin is problematic being less effective and occurring with slower kinetics [56]. A delay in repair of heterochromatic DSBs was observed in human cells. Moreover, DSBs occurring in heterochromatin are repaired by HR pathway, which leads to abnormal genome rearrangements in the presence of the closely clustered repeats contributing to human diseases such as cancer and infertility [56]. In all four cases, which are mutually non-exclusive, persistent and prolonged exposure to cumulative neuronal DNA damage causes neurons to senesce, re-enter the cell cycle and/or atrophy, and ultimately degenerate.

An everlasting debate was the question is which one comes first? Do the DNA damage and the DDR lead to chromatin defects and thus neurodegeneration? Or it is that loss of chromatin structure makes the cell more susceptible to DNA damage, increases genome instability, and therefore promotes neuropathology? A study by Pegoraro *et al*. endorses that chromatin anomalies occur prior to DNA damage. They reported that knocking down of the chromatin remodeling complex NURD, involved in establishment of heterochromatin, leads to aberrant chromatin structure indicated by loss of $H3K9^{me3}$ foci about 50h earlier than DNA damage characterized by γH2AX foci presence [57]. Our findings also support that heterochromatin defects largely precede DNA damage accumulation and the ensuing neuropathology. Embryonic *Bmi1*$^{+/-}$ neurons and 3-month old *Bmi1*$^{+/-}$ mice display reduced levels of $H2A^{ub}$ and $H3K9^{me3}$ as well as diffused distribution of HP1 protein, which largely preceded ATM/Chk2 and ATR/Chk1 activation as well as expression of neuropathological proteins. Using *Bmi1*-deficient neurons, we show that a causal relationship could be established between activation of ATM/ATR and accumulation of the pathological proteins p53 and p-TAU, strengthening further the notion that persistent DDR in post-mitotic neurons is sufficient to favour neurodegeneration. Overall, these observations suggest that epigenetic and chromatin structure changes are in the upstream of DNA damage events.

Our data revealed critical differences between familial and spontaneous AD. Heterochromatin anomalies were not present in EOAD samples, thus excluding neurodegeneration as the primary cause. We also found a molecular dichotomy between EOAD and LOAD at the level of BMI1 expression and DDR activation. This suggests that EOAD and LOAD represent two pathologies that are triggered by distinct mechanisms that ultimately result in the same neuropathology i.e. amyloid deposition and tau phosphorylation. It has been proposed that the amyloid hypothesis may only hold for familial forms of the disease but that the situation is much more complex in late-onset forms. Clinical findings from a growing number of Aβ-reducing drug trials in LOAD show that this strategy is not potent. Therefore, these observations may have important consequences in developing alternative therapies for LOAD such as upregulating BMI1 in neurons by gene therapy [58].

Bmi1 protein levels in the cortices of 15-month old *Bmi1*$^{+/-}$ mice and LOAD brains, as measured by Western blot and ChIP analyses, were severely reduced or even nonexistent in some LOAD cases. One possibility is that the Bmi1 protein, alone or in complex with Ring1b, binds to its own product (i.e. $H2A^{ub}$) or to $H3K9^{me3}$, thus creating a self-enforcing loop to amplify $H2A^{ub}$ deposition and heterochromatin formation [43]. Sub-optimal self-enforcing mechanism and the ensuing loss of chromatin association would result in Bmi1 protein destabilization and degradation. Another possibility involves miRNA-218, which was shown to promote apoptosis by downregulating BMI1 in colon cancer. Interestingly, miRNA-218 gene is localized at intergenic heterochromatin and is enriched in aged mouse cortex and hippocampus [59]. It would be interesting to analyze if miRNA-218 also targets BMI1 in the brain and regulates its decreased expression with age and AD. This suggestion could be illustrated by a regulating cycle where BMI1 represses the expression of this miRNA through its heterochromatin mediated compaction; however decreased dosage of BMI1 would favour de-repression of the miRNA-218 gene and hence lead to further BMI1 downregulation. So far, only one reported polymorphism (C18Y) in the RING domain of BMI1 gene was associated with a significant decrease in BMI1 levels in humans, inducing elevated ubiquitination and proteasomal degradation [60]. It would be interesting to evaluate if LOAD patients present this polymorphism.

In conclusion, our study is greatly pertinent in Alzheimer's disease research and in delineating the function of *Bmi1* in genomic stability (Figure 1). We provided three main novel tools and concepts.

1- Aged *Bmi1* heterozygous mice could be an interesting model for LOAD research. To our knowledge, there are no models recapitulating this form of the disease. It would be interesting to examine if *Bmi1* re-expression in neurons could rescue the pathological phenotype.

2- *Bmi1* was previously reported to associate with facultative heterochromatin. We are first to demonstrate that it is also enriched at constitutive intergenic and pericentric heterochromatin and that this association is $H3K27^{me3}$ independent,

suggesting other mechanisms for polycomb chromatin targeting. Moreover, loss of *Bmi1* enrichment correlates with increased genomic instability at heterochromatic regions.

3- We also observed that BMI1 deficiency and constitutive heterochromatic genome instability in human brains are hallmarks of LOAD but not of EOAD. This finding indicates that these two disorders differ in their triggering mechanisms however the final neuropathology is similar in both.

In order to mechanistically recapitulate the whole pathological process, treatment of WT cortical neurons with drugs that induce heterochromatin decompaction such as HDAC inhibitors is required. Conversely, treatment of *Bmi1*$^{-/-}$ cortical neurons with inhibitors of the histone demethylase Jumonji should rescue the phenotype. Furthermore, in order to demonstrate our proof of principle relating *Bmi1* loss with progression of LOAD in humans, overexpression or knocking down of *Bmi1* in LOAD and healthy cortical neurons is required. Subsequently, we can evaluate if Bmi1 overexpression rescues the pathological phenotype in LOAD neurons or if *Bmi1* knock-down in healthy neurons promotes heterochromatin decondensation and neurodegeneration. Human cortical neurons of LOAD or healthy individuals can be obtained from differentiated iPS cells. It is also highly important to evaluate if *Bmi1* deficiency and reduced H3K9^{me3} levels can also be detected in the lymphocytes of *Bmi1*$^{+/-}$ mice and LOAD patients. This is highly pertinent in terms of development of biomarkers for LOAD.

Our study opens the door to potential treatments and diagnostic biomarkers for age-related Alzheimer's disease… the question that remains is whether we can delineate the process well enough so that we can actually develop a molecular fountain of youth.

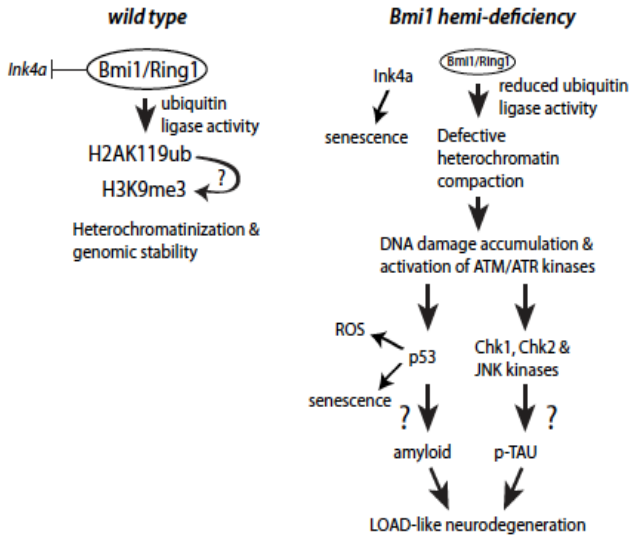

Figure 1: Working model describing the process by which epigenetic modifications of constitutive heterochromatin lead to LOAD progression. Disrupted heterochromatin results in genomic instability as well as activation of the DNA damage and chromatin stress sensors ATM and ATR. These kinases, working at the apex of the cascade, can subsequently activate p53 and the Chk1 and Chk2 kinases. This pathological cascade is sufficient, at least in mice, to induce beta-Amyloid and p-TAU accumulation, hallmarks of LOAD.

References:

1. Chatoo W., Abdouh M., et al. *The polycomb gene Bmi1 regulates antioxidant defenses in neurons by repressing p53 prooxidant activity*. J.of.Neuroscience 2009. 29(2):529-542.

2. Zhang J., Sarge K. *Identification of a polymorphism in the RING finger of the human BMI1 that causes its degradation by the ubiquitin proteasome system*. FEBS letters 2009. 583(6): 960-4.

3. Abdouh M., Chatoo W., et al., *Bmi1 is downregulated in the aging brain and displays antioxidant and protective activities in neurons*. PLos one 2012. 7(2):e31870.

4. Krishnamurthy, J., Torrice, C., Ramsey, M.R., Kovalev, G.I., Al-Regaiey, K., Su, L., Sharpless, N.E. *Ink4a/Arf expression is a biomarker of aging*. J. Clin. Invest. 2004. 114, 1299–1307.

5. Sze C., Troncoso JC., et al. Loss of the presynaptic vesicle protein synaptophysin in hippocampus correlates with cognitive decline in Alzheimer disease. J.Neuropath. Exp. Neur. 1997. 56(8):933-44.

6. Cao G., Minxia G., et al. *Bmi1 absence causes premature brain degeneration*. PLos one 2012. 7(2):e32015.

7. Querfurth H. and LaFerla F. *Alzheimer's disease*, NEJM 2010; 362:328-44

8. Forero DA, casadesus G., *Synaptic dysfunction and oxidative stress in Alzheimer's disease: emerging mechanisms*. J. Cell. Mol. Med 2006. 10(3): 796-805.

9. Subkhankulova T., Zhang X., et al., *Bmi1 directly represses p21 in Shh-induced proliferation of cerebellar granule cell progenitors*. Mol. and Cell. Neuroscience 2010. 45(2):151-162.

10. Hooper C., meimaridou E., et al., *p53 is upregulated in Alzheimer's disease and induces tau phosphorylation in HEK293a cells*. Neurosci. Lett. 2007. 418(1):34-37.

11. Lanni C., Raccchi M., et al., *p53 at the crossroads between cancer and neurodegeneration*. Free radical biology & medicine 2012. 52:1727-1733.

12. Mendoza J., Sekiya M., et al., *Global analysis of phosphorylation of Tau by checkpoint kinases Chk1 and Chk2 in vitro*. J. Proteome. Res. 2013. 12(6):2654-65.

13. Wetzel MK., Naska S., *p73 regultes neurodegeneration and p-tau accumulation during aging and Alzheimer's disease*. Neuron 2008. 59(5):709-21.

14. Liger-Mouton F., Paquet C., et al., *Oxidative stress increases BACE-1 protein levels through activation of PKR-eIF2 pathway*. Biochim.Biophys. Acta. 2012. 1822(6):885-96.

15. Borghi R., Piccini A., et al., *Upregulation of Presenilin 1 in brains of sporadic, late onset Alzheimer's disease*. Journal of Alz. Disease. 2010. 771-775.

16. Tamagno E, Parola M, et al., *Beta-site APP cleaving enzyme up-regulation induced by 4-hydroxynonenal is mediated by stress-activated protein kinases pathways*. J Neurochem. 2005. 92(3):628-36

17. Guillozet AL, Weintraub S., et al., *Neurofibrillary tangles, amyloid, and memory in aging and mild cognitive impairment.* Arch Neurol. 2006. 60(5):729-36.

18. Sparmann, A. and M. van Lohuizen, *Polycomb silencers control cell fate, development and cancer.* Nat Rev Cancer, 2006. 6(11): p. 846-56.

19. Bernstein E, Duncan EM., et al. *Mouse polycomb proteins bind differentially to methylated histone H3 and RNA and are enriched in facultative heterochromatin*. Mol Cell Biol. 2006. 26(7):2560-9.

20. Puschendorf M, Terranova R, et al. *PRC1 and Suv39h specify parental asymmetry at constitutive heterochromatin in early mouse embryos*. Nat Genet. 2008. 40(4):411-20.

21. Saurin A., Shiels C., et al., *The human polycomb group complex associates with pericentromeric heterochromatin to form a novel nuclear domain*. J. Cell. Bio. 1998. 142(4):887-898.

22. Hernandez-Munoz I., Taghavi P., et al., *Association of BMI1 with polycomb bodies is dynamic and requires PRC2/EZH2 and the maintenance DNA methyltransferase DNMT1*. Mol.Cell.Bio. 2005. 25(24):11047-11058.

23. Kallin EM., Cao R., et al. *Genome wide uH2A localization analysis highlights Bmi1-dependent deposition of the mark at repressed genes*. PLos Genetics 2009. 5(6): e1000506.

24. Braun S. and Madhani H. *Shaping the landscape: mechanistic consequences of ubiquitin modification of chromatin*. EMBO reports 2012. 13(7):619-630.

25. Nakagawa T., Kajitani T., et al. *Deubiquitylation of histone H2A activates transcriptional initiation via trans-histone cross talk with H3K4 di and*

trimethylation. Genes and dev. 2008. 22:37-49.

26. Luger K, Mäder AW, Richmond RK, Sargent DF, Richmond TJ. *Crystal structure of the nucleosome core particle at 2.8 A resolution*. Nature 1997. 389:251-60.

27. Sewalt, R.G.*, et al. Selective interactions between vertebrate polycomb homologs and the SUV39H1 histone lysine methyltransferase suggest that histone H3-K9 methylation contributes to chromosomal targeting of Polycomb group proteins.* Mol. Cell. Biol.2002. 22, 5539-5553.

28. Mungamuri SK, Benson EK, et al., *p53-mediated heterochromatin reorganization regulates its cell fate decisions*, Nat Struct Mol Biol. 2012. 19(5):478-84.

29. Zheng H, Chen L, et al., p53 promotes repair of heterochromatin DNA by regulating JMJD2b and SUV39H1 expression. Oncogene. 2013. 2013.6

30. Lei EP, Corces VG. *A long-distance relationship between RNAi and Polycomb*. Cell. 2006.124(5):886-8.

31. Grau D.J., Chapman B., et al. *Compaction of chromatin by diverse polycomb groups requires localized regions of high charges*. Gen. Dev.2011. 25:2210-21.

32. Cao L., Li W., et al., Senescence, aging, and malignant transformation mediated by p53 in mice lacking the Brca1 full-length isoform. Genes Dev. 2003.17(2):201-13.

33. Bihaqi SW, Schumacher A, et al., *Do epigenetic pathways initiate late onset Alzheimer disease (LOAD): towards a new paradigm*. Curr Alzheimer Res. 2012. 9(5):574-88.

34. Wang SC., Oeleze b., Sumacher A. *Age-specific epigenetic drift in late-Onset Alzheimer's disease*. PLos One 2008. 3(7):e2698.

35. Cedar H, Bergman Y. *Linking DNA methylation and histone modification: patterns and paradigms*. Nat Rev Genet. 2009. 10(5):295-304.

36. Mastroeni D., McKee a., et al. *Epigenetic differences in cortical neurons from a pair of monozygotic twins discordant for Alzheimer's disease*. PLos One 2009. 4(8):e6617.

37. Chouliaras L, Mastroeni D, et al., *Consistent decrease in global DNA methylation and hydroxymethylation in the hippocampus of Alzheimer's disease patients*. Neurobiol Aging. 2013. 34(9):2091-9.

38. Bollati V, Galimberti D. *DNA methylation in repetitive elements and Alzheimer disease.* Brain Behav Immun. 2011. 25(6):1078-83.

39. Li W., Jin Y., et al. *Transposable elements in TDP-43 mediated neurodegenerative disorders.* PLos One 2012. 7(9):e44099.

40. Li W, Prazak L, etal., *Activation of transposable elements during aging and neuronal decline in Drosophila.* Nat Neurosci. 2013.16(5):529-31.

41. Kaneko H, Dridi S, et al. *DICER1 deficit induces Alu RNA toxicity in age-related macular degeneration*. Nature. 2011. 471(7338):325-30.

42. Coppedè F. *One-carbon metabolism and Alzheimer's disease: focus on epigenetics*. Curr Genomics. 2010.11(4):246-60.

43. Towbin BD, González-Aguilera C, et al., *Step-wise methylation of histone H3K9 positions heterochromatin at the nuclear periphery.* Cell. 2012.150(5):934-47.

44. Niessen H., Demmers J., *Talking to chromatin: post-translational modulation of polycomb group function.* Epigenetics and chromatin 2009. 2:10.

45. Katoh Y, Ikura T., et al., *Methionine adenosyltransferase II serves as a transcriptional corepressor of Maf oncoprotein*. Mol Cell. 2011 Mar 4;41(5):554-66.

46. Chiolo I., Minoda A., et al. *Double-Strand Breaks in Heterochromatin Move Outside of a Dynamic HP1a Domain to Complete Recombinational Repair*. Cell 2011. 144(5):732-744.

47. Larson, K., et al. *Heterochromatin formation promotes longevity and represses ribosomal RNA synthesis*. PLoS Genet 2012. 8, e1002473.

48. Peters AH, O'Carroll D. et al. *Loss of the Suv39h histone methyltransferases impairs mammalian heterochromatin and genome stability*. Cell 2001.107(3):323-37.

49. Postepska-Igielska A, Krunic D, et al., *The chromatin remodelling complex NoRC safeguards genome stability by heterochromatin formation at telomeres and centromeres.* EMBO Rep. 2013.

50. Haider S., Cordeddu L., et al., *The landscape of DNA repeat elements in human heart failure*. Genome biology 2012. 13:R90.

51. Li J, Han YR, Plummer MR, Herrup K. *Cytoplasmic ATM in neurons modulates synaptic function.*Curr Biol. 2009. 19(24):2091-6.

52. Veltman J. *De novo mutations in mental retardation.* Genome Biol. 2011. 12:16.

53. Facchino, S., Abdouh, M., Chatoo, W. & Bernier, G. *BMI1 confers radioresistance to normal and cancerous neural stem cells through recruitment of the DNA damage response machinery.* J. Neurosci. 2010. 30, 10096-10111.

54. Dinant, C., and Luijsterburg, M.S. *The emerging role of HP1 in the DNA damage response.* Mol. Cell. Biol 2009. 29(24): 6335–6340.

55. Francia S, Michelini F., et al. *Site-specific DICER and DROSHA RNA products control the DNA-damage response.* Nature. 2012. 488(7410):231-5.

56. Greenberg R. *Histone tails: directing the chromatin response to DNA damage*. FEBS letters 2011. 585:2883-90.

57. Pegoraro G, Misteli T. *Ageing-related chromatin defects through loss of the NURD complex.* Nat Cell Biol. 2009. 11(10):1261-7.

58. Pimplikar SW. *Reassessing the amyloid cascade hypothesis of Alzheimer's disease.* Int J Biochem Cell Biol. 2009. 41(6):1261-8.

59. Bak M., et al., *MicroRNA expression in the adult mouse central nervous system.* RNA 2008. 14: 432-444

60. Zhang J., Sarge K. et al., *Identification of a polymorphism in the RING finger of the human BMI1 that causes its degradation by the ubiquitin proteasome system*. FEBS letters 2009. 583(6): 960-4.

ANNEXE I

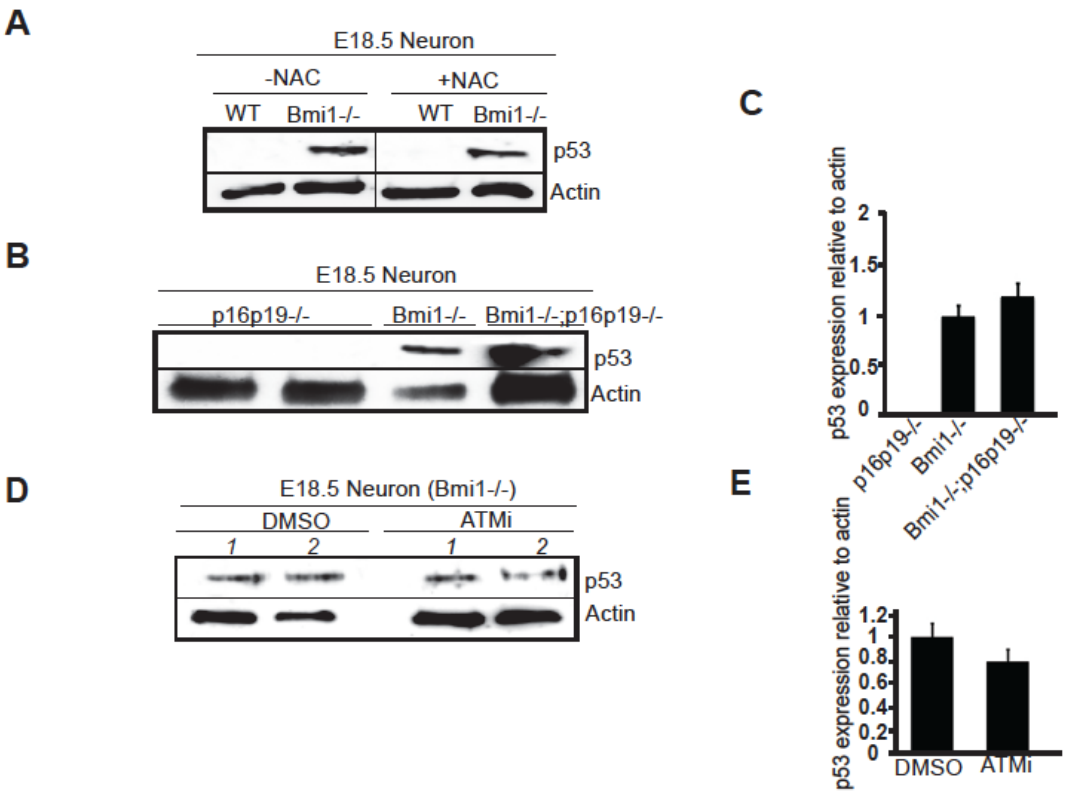

Figure 1: A. Treatment of *Bmi1*$^{-/-}$ cortical neurons with the ROS scavenger NAC did not inhibit p53 activation. **B.** DKO *Bmi1*$^{-/-}$*;INK4A/Arf*$^{-/-}$ cortical neurons did not rescue the pathological accumulation of p53. **C.** Quantification of the results in B. **D.** p53 was still upregulated in *Bmi1*$^{-/-}$ neurons even after treatment with an ATM inhibitor. E. Quantification of the results in D.

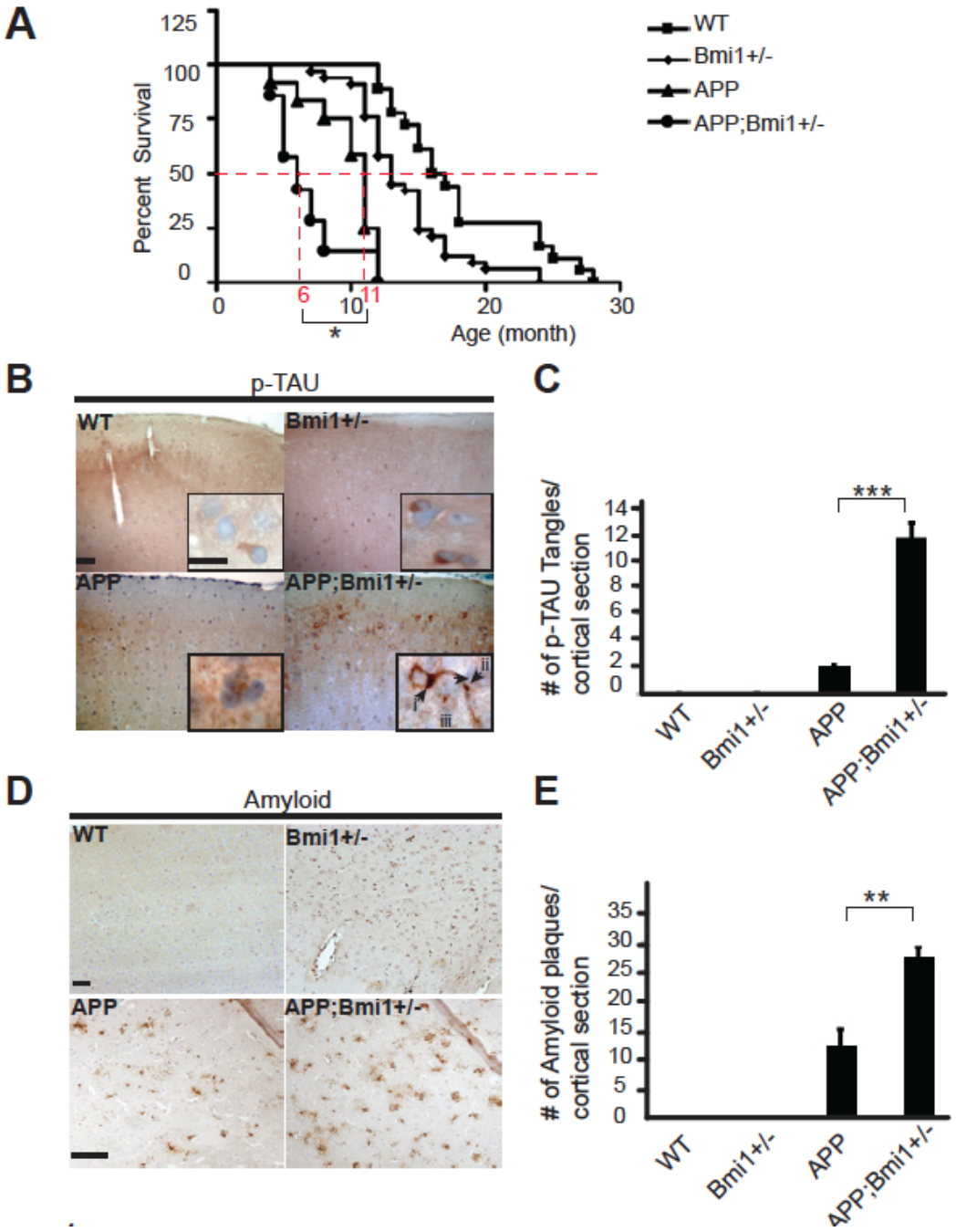

Figure 2: Genetic cooperation between *Bmi1* and *APP*. **A.** 6-month old *APP; Bmi1*$^{+/-}$ mice present a significant reduction in median lifespan. **B. & D.** 6-month old *APP; Bmi1*$^{+/-}$ mice show significant formation of p-Tau tangles and amyloid plaques deposition in several cortical sections, compared to *APP* mice cortices alone. **C. &. E.** Quantification of B. & D.

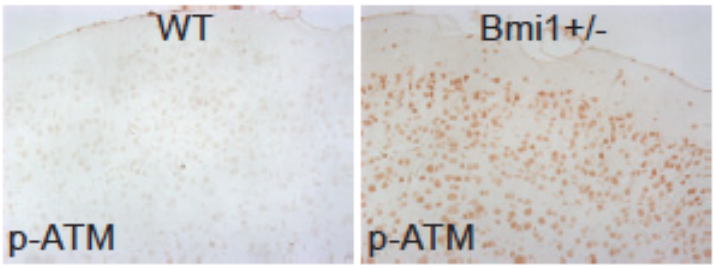

Figure 3: Immunohistochemistry on cortical sections of old WT and *Bmi1*$^{+/-}$ reveals important accumulation of p-ATM in the nucleus and cytosol of aged *Bmi1*$^{+/-}$ neurons**.**